

2002

Syntectonic fluid-rock interactions involving surficial waters in the Sevier Thrust Belt, Tendoy Mountains, Southwest Montana

Adrienne C. (Claire) Johnson
Lehigh University

Follow this and additional works at: <http://preserve.lehigh.edu/etd>

Recommended Citation

Johnson, Adrienne C. (Claire), "Syntectonic fluid-rock interactions involving surficial waters in the Sevier Thrust Belt, Tendoy Mountains, Southwest Montana" (2002). *Theses and Dissertations*. Paper 732.

This Thesis is brought to you for free and open access by Lehigh Preserve. It has been accepted for inclusion in Theses and Dissertations by an authorized administrator of Lehigh Preserve. For more information, please contact preserve@lehigh.edu.

Johnson, Adrienne
C.

Syntectonic Fluid-
Rock Interactions
Involving Surficial
Waters in the
Sevier Thrust Belt,
Tendoy...

June 2002

Syntectonic Fluid-Rock Interactions Involving Surficial Waters in the Sevier Thrust
Belt, Tendency Mountains, Southwest Montana

By

Adrienne C. Johnson

A Thesis
Presented to the Graduate and Research Committee
Of Lehigh University
In Candidacy for the Degree of
Master of Science

In
Geological Sciences
Lehigh University

May 4, 2002

This Thesis is accepted and approved in partial fulfillment of the requirements for
Master of Science.

5-14-02

Date

David J. Anastasio
Thesis Advisor

Peter Zeitler
Chairperson of Department

Acknowledgements

First, I would like to thank my advisor David Anastasio for the past two years and a great project. I have learned a lot from this experience and am glad to have had the chance to work on the veins of the Tendoy Mountains in beautiful Montana. I would also like to thank Gray Bebout, who was also a great help. Having a chance to work in the isotope lab was a great experience. I would also like to thank my third committee member Mark Evans from the University of Pittsburgh for his help with the fluid inclusions aspect of my project and the use of his laboratory. I'd also like to thank Bruce Idelman, Margie Barry, Nancy Roman, and Laurie Cambiotti. I'd also like to thank Dr. Jack Beuthin and William Brice as the University of Pittsburgh at Johnstown for the use of their labs, space, and for the entertainment. I'd also like to thank Nancy (Fluffy) Williams and Robin McDowell.

On a personal note, I'd like to thank Michael Rygel who has finally made my life complete, for the support, the encouragement, and the great stereoplot skills! A huge thanks to my father Robert Johnson, the best field assistant in the world, I couldn't have done it without you! Also thanks dad and mom, Susan, for all the discussions and reviews (it's great having parents who are geologists!), thanks for the support and love. Thanks to my brother Brian. I would also like to thank all of my friends at Lehigh, especially Jordan Vaughn and Kurt Frankel, it was a great two years and you will be missed. I would also like to thank my friends in Lima, Montana: Rosa, Ben, and Jerry. Seeing your smiling faces throughout the course of those three weeks and having a chance to live in such a beautiful part of the country, your home, was one of the most

memorable experiences I have been fortunate enough to have and I hope to visit Lima and Dell again in the future!

I would also like to thank Richard Allmendinger for the use of his stereonet programs (1995 and 2000 versions). Thanks to the Geological Society of American, the American Association of Petroleum Geologists, and the Palmer Fund through Lehigh University for the funding that made this thesis possible.

The Table of Contents

Certificate of Acceptance	ii
Acknowledgements	iii
List of Figures	vii
List of Appendixes	viii
Abstract	1
Introduction	2
Geologic Setting	5
Geology and Stratigraphy of the Tendoy Mountains	5
Geology of Sample Traverses	11
Vein Genesis	18
Vein Morphology	18
Kinematics of Vein Development	23
Textures of Veins	29
Temperature Constraints Defined and the Presence of Hydrocarbons	33
Fluid Compositions and Sources	36
Stable Isotope Analyses	36
Interpretation of Isotopic Results	41
Fluid Sources	44
Paleohydrology Reconstructions	45
Conclusions	50
References	52

Appendices

62

Vita

117

List of Figures	Page
Figure 1 – Cartoon of fluid flow regimes	3
Figure 2 – A) Geologic map	6
B) Cross-sections	7
Figure 3 – Stratigraphic column	10
Figure 4 – Little Sheep Creek traverse sketch and cross-section	12
Figure 5 – Big Sheep Creek traverse sketch and cross-section	13
Figure 6 – McKnight Canyon traverse	15
Figure 7 – Easternmost Four Eyes Canyon traverse sketch and cross-section	16
Figure 8 – Westernmost Four Eyes Canyon/Medicine Lodge traverse sketch and cross-section	17
Figure 9 - Stereoplots of Poles to Bedding	19
Figure 10 – Vein textures and styles of veining in the field	20
Figure 11 - Sketch of irregular veins in the western Four Eyes Canyon traverse	22
Figure 12 – Tendoy thrust sheet orientation analyses:	
A) Plots and cross-cutting relationships	22
B) Tendoy kinematic summary	26
Figure 13 – Four Eyes Canyon and Medicine Lodge thrust sheets orientation analyses	
A) Plots and cross-cutting relationships	28
B) Four Eyes Canyon and Medicine Lodge kinematic summary	30
Figure 14 – Vein textures in thin sections	31
Figure 15 – Stable isotope results A) Undeformed host-rock, microlithons,	

and selvages B) Tie lines of veins to corresponding host-rock	38
Figure 16 – Stable isotope results	
A) Cretaceous veins for Tendoy thrust sheet B) Cretaceous veins for the Four Eyes Canyon/Medicine Lodge thrust sheets	39
C) Eocene veins for the Four Eyes Canyon/Medicine Lodge thrust sheets	42
Figure 17 – $\delta^{18}\text{O}$ variation in North America	46
Figure 18 – Paleogeography of the Late Cretaceous and Eocene	48
Appendixes	
Appendix 1. Topographic index map and individual topographic/geologic maps for each traverse	62
Appendix 2. Traverse photo mosaics with sample locations	70
Appendix 3. Little Sheep Creek collapse cave photographs	75
Appendix 4. Styles of veining photographs: outcrop and thin sections	76
Appendix 5. Orientation data sets	77
Appendix 6. Fluid inclusion table of results, diagram of observations, and photographs	100
Appendix 7. Stable isotope data sets	103

Abstract

Structural, petrographic, and isotopic analyses of calcite veins and their carbonate host-rocks from the Sevier thrust front of southwestern Montana record syntectonic meteoric fluid infiltration and hydrocarbon migration. The calcite veins record fluid pathways and fluid flow history during thrust emplacement. Vein fillings occurred during single or multiple fluid flow events. Orientation analysis of mutually crosscutting, high-angle vein sets suggest development concurrent with Four Eyes Canyon and Medicine Lodge thrusting and folding, but prior to Tendoy thrusting and folding. Syn-folding bed-parallel shear veins are found in all thrust sheets. Irregular veins that transect Sevier structures in the Four Eyes Canyon and Medicine Lodge thrust sheets were likely reactivated during Eocene extensional deformation. Analyses of $\delta^{18}\text{O}_{\text{V-SMOW}}$ and $\delta^{13}\text{C}_{\text{V-PDB}}$ of veins and host-rocks allow reconstruction of fluid-rock interactions during deformation. Low salinity ($T_m = -0.6^\circ\text{C}$ to $+3.6^\circ\text{C}$) and low temperature (80-100°C for Cretaceous veins, 40-80°C for Eocene veins) fluids interacted with hanging wall carbonates at shallow depths (3-4 km Cretaceous, 1-2 km Eocene). Undeformed carbonate host-rocks have a $\delta^{18}\text{O}$ mean value of $+22.2 \pm 3\text{‰}$ (1σ). All veins show significant variation in $\delta^{18}\text{O}$ and $\delta^{13}\text{C}$. Variation in $\delta^{13}\text{C}$ is likely due to the presence of hydrocarbons. Tendoy veins related to Cretaceous thrusting have calcite $\delta^{18}\text{O}$ values of +8.9 to +28.8‰. In the Four Eyes Canyon and Medicine Lodge thrust sheets, Cretaceous veins have calcite $\delta^{18}\text{O}$ values of +5.9 to +21.6‰ and Eocene veins have $\delta^{18}\text{O}$ values of +5.9 to +17.0‰. Calculated fluid $\delta^{18}\text{O}$ as H_2O , using calcite $\delta^{18}\text{O}$ values for Cretaceous veins are interpreted to be -11 to -9‰ (80°

and 100° C) as compared to Eocene fluid $\delta^{18}\text{O}$ values of -19‰ to -13‰ (40° and 80° C). Isotope data indicates infiltration of foreland thrust sheets by evolved meteoric waters, during both the Cretaceous and the Eocene. Surficial fluids infiltrated into the thrust sheets by topographic recharge and migrated updip towards the foreland resulting in varying degrees of fluid-rock interactions producing higher $\delta^{18}\text{O}$ veins. Degraded hydrocarbon found in fluid inclusions indicate that hydrocarbons migrated with freshwater fluids.

Introduction

Evolution of orogens and foreland basins is profoundly influenced by crustal fluids, which impact deformation mechanics (Forster and Smith, 1990; Davis et al., 1983; Hubbert and Rubey, 1959) and the transport of hydrocarbons (Oliver, 1986). Numerous fluid sources and flow regimes have been distinguished and studied in orogens; examples include deep, diffuse flow of metamorphic and magmatic fluids being driven in front of thrust sheets (Oliver, 1986), shallow flow of meteoric fluids through fractures in a fold and thrust front (Hutcheon et al., 2000; Ge and Garvin, 1994), and a flow regime consisting of both deep and shallow diffuse flow along fractures with interaction between metamorphic, magmatic, and meteoric fluids (Koons and Craw, 1991) (Figure 1). Additionally, aquifer systems can be stratified with distinct zones at varying depths between which there is no mixing or exchange of fluids, but through which there is fluid flow and fluid-rock interaction (Evans and Battles, 1999). Bebout et al. (2001) have shown that in the Lost River Range, Idaho

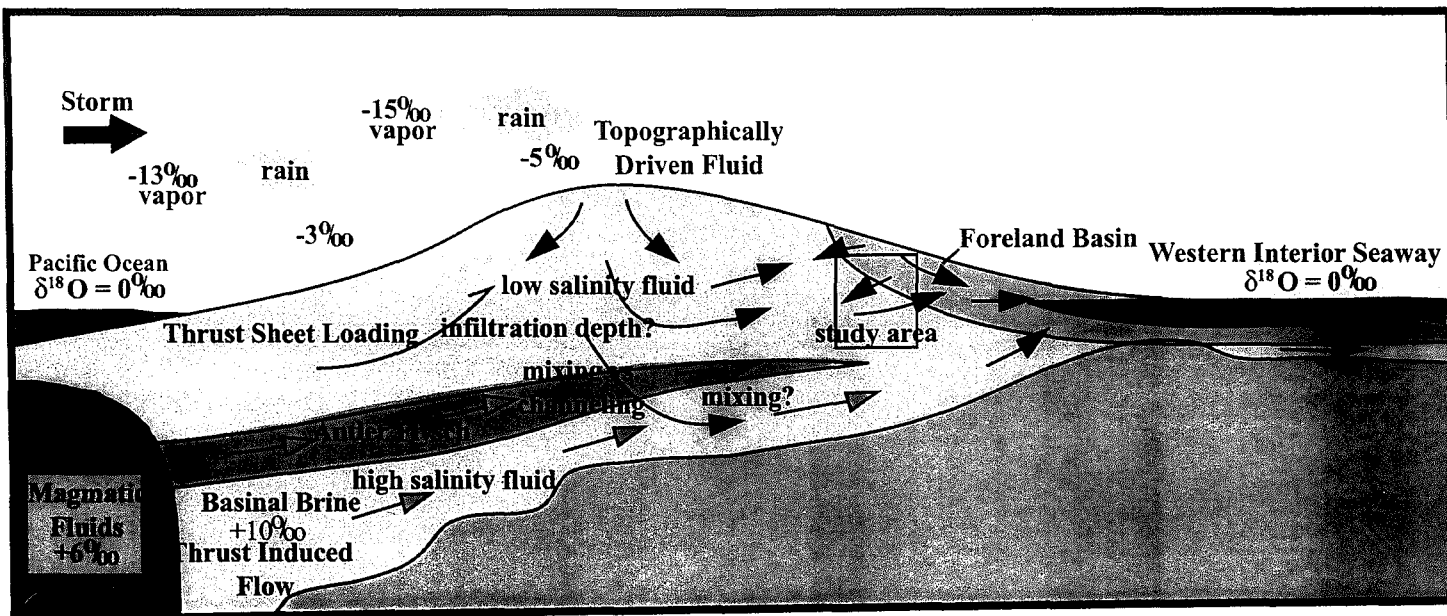


Figure 1. Cartoon of fluid flow regimes in a fold and thrust belt setting: different fluid sources, $\delta^{18}\text{O}$ compositions, pathways, and driving mechanisms (modified from Koons and Craw, 1991; Anastasio in prep., 2002).

there was deep infiltration of meteoric fluids. The lack of deep magmatic or metamorphic fluids in that region is perhaps related to the presence of a thick section of the Antler flysch, an ideal aquitard, preventing them from mixing with shallower meteoric fluids. The purpose of this study was to look for evidence of the infiltration of meteoric water further to the east in the Tendoy Mountains of the Beaverhead Range. Absence of Antler flysch beneath frontal thrust sheets provides an opportunity to investigate the generation of devolatilized hinterland fluids in the thrust belt (e.g. Oliver, 1986; Evans and Battles, 1999). The Tendoy Mountains experienced a period of compression during the Cretaceous when the Western Interior Seaway was present (a potential water source) and subsequent extension during the Eocene when the seaway no longer occupied the continent's interior (Kalakay, 2001). Variations in fluid regimes during these two periods of deformation are explored to evaluate the effect of fluid source variation on fluid-rock interactions.

Samples in this study were collected from traverses both along- and cross-strike in the Tendoy, Four Eyes Canyon, and Medicine Lodge thrust sheets. These samples were analyzed for variations in fluid pathways and fluid compositions due to spatial, temporal, and structural positioning. The excellent exposures in all three thrust sheets allows for investigation of the spatial variation within the thrust sheets. Additionally, sampled veins that developed during both the periods of Cretaceous compression and Eocene extension provide a framework to explore for temporal variability. Finally, the emerging thrust sheets have a complex deformational history

of in- and out- of sequence faulting and numerous folded sections that provide ample structural variability over a substantial time period (Perry et al., 1988).

A multidisciplinary approach using structural and geochemical methods were applied to the Tendoy, Four Eyes Canyon, and Medicine Lodge thrust sheets in order to understand the evolution of fluid pathways, fluid flow, and fluid sources in the Tendoy Mountains. Orientation and petrographic analyses of veins were used to study variations in fluid pathways due to temporal variations in tectonic regime.

Environmental conditions, such as temperature, influence the calculations of isotopic composition of the fluid and how one would interpret the fluid source. In order to constrain deformation fluid temperatures fluid inclusion analyses were conducted and estimates about rock and fluid temperatures from other studies were used. Finally, stable isotope analyses of veins ($\delta^{18}\text{O}_{\text{V-SMOW}}$ and $\delta^{13}\text{C}_{\text{V-PDB}}$) were conducted to study the evolution of fluids and fluid-rock interactions in the Tendoy Mountains and reconstruct the paleohydrology of the frontal thrust sheets.

Geologic Setting

Geology and Stratigraphy of the Tendoy Mountains

The Tendoy Mountains contain the frontal thrust sheets (Tendoy, Four Eyes Canyon, and Medicine Lodge) of the Sevier fold and thrust belt in southwestern Montana (Figure 2A and 2B). The formation of the syntectonic Beaverhead Group records the sequence of thrusting. As the thrust sheets emerged they shed additional material into the foreland, thickening the package of syntectonic conglomerate

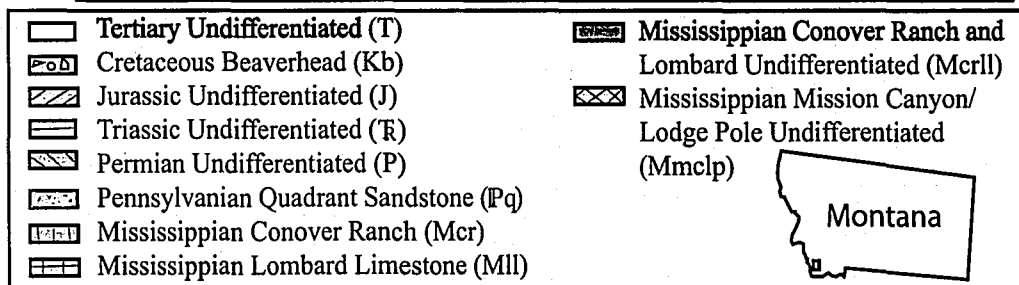
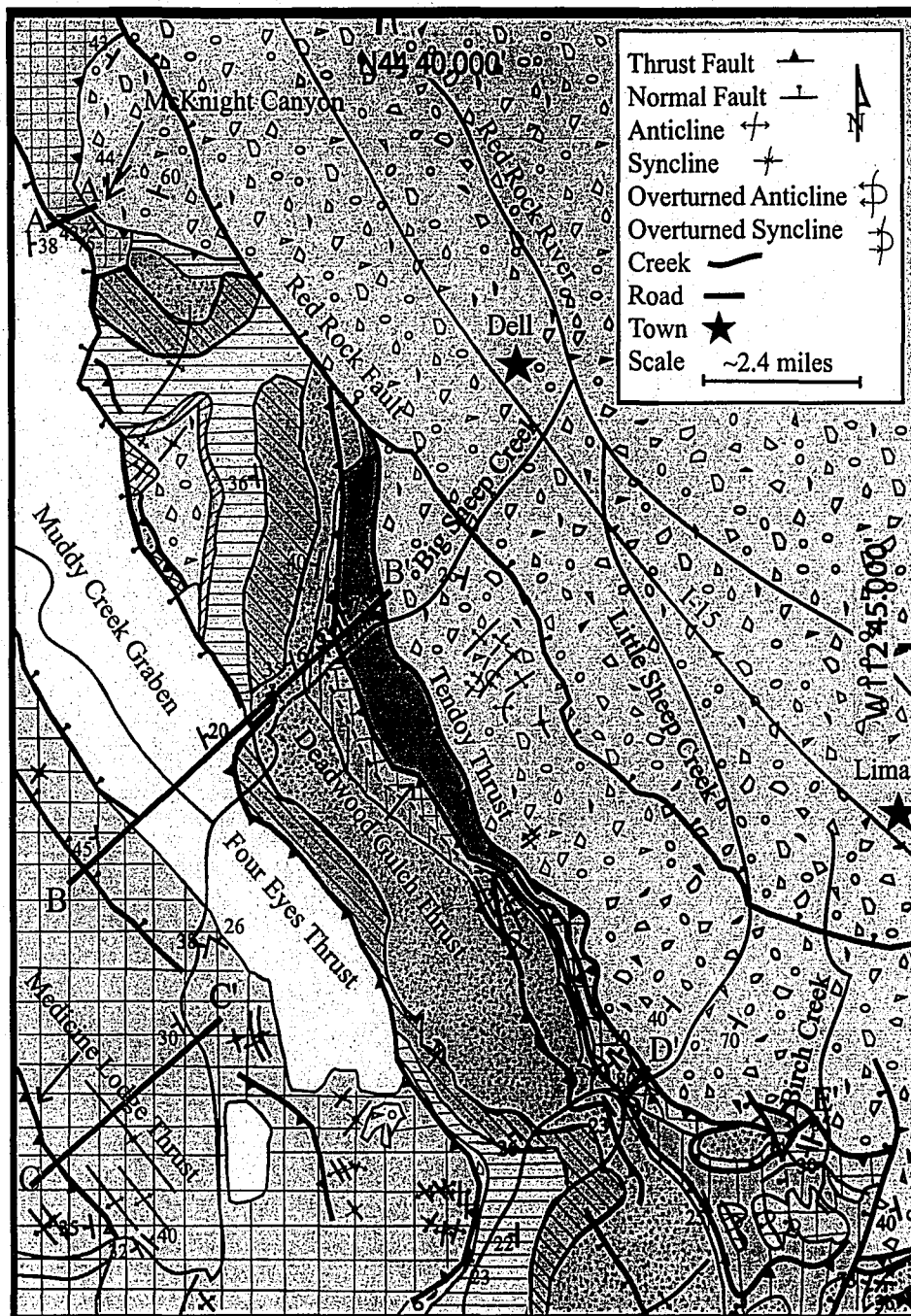


Figure 2: A) Simplified geologic map from Lonn et al., 2000; McDowell, 1992; Williams and Bartely, 1988; and with additional data from this thesis research, Johnson 2002, and Harkins, 2002.

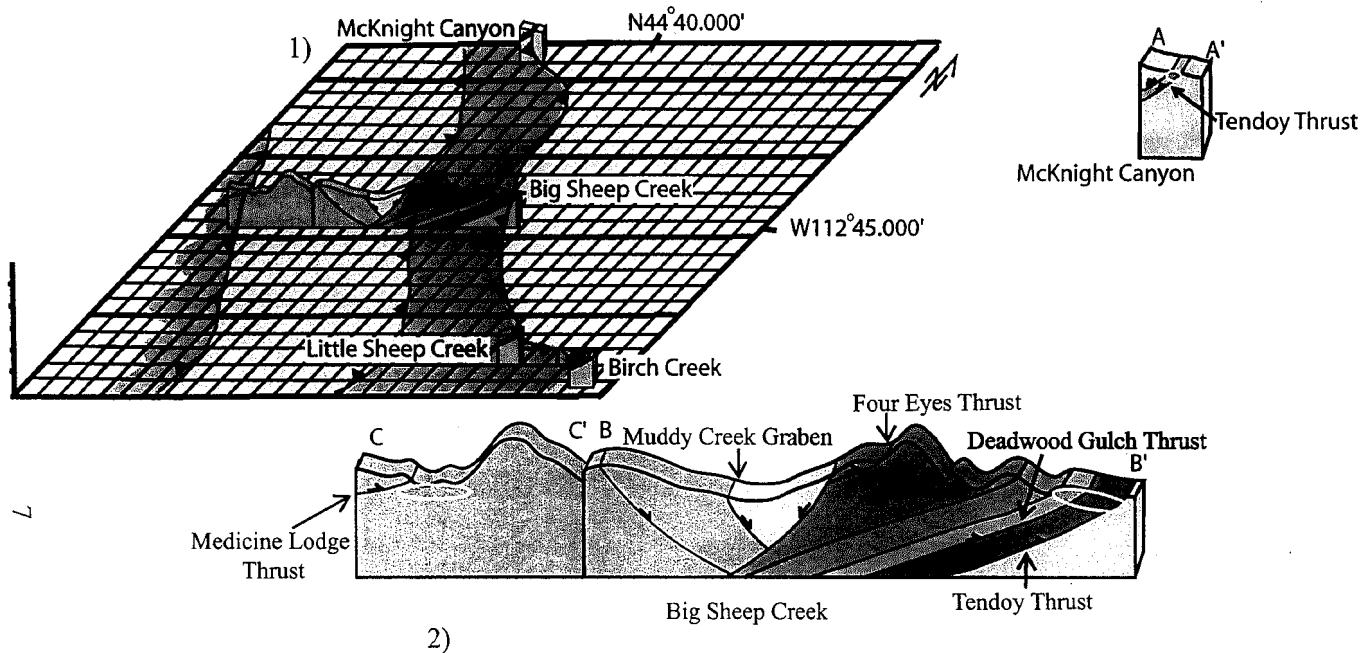
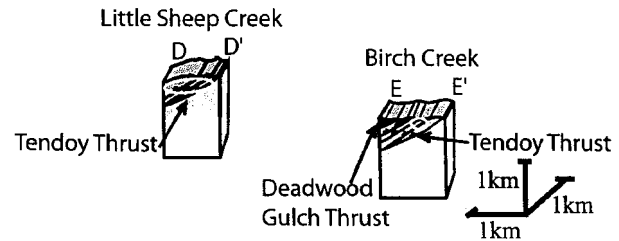


Figure 2B. 1) A 1km² grid, with a 1km vertical scale showing the position of sampling traverses. The frontal most thrust in each cross-section is the Tendoy thrust fault. 2) Simplified cross-sections of the sample traverses, to scale spatially along and cross-strike and vertically. All lines with arrows are faults and all other lines are contacts between formations. See Figure 2A for gray scale legend of formations and cross-sections lines. The Birch Creek cross-section was modified from McDowell (1992, 1997), the Little Sheep Creek and McKnight Canyon cross-sections were developed from this study and the Big Sheep Creek cross-section was developed from this study and Harkins (unpublished data, 2002).



(Schmitt et al., 1995). In some cases individual thrust sheets override units of the Beaverhead Group that were shed from the emplacement of previously emerging thrust sheets (Perry et al., 1988; Perry and Sando, 1983). Similar crosscutting relationships established the emplacement of the frontal Tendoy faults, about 79-76 Ma, about 30 km to the north (Kalakay, 2001). During the Sevier orogeny, the imbricate faults of the Tendoy Mountain thrust system formed in sequence (Medicine Lodge, Four Eyes Canyon, Tendoy) with out of sequence faulting of the Cabin thrust behind the Medicine Lodge thrust (Perry et al., 1988; Skipp, 1988). These major NW-SE trending thrust faults contain folded carbonates in their hanging walls. The faults steepened northeastward upon encountering Laramide Blacktail-Snowcrest Uplift (Perry et al., 1983). This induced out of sequence faulting within the Tendoy thrust sheet (e.g. Deadwood Gulch Fault, DWG) (McDowell, 1997 and 1992; Perry et al., 1988) and potential reactivation and out of sequence movement of the Four Eyes Canyon thrust (Anastasio et al., 2002).

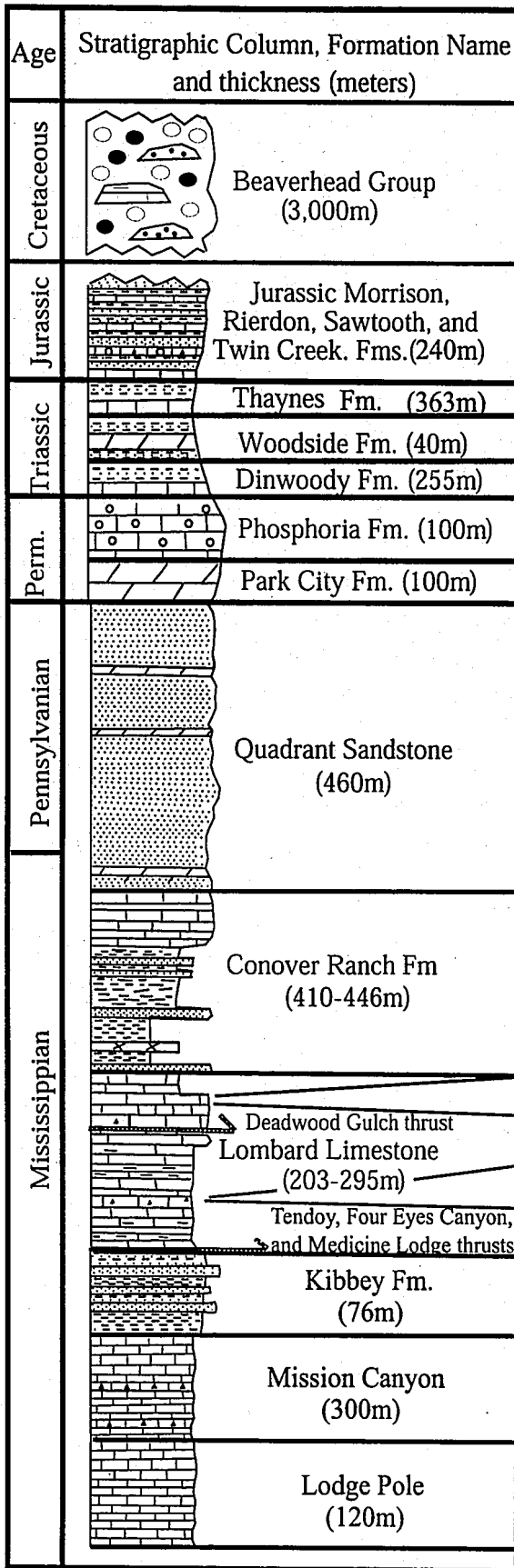
Eocene volcanism generated ash falls and scattered lava flows, which cover portions of the Four Eyes Canyon and Medicine Lodge thrust sheets. During this time there was also Basin and Range extension creating numerous normal faults in the study area (e.g. the Muddy Creek Graben) (Janecke et al., 1999). Eocene deformation proved to be important in the development of some vein sets in the study area.

The study focused on the Tendoy thrust, which emplaces Mississippian limestone on the Upper Cretaceous Beaverhead Group. There is approximately 5 km




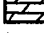


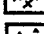
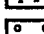

of offset on the Tendoy thrust fault (McDowell, 1992). The Four Eyes Canyon and Medicine Lodge thrusts also carry Mississippian carbonates in their hanging walls.

The carbonate rocks contained in the immediate hanging walls of all three thrust sheets are folded, while the beds within the immediate hanging wall of the Deadwood Gulch Thrust are relatively flat laying. Fold axes are oriented perpendicular to the direction of fault emplacement, that is their fold axes are parallel to the trend of the thrust faults. Folding occurred during the emplacement of the thrust sheets (McDowell, 1997). Several of the northeast-verging folds found in the Birch Creek area are interpreted to be fault-tip or fault-propagation folds that formed from splays rooted off of the basal detachment (McDowell, 1997).

Samples of calcite vein and limestone protolith were collected from the Mississippian Lombard Limestone (Mll) (Figure 3), which is 203-295 m thick and lies immediately above the Tendoy, Four Eyes Canyon, and Medicine Lodge Faults. The Lombard Limestone consists predominately of wackestone/packestone limestone, with varying amounts of fossils, and is interbedded with calcareous shale, lime mudstones, and arenaceous siltstones. Moving from the Big Sheep Creek and Little Sheep Creek traverses towards the Birch Creek and McKnight Canyon traverses the Tendoy fault cuts up-section in the Lombard Limestone (McDowell, 1997 and 1992). Immediately above the Lombard Limestone is a package of Mississippian- through Jurassic-aged sedimentary rocks, ~2 km thick (McDowell, 1997 and 1992). The nonmarine Cretaceous Beaverhead Group (Kb) is a minimum of 2800m thick in the Tendoy footwall, thicknesses vary from location to location. Presumably the Beaverhead



Key

-  conglomerate
-  sandstone
-  limestone
-  dolomite
-  shale/mudstone
-  siltstone
-  gypsum
-  chert
-  oolite

Samples: 13-21, 23, 63

Samples: 24-26 (BSC)

Samples: 2-12, 22, 35-43 (LSC, BC, McK)
27-34, 44-46

Samples: 49-58, 59+60, 61+62 (4Eyes, Med. L., Cabin)

Figure 3. Stratigraphic column of the Tendoy Mountains (Modified from McDowell, 1992 and 1997; Schmitt et al., 1995; Johnson, unpublished data 1999)

Group is thinner in the hanging wall (McDowell, 1997 and 1992; Schmitt et al., 1995; William and Bartley, 1988).

Geology of Sample Traverses

Several sampling traverses were chosen along the strike of the Tendoy thrust sheet and across strike into the Four Eyes Canyon and Medicine Lodge thrust sheets to study the spatial and temporal variation in fluid-rock interaction (Figure 2; Appendices 1-3). The southernmost Tendoy traverse was at Birch Creek (Figure 2), where samples were collected from northeast-verging fault propagation folds in the Lombard and Conover Ranch Formations less than 0.5 km from the Tendoy fault (McDowell, 1992).

The Little Sheep Creek traverse is 4 km to the north (Figure 2) where the unexposed Tendoy fault makes up the easternmost margin of a one-kilometer long traverse. McDowell (1997 and 1992) interpreted out of sequence thrusting of two smaller thrust faults and the Deadwood Gulch fault after folding and emplacement of the Tendoy fault as evidenced by the repeated stratigraphic section and displaced folds. Bedding within these imbricate faults is nearly vertical. An anticline-syncline pair, a small thrust fault, and an isolated anticline are located between the westernmost of the two imbricate faults and the Deadwood Gulch fault (Figure 4).

Continuing along strike is the Big Sheep Creek traverse (Figures 2 and 5). The easternmost margin is defined by the Tendoy fault; the western margin (2 km due

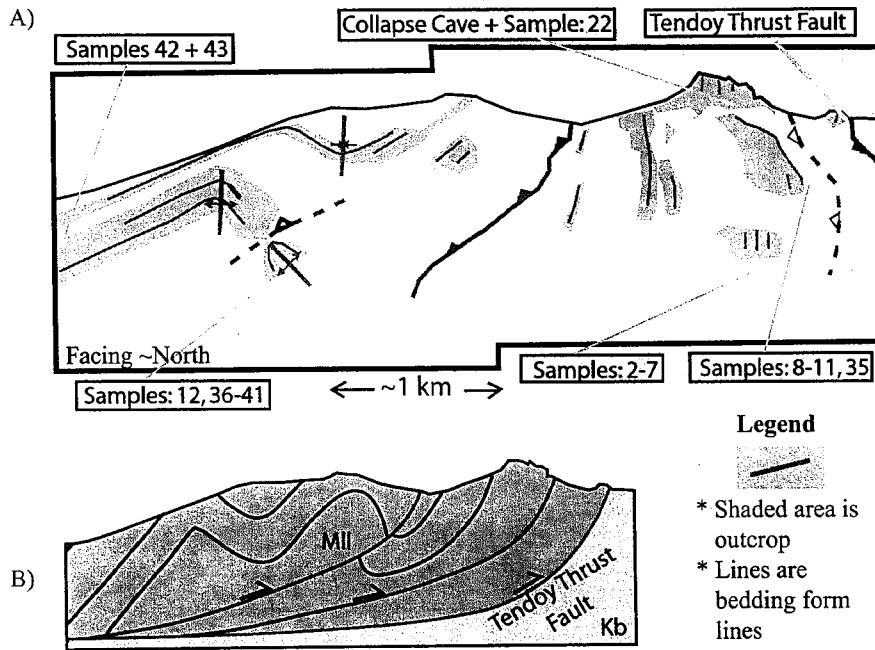
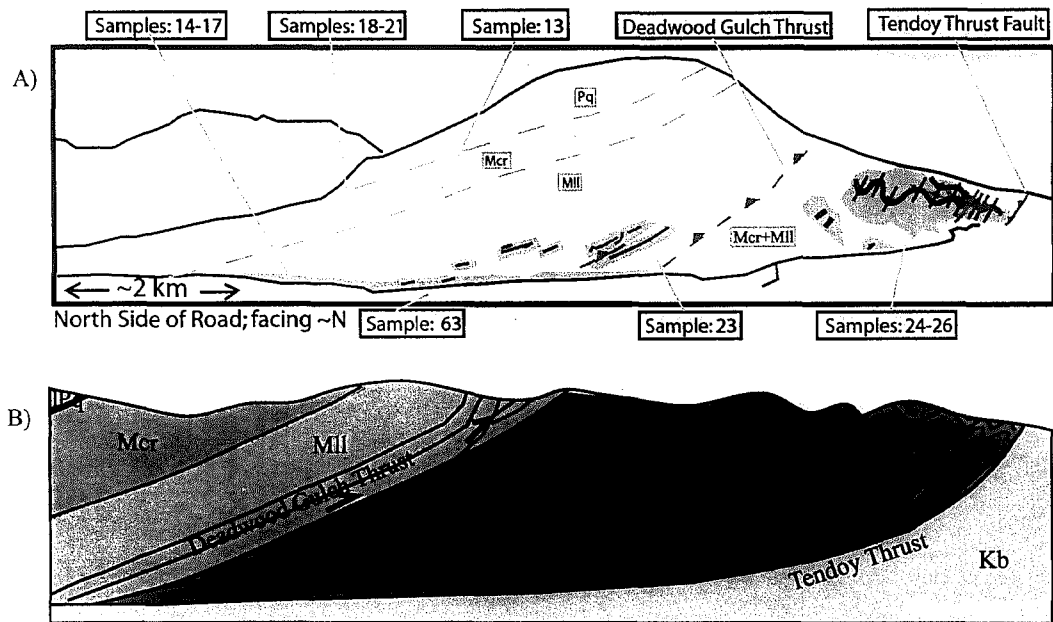


Figure 4. A) Tracing of Little Sheep Creek traverse with major structures and sampling sites.
 B) Interpretive cross-section of Little Sheep Creek.

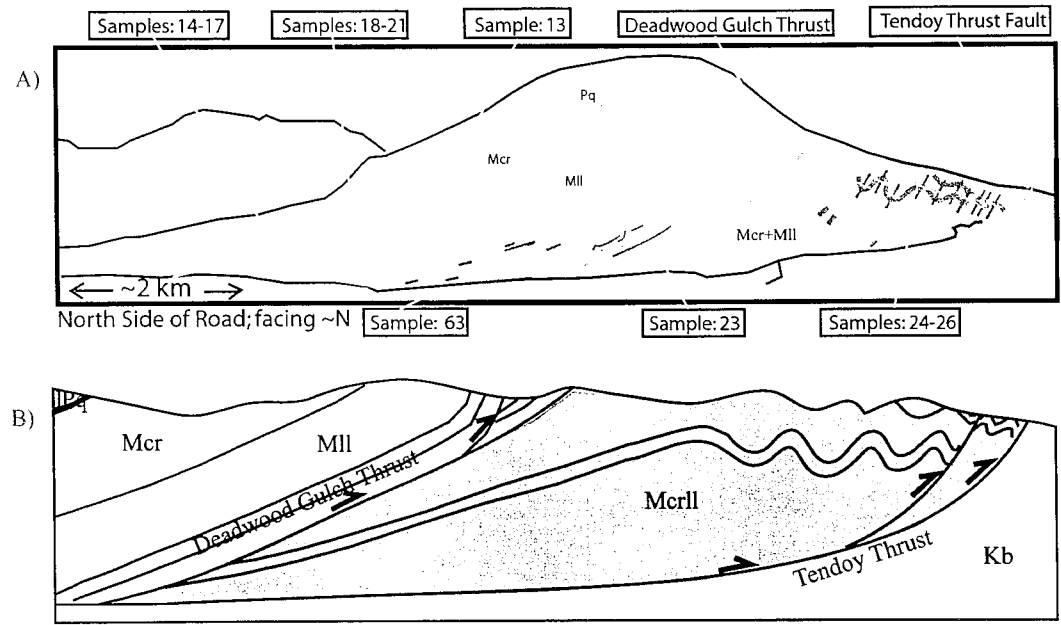


Legend

- * Shaded area is outcrop
- * Lines are bedding form lines

Figure 5. A) Tracing of Big Sheep Creek traverse with major structures and sampling sites.

B) Interpretive cross-section of Big Sheep Creek.



Legend

Figure 5. A) Tracing of Big Sheep Creek traverse with major structures and sampling sites.
 B) Interpretive cross-section of Big Sheep Creek.

- * Shaded area is outcrop
- * Lines are bedding form lines

13

west) extends into an area where the Tendoy fault had less of an immediate effect on veining. The traverse consists of two packages. The first package, immediately above the Tendoy fault, is an intensely folded section of Mississippian Lombard Limestone and Conover Ranch Formations. The second package, contained in the hanging wall of the Deadwood Gulch thrust, comprises relatively unfolded, flat lying Lombard Limestone and Conover Ranch Formations.

The McKnight Canyon traverse is located the furthest north along strike in the Tendoy thrust sheet (Figure 2). The Tendoy fault is exposed at this location; samples collected immediately above the fault in the hanging wall (Figure 6). The Lombard Limestone is highly brecciated adjacent to the fault.

Two sampling traverses were located further west in the Four Eyes Canyon and Medicine Lodge thrust sheets (Figure 2). The easternmost traverse in the Four Eyes Canyon (Figures 2 and 7) consists of tightly folded limestone. Further west, in the rear of the Four Eyes Canyon thrust sheet and adjacent to the Medicine Lodge thrust sheet, are a series of folded limestone beds (Figures 2 and 8). Sampling at this site in the Four Eyes Canyon was conducted in one anticline on both limbs and in the hinge region. Several samples were taken from the Medicine Lodge thrust. All sampling traverses were positioned to investigate spatial and temporal variation in fluids as well as to study the effect of varying structural positions on fluids and fluid flow.

Stereographic analysis was used to establish the structural framework in which veins were formed in the Tendoy thrust sheet. Due to similarities seen in structural

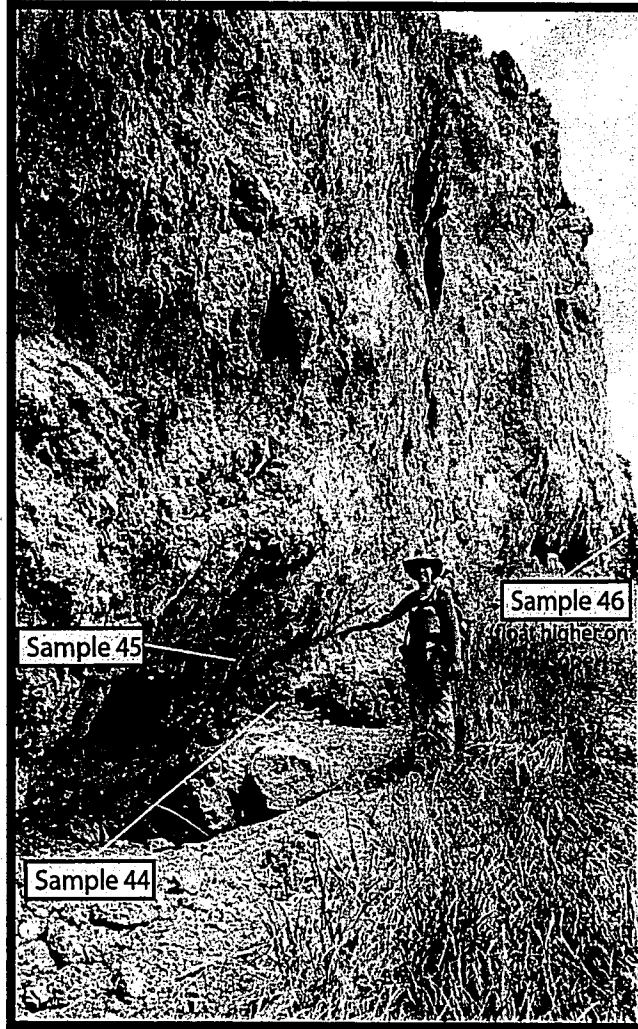


Figure 6. The exposure of the Tendoy thrust fault at the McKnight Canyon traverse. Brecciated zone in the hanging wall of the fault.

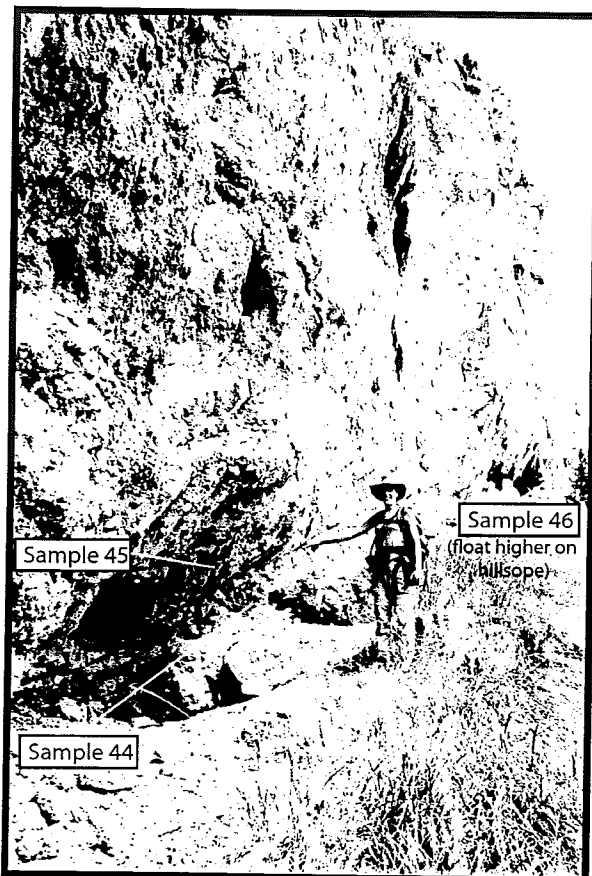


Figure 6. The exposure of the Tendoy thrust fault at the McKnight Canyon traverse. Brecciated zone in the hanging wall of the fault.

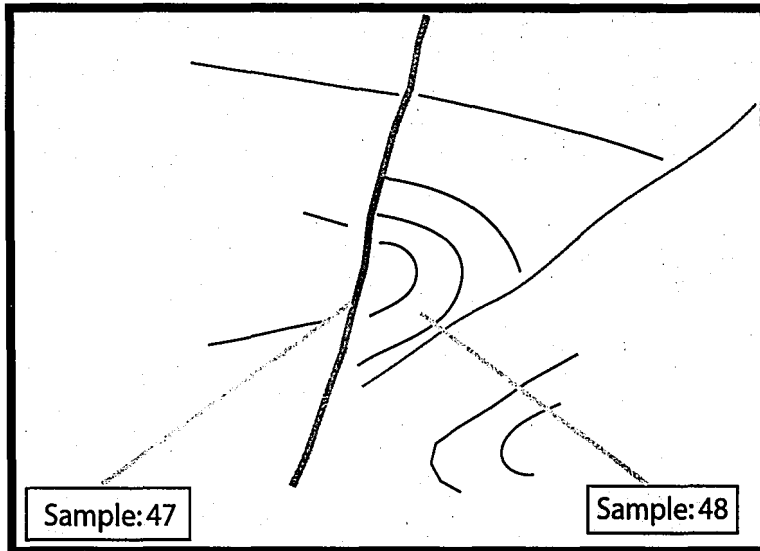


Figure 7. Photograph and tracings of sampling traverse in eastern part of the Four Eyes Canyon thrust sheet. Near vertical veins cut across Cretaceous compressional structures.

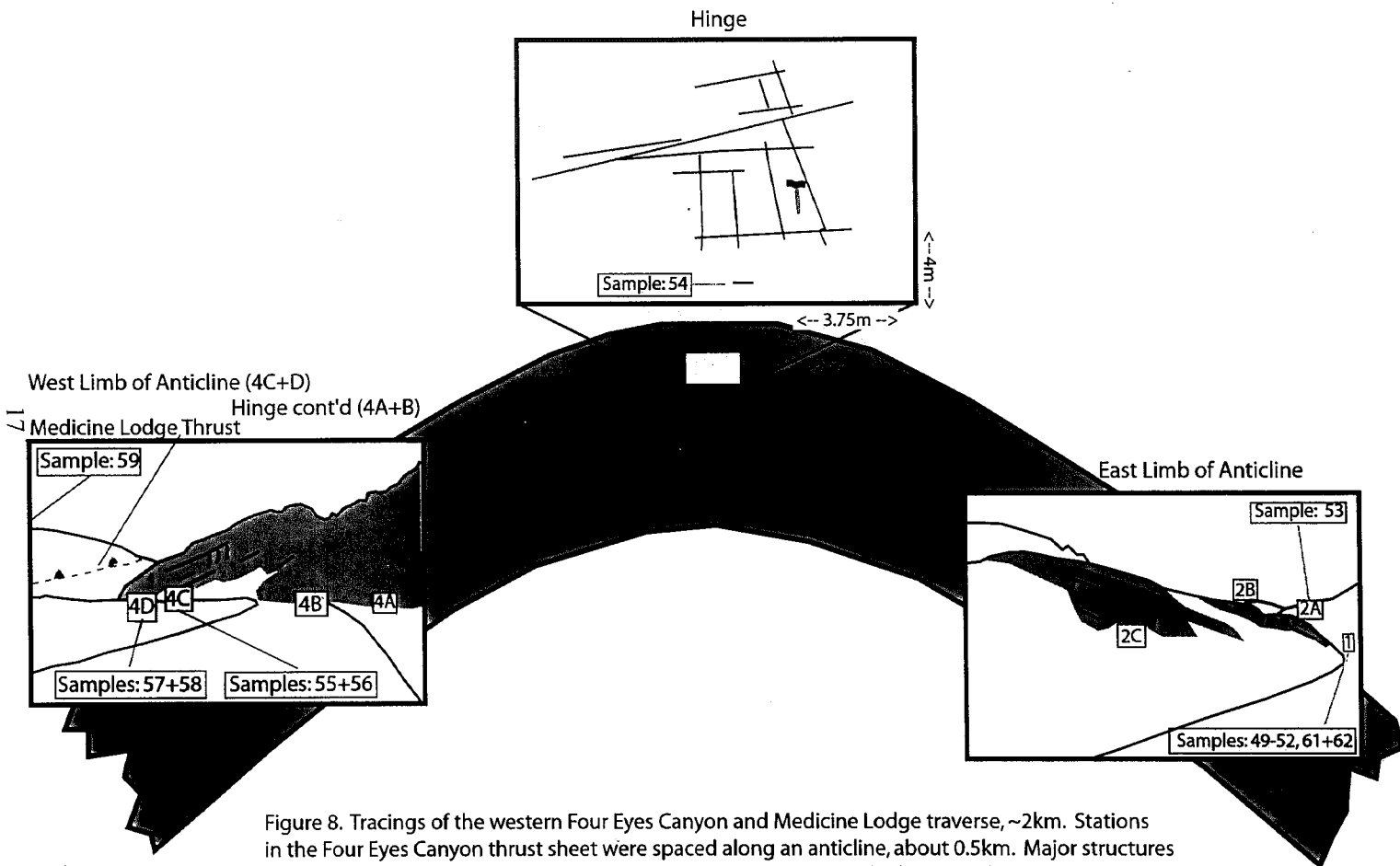


Figure 8. Tracings of the western Four Eyes Canyon and Medicine Lodge traverse, ~2km. Stations in the Four Eyes Canyon thrust sheet were spaced along an anticline, about 0.5km. Major structures are shown as well as cross-cutting relationships between veins in the hinge of the anticline.

styles of sample traverses, poles to all beds within the Tendoy thrust sheet were plotted on a single stereoplot (Figure 9A). A cylindrical best fit to the data indicates an overall fold axis to folds in the Tendoy thrust sheet to have a trend and plunge of $322^{\circ}, 06^{\circ}$, which is consistent with NE emplacement of thrust sheets and northeast verging symmetric, upright, horizontal folds. The cylindrical, open folds are second to third order folds. In the Four Eyes Canyon and Medicine Lodge thrust sheets the general structural grain is similar to that of the Tendoy thrust sheet with a fold axis oriented $330^{\circ}, 13^{\circ}$ (Figure 9B).

Vein Genesis

Veins are major fluid conduits in the fluid flow system of an orogen. They record the paleohydrology of the resulting mountain belts. The geometry of veins is dependent on the strain history of the deforming orogen. In order to piece together the evolution of fluid pathways it is necessary to understand vein set orientations and crosscutting relationships between veins of different orientations (Appendix 4). Orientation analyses were conducted to determine the number and timing of vein sets. Petrographic analyses established how the fractures opened and sealed.

Vein Morphology

Veins observed in the sample sites were either composed of a single layer or generation of flow (Figure 10A) or had multiple flow opening and filling histories (Figure 10B). In some instances, textural and color variation between layers indicates

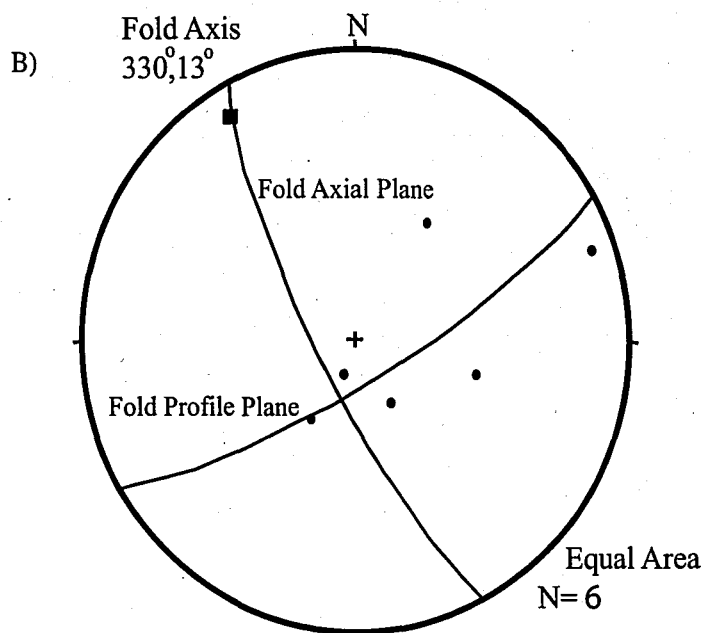
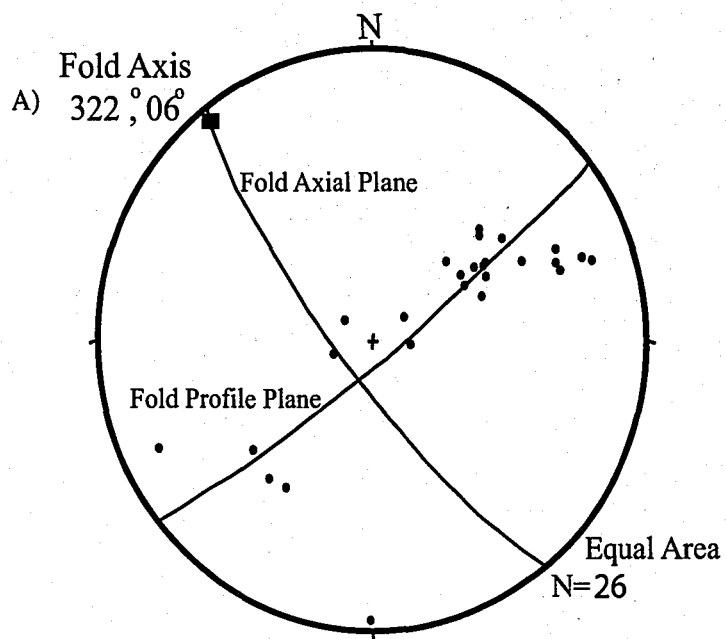


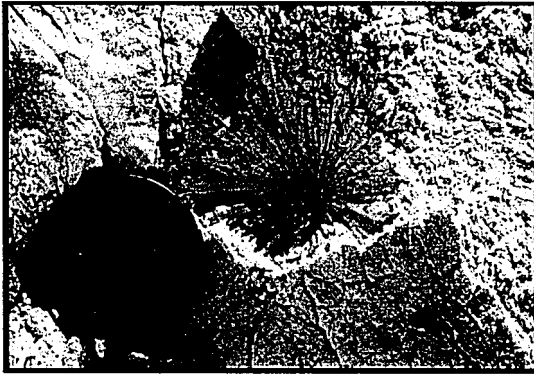
Figure 9. A) Stereoplot of poles to bedding in the Tendoy thrust sheet.
B) Stereoplot of poles to bedding in the Four Eyes Canyon and Medicine Lodge thrust sheets.



A)



B)



C)



D)



E)

Figure 10. A) Single layered vein, 3mm wide. B) Multi-layered vein - each layer represents a different period of flow, different layers have textural and color variation. C) Fibrous bundle (starburst) of calcite growing off of a host-rock inclusion within one of the layers of a multi-layered vein. D) Longitudinal (left to right) and transverse (up and down) systematic vein sets (hammer for scale). E) Randomly orientated, nonsystematic veins found in brittle deformation zones of thrust fault hanging walls (1mm wide veins).

that these multi-layered veins consist of up to 12 generations of flow. Within some individual layers there are wall rock fragments of limestone protolith. Associated with these inclusions are elongate bundles of calcite crystals radiating away from the clast (Figure 10C). These clasts behaved as nucleation sites for calcite crystal growth, producing "starburst" structures of calcite ranging anywhere from 1 cm to 8 cm in diameter depending on the size of the clast. Clearly, fluid pathways must have been wide enough to allow free floating clasts and the growth of radiating crystal bundles.

Field observations revealed five vein sets: bed-parallel veins; longitudinal, high angle veins striking parallel to structural grain (see Figure 9); transverse, high angle veins trending in the dip direction (see Figure 9); and a steep near vertical to irregular set that cut across compressional structures. The longitudinal and transverse sets are regularly spaced and very prominent (Figure 10D). Bed-parallel veins are associated with folds and are not found in flat-lying beds (e.g. the Big Sheep Creek-Deadwood Gulch packages). Several crosscutting relationships were observed between vein sets. In the Tendoy thrust sheet the longitudinal and transverse sets mutually crosscut one another, and they are both cut by the bed parallel shear veins. In the Four Eyes Canyon and Medicine Lodge thrust sheets longitudinal, transverse, and bed-parallel veins mutually cross-cut one another. Near vertical veins cut all previously mentioned veins and all other compressional structures. In several instances at the western Four Eyes Canyon/Medicine Lodge traverse veins of irregular orientation were observed cutting through beds; occasionally these veins reoccupy the paths of preexisting longitudinal, transverse, and bed-parallel veins (Figure 11). In the

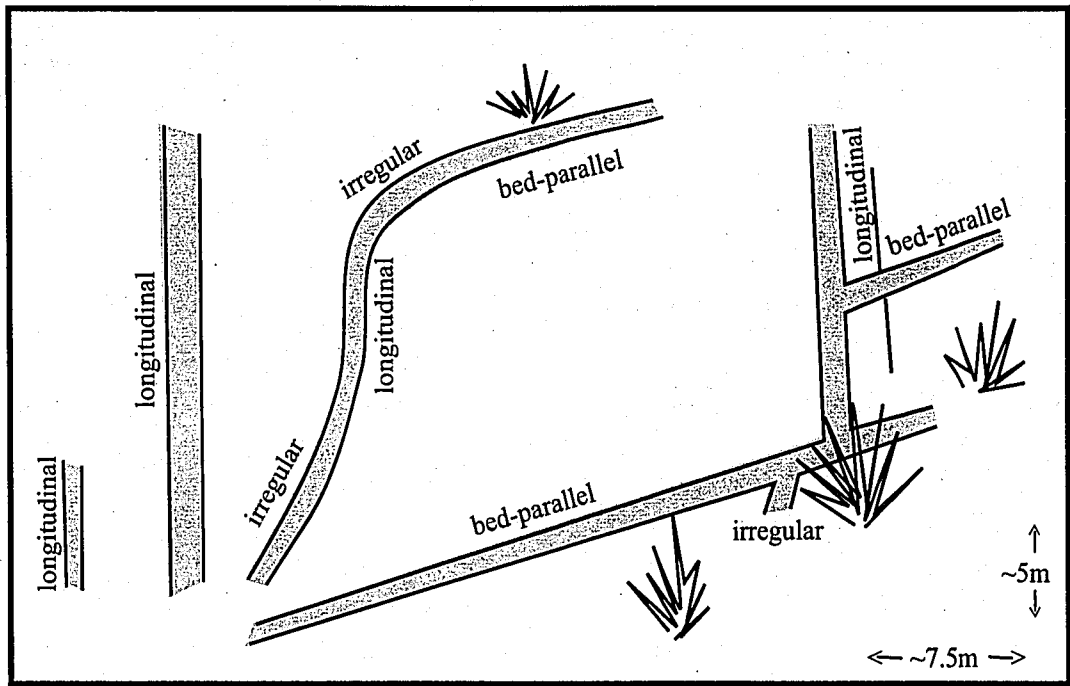


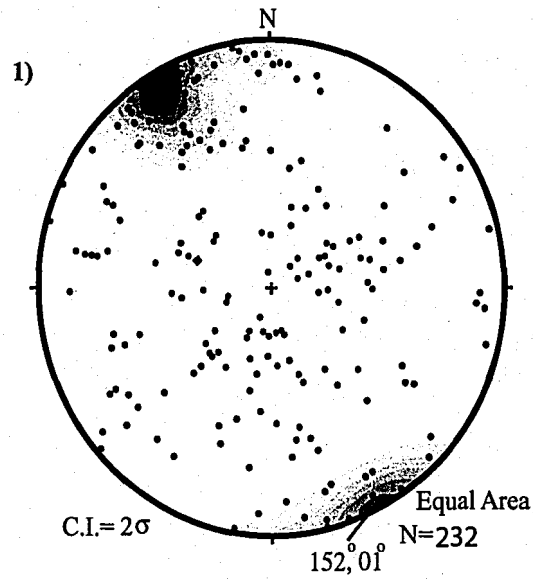
Figure 11. Schematic sketch of irregular veins in the western portion of the Four Eyes Canyon thrust sheet. One set is observed flowing into another and in some cases a vein will be randomly oriented and then join with another vein, like the bed-parallel veins.

immediate hanging-wall of the major thrust faults, a network of thin (~1 mm), randomly oriented veins occupy fractures caused by shattering of bedrock in the brittle deformation zones (Figure 10E). These veins were omitted from the following analyses.

Kinematics of Vein Development

The orientations of over 200 veins were analyzed stereographically in order to constrain the evolution of fluid pathways throughout the different stages of deformation (Appendix 5). The tightness of concentrations of poles to veins was assessed in both the current (geographic) position and in the original (stratigraphic) position. This type of analysis was used to evaluate and distinguish vein sets

Field observations suggested the presence of three common vein sets: transverse, longitudinal, and bed-parallel at each locality. Thus, all veins for the Tendoy thrust sheet were analyzed together in their geographic coordinates (Figure 12A). Kamb contouring indicates only a single concentration of poles with a mean orientation of $\sim 152^\circ, 01^\circ$ (Figure 12A-1). This vein set is interpreted as a transverse set because its orientation is close to the dip direction of beds and is parallel to the fold profile plane in the Tendoy thrust sheet (see Figure 9A). However, in the field, this transverse vein set mutually crosscuts a longitudinal, high angle vein set which is oriented parallel to regional strike (Figure 12A-2). Although this longitudinal set is scattered in geographic coordinates, it is concentrated in stratigraphic coordinates (Figure 12A-3). Kamb contours of rotated veins show that there are two distinct



2)

	Tendoy Thrust Sheet
Longitudinal cuts Transverse	9
Transverse cuts Longitudinal	10
Longitudinal cuts Bed-parallel	0
Transverse cuts Bed-parallel	0
Bed-parallel cuts Longitudinal	2
Bed-parallel cuts Transverse	1

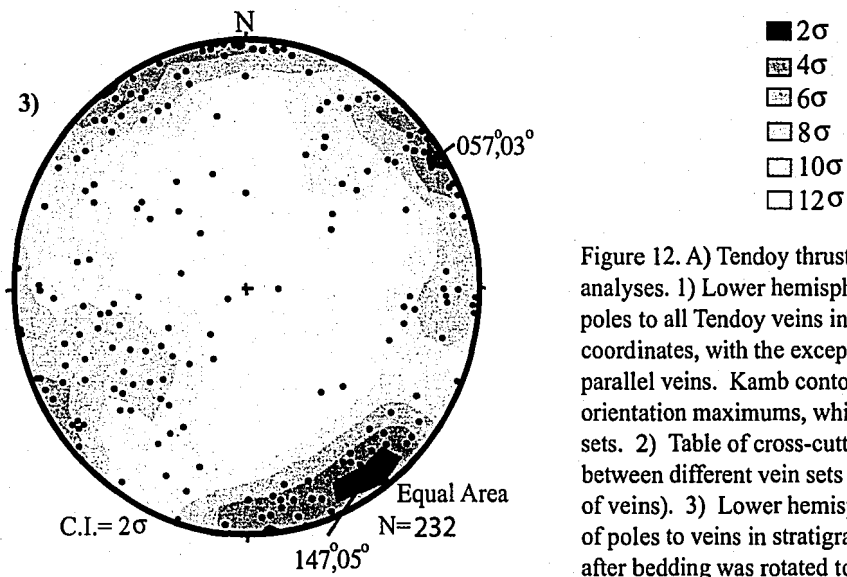


Figure 12. A) Tendoy thrust sheet orientation analyses. 1) Lower hemisphere stereoplot of poles to all Tendoy veins in geographic coordinates, with the exception of bed-parallel veins. Kamb contouring indicates orientation maximums, which represent vein sets. 2) Table of cross-cutting relationships between different vein sets (represents 11% of veins). 3) Lower hemisphere stereoplot of poles to veins in stratigraphic coordinates after bedding was rotated to horizontal.

orientation maximum of veins with mean orientations of 147° , 05° and 057° , 03° . The first orientation maximum is the same transverse vein set. This set is slightly less concentrated than the transverse set because the few veins which were not oriented exactly perpendicular to the fold axis experienced minor amounts of rotation upon returning beds to horizontal. The second orientation maximum is interpreted as a longitudinal set because it has an orientation approximately strike parallel to the fold axial plane (Figure 9A) in the Tendoy thrust sheet. These two sets most likely formed while beds in the Tendoy thrust sheet were still flat-lying. During folding the longitudinal veins underwent reorientation around folds. Bed-parallel shear veins were observed only in folded beds within the Tendoy thrust sheet. During folding bed-parallel shear veins form due to flexural slip along bedding planes. This interpretation is supported by the observation of bed-parallel veins cutting across all transverse and longitudinal veins (Figure 12A-2). Therefore, the bed-parallel vein set is interpreted to have formed during emplacement and folding of the Tendoy thrust sheet. A summary of the kinematics for vein formation during regional Cretaceous compression is shown in Figure 12B for the Tendoy thrust sheet.

In the Four Eyes Canyon and Medicine Lodge thrust sheets vein sets similar to Tendoy sets were observed (i.e. bed-parallel, longitudinal, and transverse sets). In addition, there were high angle veins that cut across all structural features (Figure 7) and veins that were of irregular orientation cutting across structures and at times using preexisting bed-parallel or longitudinal veins (Figure 11). These two types of veins are interpreted to be post-compression veins.

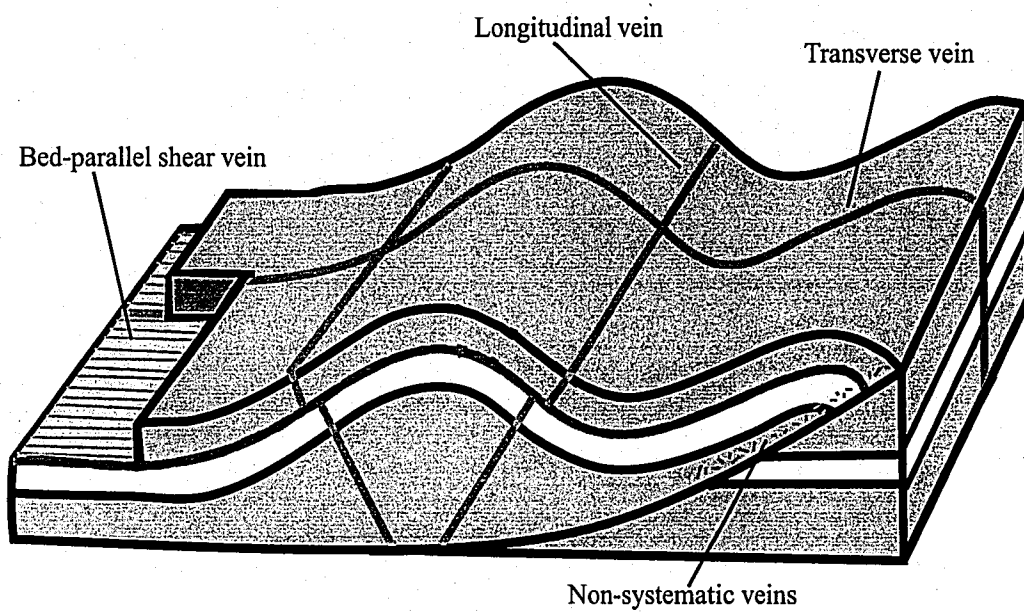
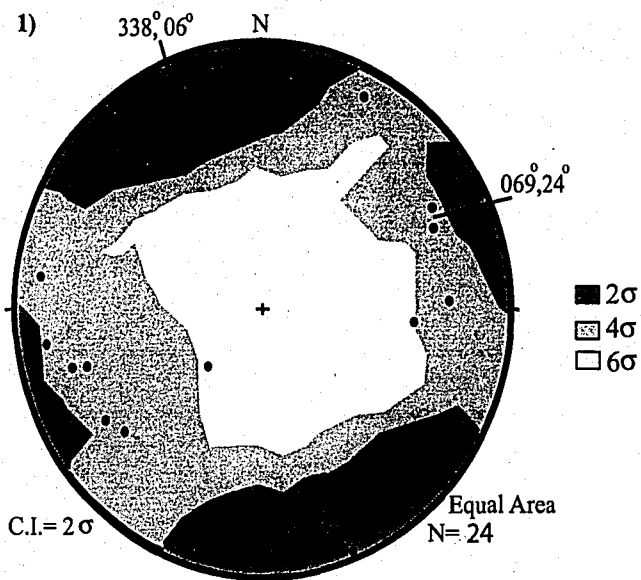


Figure 12. B) Schematic summary of vein sets. A) In the Tendoy thrust sheet longitudinal and transverse veins formed while beds were flay lying. Later, folding and faulting in the Tendoy thrust sheet reoriented these veins and bed-parallel shear veins developed as a result of flexural slip. Non-systematic veins are associated with brittle deformation zones in the immediated hanging wall of thrust faults.

There are two distinct concentrations of data when veins related to Cretaceous compression are plotted with respect to a geographic reference frame (Figure 13A-1). The mean orientations of these two sets are $338^{\circ}, 06^{\circ}$ and $069^{\circ}, 24^{\circ}$. The first concentration is oriented almost perpendicular to the mean fold axes of folds in the Four Eyes Canyon and Medicine Lodge thrust sheets (see Figure 9B) making this set analogous to Tendoy transverse veins. The other set is oriented approximately parallel to the mean structural grain in the region (see Figure 9B), and is thus interpreted as a longitudinal set analogous to Tendoy longitudinal veins. Longitudinal, transverse, and bed-parallel veins are all mutually crosscutting in the Four Eyes Canyon thrust sheet (Figure 13A-2). Based on the higher concentrations of orientation maximum for veins in their geographic coordinates and their crosscutting relationships, these three veins sets formed during folding of the Four Eyes Canyon and Medicine Lodge thrust sheets. Subsequent to Cretaceous compression, irregular veins and high-angle veins were formed (Figure 13A-3). These multi-layered veins are relatively wide and have coarse crystalline textures. Because many of the bed-parallel, longitudinal, and transverse vein sets are multi-layered with textures and widths, they were likely reactivated during this period of later extension. Post-Cretaceous compression veins are found only in the Four Eyes Canyon and Medicine Lodge thrust sheets where there was significant Basin and Range extension and volcanism during the Eocene. The Muddy Creek Graben, other extensional faults, and volcanic deposits are found only in the Four Eyes Canyon and Medicine Lodge thrust sheets and are not present in the



2)

	Four Eyes Canyon + Medicine Lodge
Longitudinal cuts Transverse	6
Transverse cuts Longitudinal	4
Longitudinal cuts Bed-parallel	1
Transverse cuts Bed-parallel	2
Bed-parallel cuts Longitudinal	0
Bed-parallel cuts Transverse	2

- Bed-parallel veins
- ▲ Irregular veins
- Reactivated longitudinal and transverse veins and other high angle veins

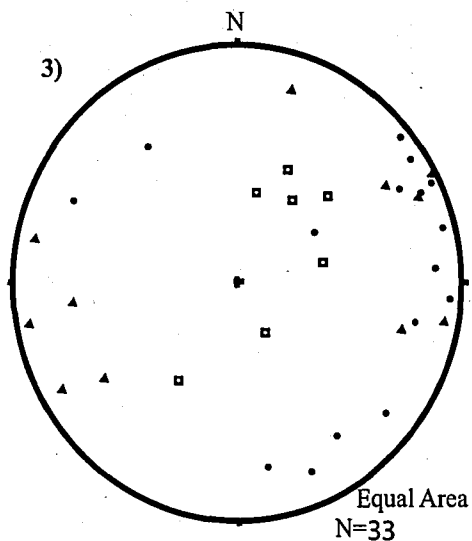


Figure 13. A) Four Eyes Canyon and Medicine Lodge thrust sheets orientation analyses. 1) Lower hemisphere stereoplots of poles to Cretaceous veins, with the exception of bed-parallel veins in geographic coordinates. Kamb contouring indicates orientation maximums, which represent vein sets. 2) Table of crosscutting relationships between different vein sets (represents 8% of veins). 3) Lower hemisphere stereoplots of Eocene veins in geographic coordinates.

Tendoy thrust sheet. Therefore, these vein sets are interpreted to have formed during Eocene extension. A summary of the kinematics of vein formation is shown in Figure 13B for the Four Eyes Canyon and Medicine Lodge thrust sheets.

Textures of Veins

Twenty samples were collected from representative vein sets in the Tendoy, Four Eyes Canyon, and Medicine Lodge thrust sheets. Petrographic analysis of these samples was used to establish filling behavior and to reconstruct the history of these fluid pathways. Most of the Cretaceous Tendoy veins are single-layered veins. In contrast, many of the Cretaceous and Eocene veins in the Four Eyes Canyon and Medicine Lodge thrust sheets are multi-layered.

The majority of veins consist of euhedral crystals that range in size from 120 μ m to 6mm, very few contain elongated crystal fibers (Figure 14A). High fluid pressures would allow wider fractures to form and give the minerals a longer period of time to precipitate larger euhedral crystals as flow would be more continuous (Cosgrove, 2001; Fisher and Brantley, 1992). Some layers consist entirely of fine-grained crystals ranging from 8 to 120 μ m in size (Figure 14A). Generally, fine-grained calcite crystals are found along the walls of the veins from which the larger crystals nucleate (Figure 14B). The smaller crystals, or seed nuclei, which have the preferred crystallographic orientations become larger growing towards the vein center (Fisher and Brantley, 1992). In most cases the crystals were observed to grow from both vein walls towards the center of the vein. Both uni- and bi-directional growth

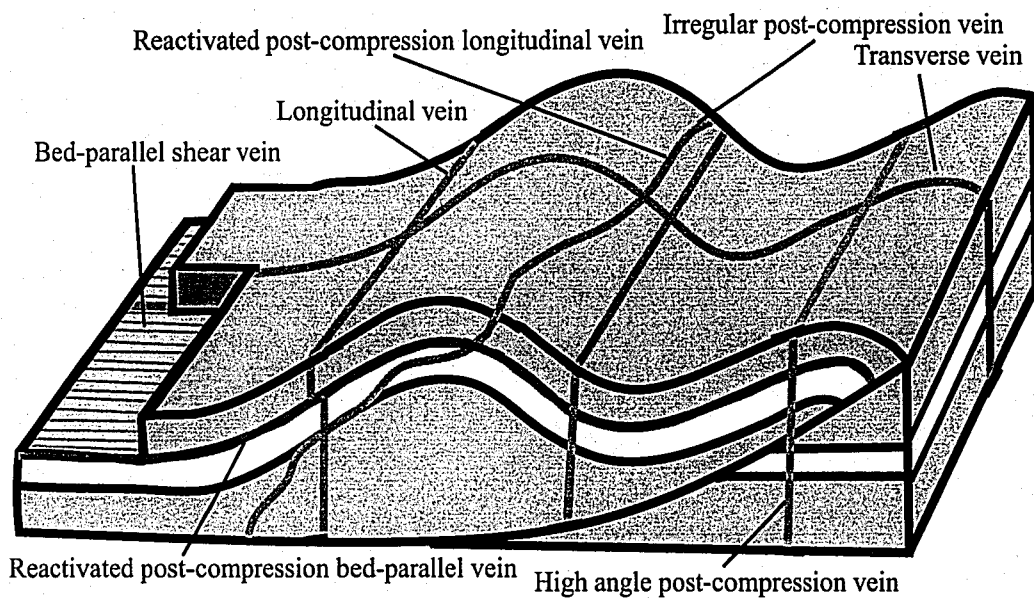
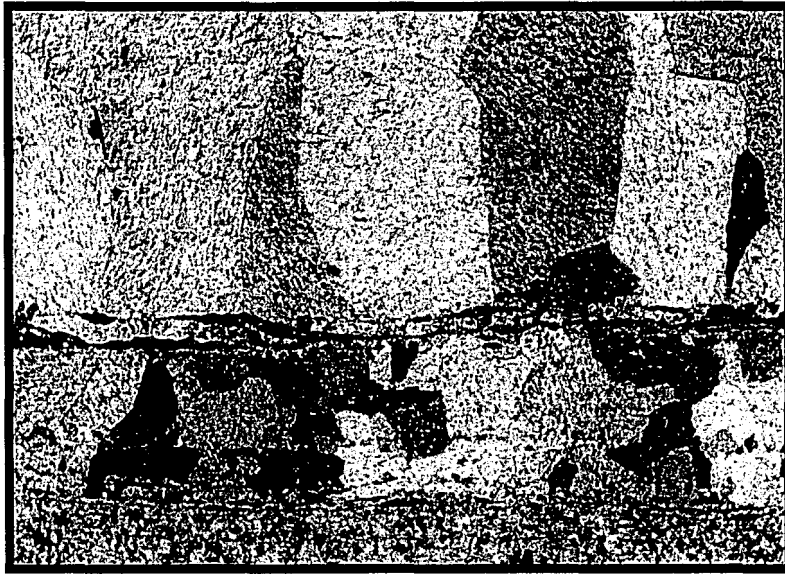
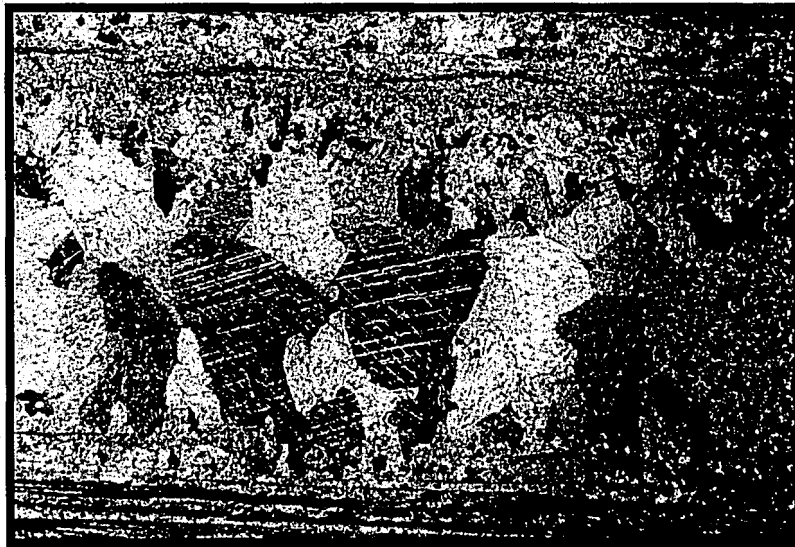


Figure 13. B) Schematic summary of vein sets. In the Four Eyes Canyon and Medicine Lodge thrust sheets longitudinal, transverse, and bed-parallel veins formed during folding and faulting and have mutually cross-cutting relationships. In a post-compression regime some Sevier compressional veins were reactivated and irregular and high angle veins were formed cutting across all compressional structures.



A)



B)

Figure 14. A) Thin section showing multiple layers with differences in crystal size from the smallest crystals which are ~ 8 to $120\mu\text{m}$ and the largest crystals which are $\sim 120\mu\text{m}$ to 6mm in size. B) Multiple layered vein showing bi-directional growth of calcite off of seed nuclei ($\sim 8\mu\text{m}$) on the vein walls inwards towards the center where larger ($\sim 2\text{mm}$ on average) crystals grow. In a few of the larger calcite crystals are twin lamellae in one and two sets.

was observed. One or two sets of calcite twin lamellae are present in most veins. These lamellae are thin and relatively sparse, indicating low amounts of stress and strain (Ferrill, 1991). In the limestone protolith minor amounts of pressure solution were observed as selvages. In several of the multi-generation veins there were rip up clasts of protolith, which were about 2mm in size. In most cases these rip-up clasts act as nucleation sites for calcite radial growth (Lindholm, 1974), similar to what was observed at the macro- scale in the field. The samples collected from the reactivated Four Eyes Canyon veins contained numerous large elongated, sparry crystals. Both the radiating bundles and large sparry crystals indicate that some of the vein layers were conduits for significant volumes of fluid.

Field observations, orientation analysis, and petrographic analysis it has been established that there are several vein sets. These veins formed during both Sevier compression (Cretaceous) and during a later period of extension (Eocene). Similar textures in all vein sets suggests that they all formed via similar processes. Initially fractures of varying width opened. Fractures were then sealed with uni- and bi-directional growth from one or both vein walls. This process occurred several times in the veins containing multiple generations. Vein systems, particularly those with multiple generations, form the framework for isotopic study.

Temperature Constraints and the Presence of Hydrocarbons

Knowledge of the environmental conditions during deformation is key in determining fluid compositions and sources because fluid temperature has a large effect on the fractionation of oxygen between calcite and water at low temperatures. Ferrill (1991) notes that thin twin lamella similar to those observed in the Tendoy Mountains generally indicate rock temperatures less than 200° C. Conodont color alteration index (CAI) values of 1 from the Tendoy thrust sheet indicate temperatures less than 80° C (Epstein et al., 1977; Perry et al., 1981). In addition, vitrinite reflectance values of 0.35% R_o (Perry et al., 1981 and 1983) indicate temperatures of about 51° C (Barker and Pawlewicz, 1994). Perry et al. (1983) interpreted a geothermal gradient of 20° C/km by using vitrinite reflectance data and deep drill-hole temperatures established for the Centennial Basin. A mean surface temperature of 22° C was chosen for temperature calculations (Perry et al., 1983). In order to calculate the rock temperature (via the geothermal gradient), it is necessary to establish the maximum burial depth to the Tendoy, Four Eyes Canyon, and Medicine Lodge thrusts. While vitrinite reflectance and conodont color alteration values suggest shallow burial in the Tendoy thrust sheet, the fault must have been at least 2300 m deep to accommodate the preserved section of Mississippian-Cretaceous rocks. With the addition of a few hundred meters of Cretaceous syntectonic conglomerates (Perry et al., 1983) this suggests a maximum burial depth of ~3 km and a rock temperature of ~82° C. This temperature is broadly consistent with conodont and vitrinite data, both of which develop as a function of both time and temperature. In the Four Eyes

Canyon and Medicine Lodge thrust sheets conodont color alteration values are slightly higher (~1.5). Perry et al. (1983) interpreted these values to record burial depths of ~4 km. Given the CAI values and the estimated geothermal gradient a rock temperature of ~102° C is predicted for the Four Eyes Canyon and Medicine Lodge thrust sheets. Many of the Four Eyes Canyon veins were precipitated after Cretaceous regional compression, during the Eocene. At this time the Mississippian rocks in the hanging walls of the Four Eyes Canyon and Medicine Lodge thrust sheets had been fully emplaced on or near the synorogenic surface. The rocks which were sampled at the surface today could have been as deep as 1-2 km, if assuming low erosion rates of about 1/40 or 1/20 of a millimeter over the last ~40 MA. The paleotemperatures during Eocene deformation are not well constrained. If it were assumed that temperature conditions were the same as during the Cretaceous, regional compression of these rocks probably at temperatures of 42-62° C, for 1-2 km respectively. Volcanism during the Eocene may have raised temperatures as high as 80° C. Fluid temperatures can be different than rock temperatures so fluid inclusions were analyzed.

Fluid inclusion analyses were conducted on samples from the study area, in order to obtain fluid temperature and composition constraints (Appendix 6). Many of the inclusions were clear (either aqueous, calcite, methane, or decrepitated inclusions) without vapor bubbles. However, there were a few inclusions with vapor bubbles that were measured. In general, inclusions were 2-5 μm in size and located along planes or in trains healing microfractures making them secondary inclusions (Roedder, 1984).

Upon heating and cooling the clear inclusions exhibited no phase change and were not useful in finding the homogenization temperature (T_h). However, phase changes did occur in a few inclusions providing two homogenization temperatures. The homogenization temperatures that were obtained from two aqueous fluid inclusions were $+44^\circ\text{C}$ and $+160^\circ\text{C}$. On the lower end, this is consistent with the rock temperatures, but the higher end is 60°C outside rock temperatures expected for the thrust front. While this is too little data to tightly constrain the actual range of fluid temperatures, the values are consistent with low fluid temperatures. Therefore, it will be necessary to assume that fluid temperatures are close to rock temperatures and use the temperatures derived from the CAI values, vitrinite reflectance data, and the geothermal gradient to use as working fluid temperature: $80\text{-}100^\circ\text{C}$ for Cretaceous veins and $40\text{-}80^\circ\text{C}$ for Eocene veins.

Fluid density and salinity can be determined from the measured temperature when melting occurred (T_m) after inclusions were frozen (Roedder, 1984). The lower the temperature is the more saline the fluid. Fluids which can retain their solid phase at temperatures exceeding freezing are metastable superheated ice and indicate very fresh water (Roedder, 1984). The melting temperatures obtained from the Tendoy samples (-0.6 to $+3.6^\circ\text{C}$) indicate the presence of metastable superheated ice, which is low salinity freshwater. Both low temperature and fresh/low salinities are consistent with a meteoric source.

Brown inclusions were found in planar clusters or trains healing microfractures. These brown inclusions were frozen and exposed to ultraviolet

radiation to see if they were petroleum (Burruss, 1981). The brown inclusions in the Tendoy samples are interpreted to be degraded petroleum because they did not develop a vapor bubble nor did they fluoresce (e.g. Roedder, 1984; Burruss, 1981). Because the hydrocarbons heal microfractures in conjunction with the fluids they were probably present in the calcite forming fluid. Methane does not appear to be present because vapor bubbles did not appear upon freezing. Well log data (Amoco, 1986) and organic geochemical analyses (Swetland et al., 1978) do show the presence of methane and high hydrocarbon/organic carbon ratios and of hydrocarbons in the Tendoy Mountains. However, the hydrocarbons were most likely generated in unit(s) other than the Lombard Limestone (Perry et al., 1983). Given the presence of degraded hydrocarbons in the veins, fractures were clearly pathways for both hydrocarbons and freshwater during deformation.

Fluid Compositions and Sources

Stable Isotope Analyses

Stable isotope analyses were conducted on host rocks and systematic veins found in the Tendoy, Four Eyes Canyon and Medicine Lodge thrust sheets (Appendix 7). Microsamples of calcite vein material and carbonate protolith representing the different deformational stages were analyzed for oxygen and carbon isotopes following McCrea's techniques (1950) and the resulting CO₂ gases were analyzed on the Finnigan MAT 252 at Lehigh University. Oxygen and carbon were reported relative to the Vienna standard mean ocean water (V-SMOW) and PeeDee

Belemnite (PDB), respectively, and reported in the standard notation of ‰ after the following:

$$\delta^{18}\text{O} = 1000\left[\left(\frac{^{18}\text{O}/^{16}\text{O}}{^{18}\text{O}/^{16}\text{O}}\right)_{\text{sample}} / \left(\frac{^{18}\text{O}/^{16}\text{O}}{^{18}\text{O}/^{16}\text{O}}\right)_{\text{standard}} - 1\right] \quad (1)$$

$$\delta^{13}\text{C} = 1000\left[\left(\frac{^{13}\text{C}/^{12}\text{C}}{^{13}\text{C}/^{12}\text{C}}\right)_{\text{sample}} / \left(\frac{^{13}\text{C}/^{12}\text{C}}{^{13}\text{C}/^{12}\text{C}}\right)_{\text{standard}} - 1\right] \quad (2)$$

Standardization of oxygen and carbon results was verified using known laboratory standards (calcite 8-3-7v-CO₃ and international carbonate standards).

Analyses of undeformed host-rocks and microlithons and selvages in deformed samples (Figure 15A) show high $\delta^{18}\text{O}$ values (between +20‰ and +27‰) and a wide range of $\delta^{13}\text{C}$ values (+0.6 to +5.6‰). Values for undeformed host-rocks (host-rocks showing no obvious penetrative deformation or cleavage formation) overlap with values for microlithons and selvages in deformed rocks. The smaller number of selvages shows a more restricted range in $\delta^{13}\text{C}$. Overall, tie lines from veins to their respective host-rocks (Figure 15B) show that there is a systematic shift from ^{13}C and ^{18}O -enriched host-rocks to lower $\delta^{18}\text{O}$ and lower $\delta^{13}\text{C}$ veins, with only a few exceptions.

Significant variation is seen in both $\delta^{18}\text{O}$ and $\delta^{13}\text{C}$ of microsampled calcite from Cretaceous Tendoy veins, Cretaceous Four Eyes Canyon and Medicine Lodge veins, and Eocene Four Eyes Canyon and Medicine Lodge veins (Figure 16). The Cretaceous Tendoy veins show the largest variation in $\delta^{13}\text{C}$, ranging from -0.9 to +4.8‰ (Figure 16A-1). The Cretaceous Tendoy veins also show the most significant variation in $\delta^{18}\text{O}$ from +8.9 to +28.8‰. The more $\delta^{18}\text{O}$ -enriched veins have values similar to those of the undeformed host-rocks. Analysis of the different vein sets in the

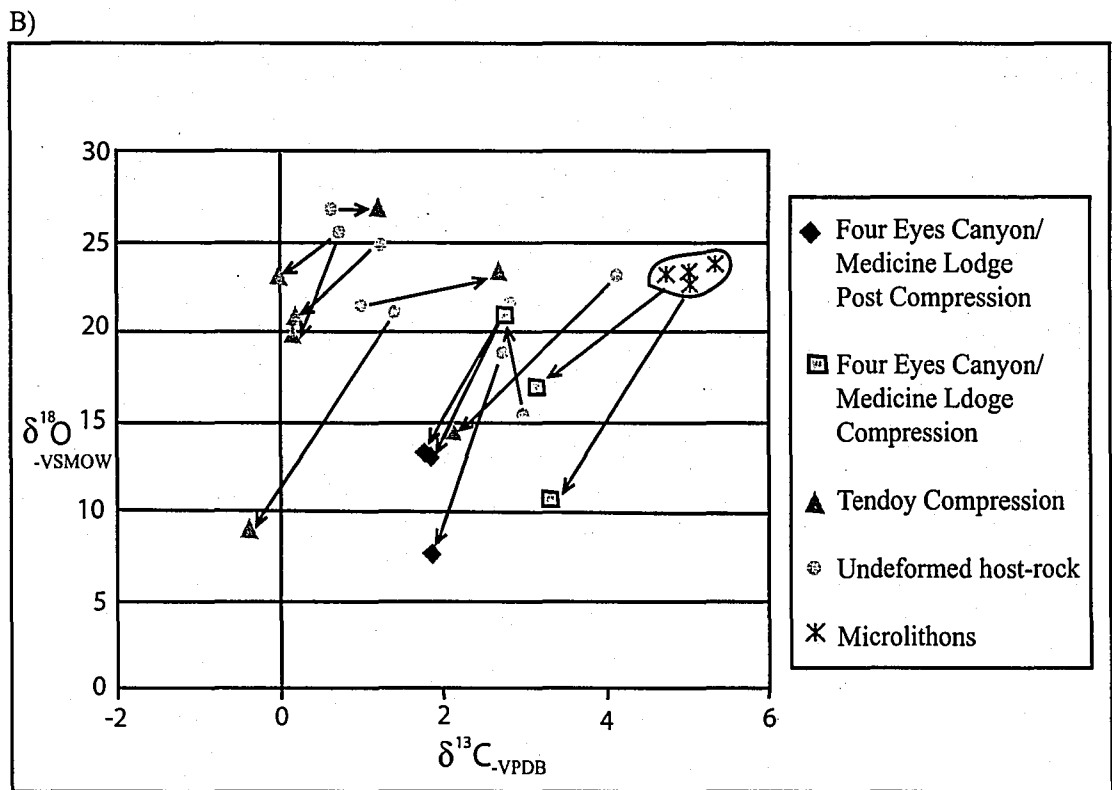
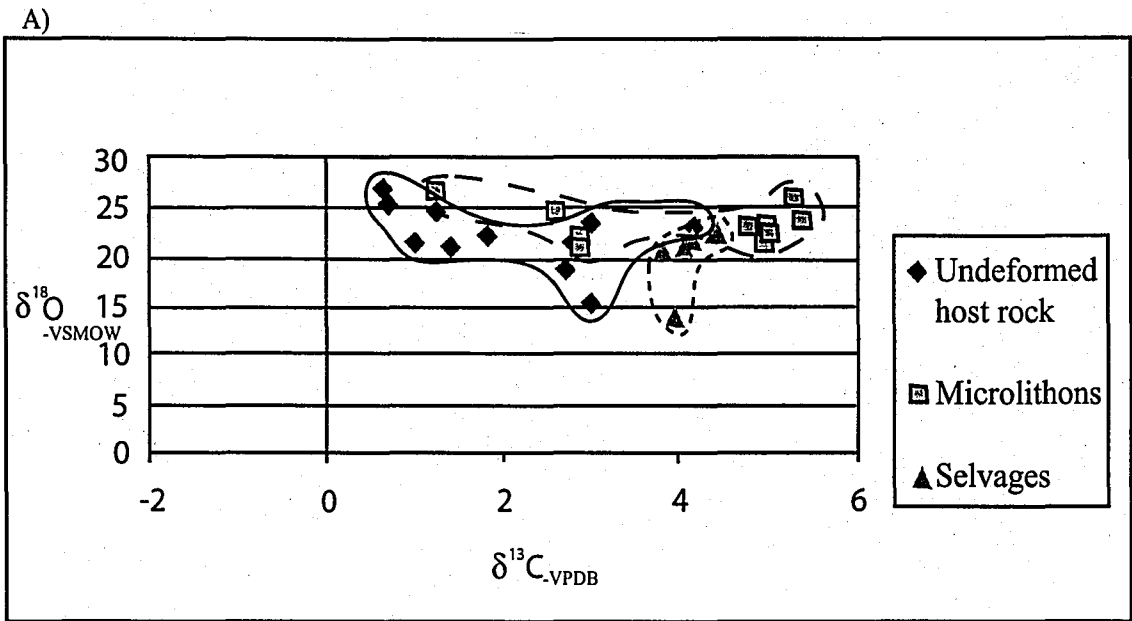
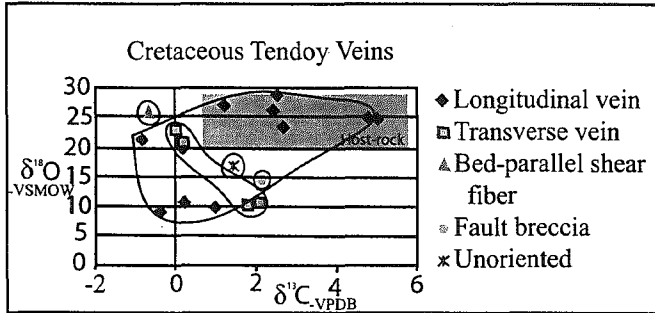
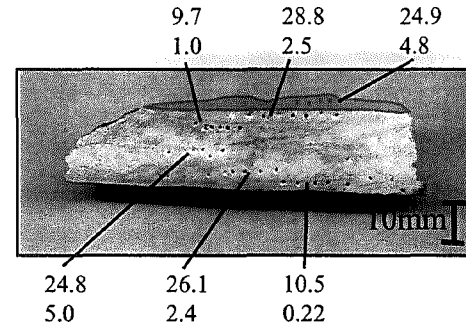


Figure 15. A) Undeformed host-rock and microlithons and selvages in deformed samples have compositions with a mean of +22.2 and a standard deviation of +/- 3‰. This range is shown on other plots as a shaded region. B) Tie lines between host-rock and corresponding veins.

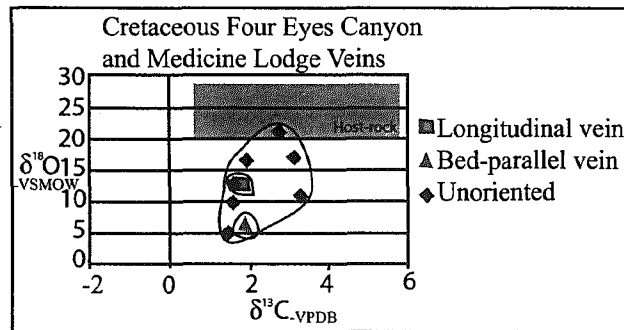
A) 1)



2)



B) 1)



2)

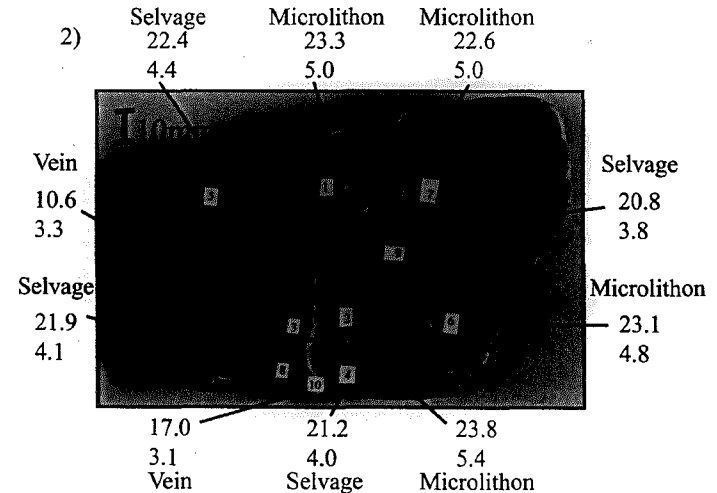


Figure 16. A) Cretaceous Tendoy veins. 1) Plot of all Tendoy thrust sheet isotope data. 2) Sample from the Tendoy thrust sheet. B) 1) Cretaceous Four Eyes Canyon and Medicine Lodge isotope data. 2) Sample from the Four Eyes Canyon (Chizmadia and Bebout, unpublished data) samples of microlithons, selvages, and vein.

Key for Multi-layered Veins
 $\delta^{18}\text{O} = 9.7\text{‰}$
 $\delta^{13}\text{C} = 1.0\text{‰}$

Tendoy thrust sheet (Figure 16A-1) was conducted in order to identify any distinct variation among the different sets, which formed at different periods in the Tendoy thrust sheet's deformational history. Veins related to pre-Tendoy folding and faulting (longitudinal and transverse) show significant variation in $\delta^{18}\text{O}$ and $\delta^{13}\text{C}$. The longitudinal veins have the largest range in $\delta^{18}\text{O}$ and $\delta^{13}\text{C}$. Bed-parallel shear fibers and fault breccia fall within the range of the pre-Tendoy deformation veins. Bed-parallel shear fibers have high $\delta^{18}\text{O}$ values, in the range of undeformed host rock, while the fault breccia has somewhat lower $\delta^{18}\text{O}$. A single Cretaceous Tendoy multi-layered vein has two distinct calcite isotopic compositions differing by about +15‰ in $\delta^{18}\text{O}$ (Figure 16A-2). Both $\delta^{18}\text{O}$ and $\delta^{13}\text{C}$ have systematic shifts from higher to lower values along the traverse.

The Cretaceous Four Eyes Canyon and Medicine Lodge veins have $\delta^{18}\text{O}$ values of +5.2 to +20.9‰ (Figure 16B-1). Overall, the veins in the Four Eyes Canyon/Medicine Lodge traverse show lower $\delta^{18}\text{O}$ and a smaller range of $\delta^{13}\text{C}$ when compared to the Tendoy veins. Orientation analysis revealed that the Four Eyes Canyon and Medicine Lodge vein sets formed during folding and faulting of these two thrust sheets (Figure 16B-1). The bed-parallel vein, which is dilatent, has significantly lower $\delta^{18}\text{O}$ than the bed-parallel shear vein analyzed in the Tendoy thrust sheet (see Figure 16A-1). A longitudinal vein has $\delta^{18}\text{O}$ lower than undeformed host-rock and within the range of other Four Eyes Canyon, Medicine Lodge, and Tendoy veins. A Cretaceous Four Eyes Canyon specimen was collected in a previous study (L.

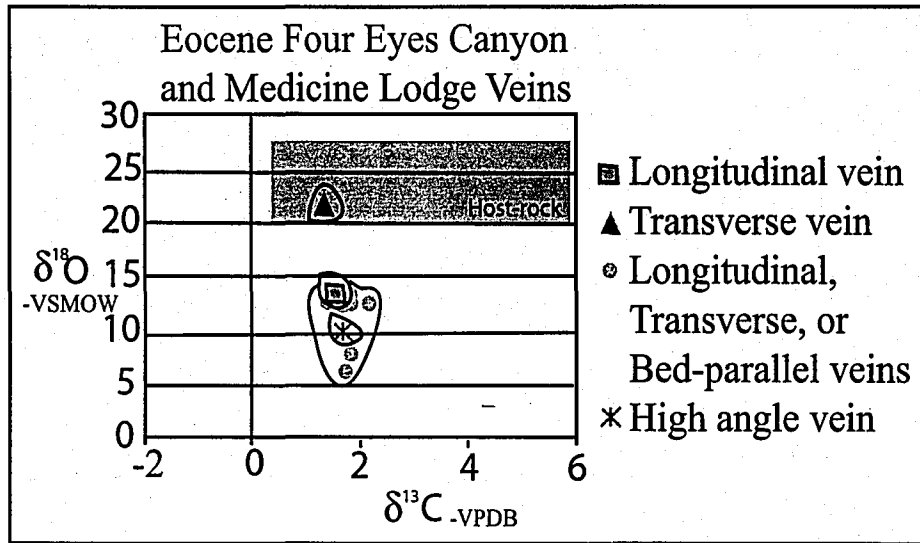
Chizmadia and G. Bebout, unpublished data) and includes ten microdrilled samples of microlithons, selvages, and vein material (Figure 16B-2). There are two distinct vein compositions and there is the same shift from higher $\delta^{18}\text{O}$ and $\delta^{13}\text{C}$ in microlithons to lower values in selvages and even lower values for the two veins in this sample.

The Eocene Four Eyes Canyon and Medicine Lodge veins have $\delta^{18}\text{O}$ values of +5.9 to +21.6‰, but mostly less than +15‰ (Figure 16C-1). Generally, there is much less variation in $\delta^{18}\text{O}$ and $\delta^{13}\text{C}$ than for the Cretaceous veins. An Eocene multi-layered vein from the Four Eyes Canyon thrust sheet was also analyzed (Figure 16C-2). This vein had layers of uniform composition. There is a systematic shift from undeformed host-rock with high $\delta^{18}\text{O}$ to lower $\delta^{18}\text{O}$ in veins. Data for an Eocene sample (either longitudinal or transverse, not determined) collected from an earlier study in the Medicine Lodge thrust sheet are shown in figure 16C-3. Two distinct vein isotopic compositions are observed and there is the same systematic shift from higher $\delta^{18}\text{O}$ and $\delta^{13}\text{C}$ undeformed host-rock to lower $\delta^{18}\text{O}$ and $\delta^{13}\text{C}$ in veins.

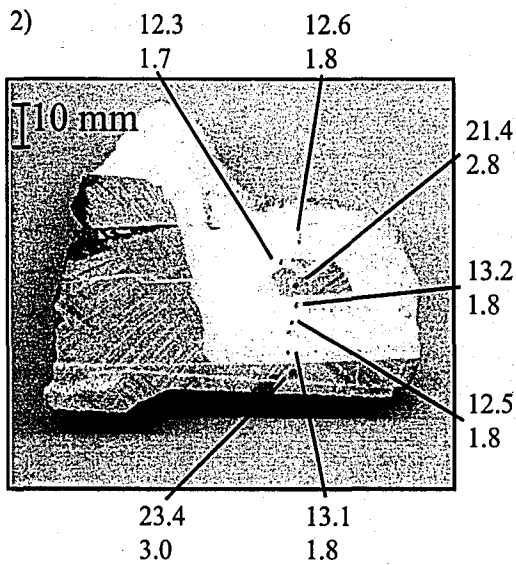
Interpretation of Isotopic Results

In general, undeformed host rock, microlithons, and selvages have ^{18}O -enriched compositions (+20 to +27‰), which are consistent with values characteristic of marine carbonate rocks (Bebout et al., 2001). The variation in carbon is possibly related to the presence of hydrocarbons in the Mississippian carbonate rocks (Perry et al., 1983). There is a great deal of variation in the oxygen and carbon isotope compositions of the veins studied. The ranges of isotopic compositions are fairly

1)



2)



3)

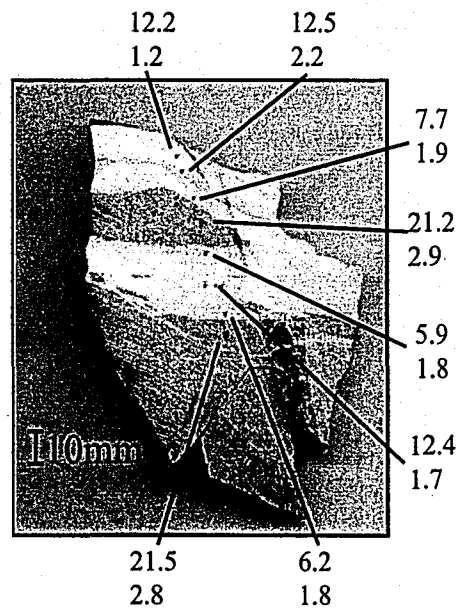


Figure 16. C) Eocene vein stable isotope results. 1) Eocene vein data for the Four Eyes Canyon and Medicine Lodge thrust sheets. 2) Sample from the Four Eyes Canyon thrust sheet. 3) Sample from the Medicine Lodge thrust sheet, taken in an earlier study, either longitudinal or transverse.

Key for Multi-layered Veins

$$\delta^{18}\text{O} = 12.3\text{‰}$$

$$\delta^{13}\text{C} = 1.7\text{‰}$$

similar for the Cretaceous and Eocene veins, although the Cretaceous veins have the largest range for both oxygen and carbon. This range of compositions for both isotopes was observed in each of the thrust sheets, vein sets, and in several multi-layered veins. That is, there is no distinct segregation of compositions between any given thrust sheet or vein set.

Overall, there is a systematic shift from ^{13}C - and ^{18}O -enriched host-rock to lower $\delta^{18}\text{O}$ and $\delta^{13}\text{C}$ veins as seen in the tie lines connecting veins to their respective host-rocks. This implies that the fluids were not equilibrating with the host-rock and is consistent with open-system behavior. The one exception is a bed-parallel shear vein found in the Tendoy thrust sheet. This fibrous vein has $\delta^{18}\text{O}$ compositions very similar to undeformed host-rock indicating a closed system and local diffusion of material along that particular bed plane consistent with vein texture (e.g. Durney, 1972).

The large range in $\delta^{18}\text{O}$ may be due to varying degrees of fluid-rock interactions which may have occurred as the more ^{18}O -depleted fluids interacted with the more ^{18}O -enriched carbonate rock (Nesbitt and Muehlenbachs, 1989 and 1991). As the fluid flowed through the fractures it and the host rock attempted to equilibrate through an exchange of oxygen and carbon isotopes. Depending on the degree of fluid-rock interaction, some fluids fully equilibrated with the host rock (veins with $\delta^{18}\text{O}$ values $> 20\text{‰}$) while others remained more depleted in ^{18}O (values with $\delta^{18}\text{O}$ values $< 20\text{‰}$). Less fluid-rock interactions (low $\delta^{18}\text{O}$ values) may result from

influxes of fluid into the system (Rye and Bradbury, 1988). This is seen in the bed-parallel vein found in the Four Eyes Canyon thrust sheet, which is not a fibrous vein, but is in fact dilatant and part of the open system of fluid flow with low $\delta^{18}\text{O}$. The relatively low $\delta^{18}\text{O}$ value for the fault breccia found in the hanging wall of the Tendoy thrust fault is also consistent with large volumes of fluid per volume of rock in the fault zone.

Fluid Sources

Open system behavior leaves several choices for fluid sources (see Figure 1). Any available fluids from deeper sources would have been capable of producing heavier vein $\delta^{18}\text{O}$. Magmatic fluids have $\delta^{18}\text{O}$ values of +5 to +10‰ (Sheppard, 1996) and metamorphic fluids generally have higher $\delta^{18}\text{O}$ values, up to +20‰ (Nesbitt and Muehlenbachs, 1989 and 1991). However, the possibility of deeper magmatic or metamorphic fluids seems unlikely since there are no igneous or metamorphic rock units found in the hanging walls and footwalls of the Tendoy, Four Eyes Canyon, and Medicine Lodge thrust sheets (see Figure 4) (McDowell, 1992 and 1997; Perry et al., 1988) and values of magmatic fluids would have been inadequate.

Although a number of factors could have caused the higher $\delta^{18}\text{O}$ values, it is possible to draw conclusions about fluid sources from the minimum $\delta^{18}\text{O}$ values. Using calcite- H_2O fractionation factors (O'Neil, 1996) fluid compositions were calculated from the vein $\delta^{18}\text{O}$ values, for the various temperature ranges calculated. During the Cretaceous minimum $\delta^{18}\text{O}$ for fluids generally are around -11‰ to -9‰,

calculated for 80° C and 100° C respectively, near the -7.5‰ values of Bebout et al. (2001). Eocene minimum values are typically between -19‰ and -13‰ (calculated for 40° C and 80° C respectively) and are significantly lighter than the compressional fluids. These values for the Cretaceous and Eocene (both of which are far lower than those for magmatic and metamorphic fluids) could reflect the compositions of meteoric water at low temperatures (Kendall et al., 1969; Nesbitt and Muehlenbachs, 1989 and 1991). Bebout et al. (2001) found similar fluid values for Sevier compressional veins in the Lost River Range, Idaho further west in the hinterland, -7.5 to +2.5‰ (150° C to 250° C), which have also been interpreted as influxes of meteoric water.

Paleohydrology Reconstruction

Results from kinematic, textural, and stable isotope analyses can be synthesized to provide insight into the source of the meteoric water and the paleohydrology of the Tendoy, Four Eyes Canyon, and Medicine Lodge thrust sheets. Ocean water by definition has a composition of 0‰ and nearshore fluids can have oxygen isotope values not much lower, e.g. -5‰ (Kendall et al., 1969). Continual precipitation results in depletion of oxygen isotopes from clouds (see Figure 1) to as low as -16‰ in the Rocky Mountains (Figure 17) (Siegenthaler, 1979; Yurtsever and Gat, 1981). The regional, late Cretaceous compression, which folded and emplaced the Medicine Lodge, Four Eyes Canyon, and Tendoy thrust sheets also caused veining (Kalakay, 2001). During the period of frontal thrust emplacement, the Western

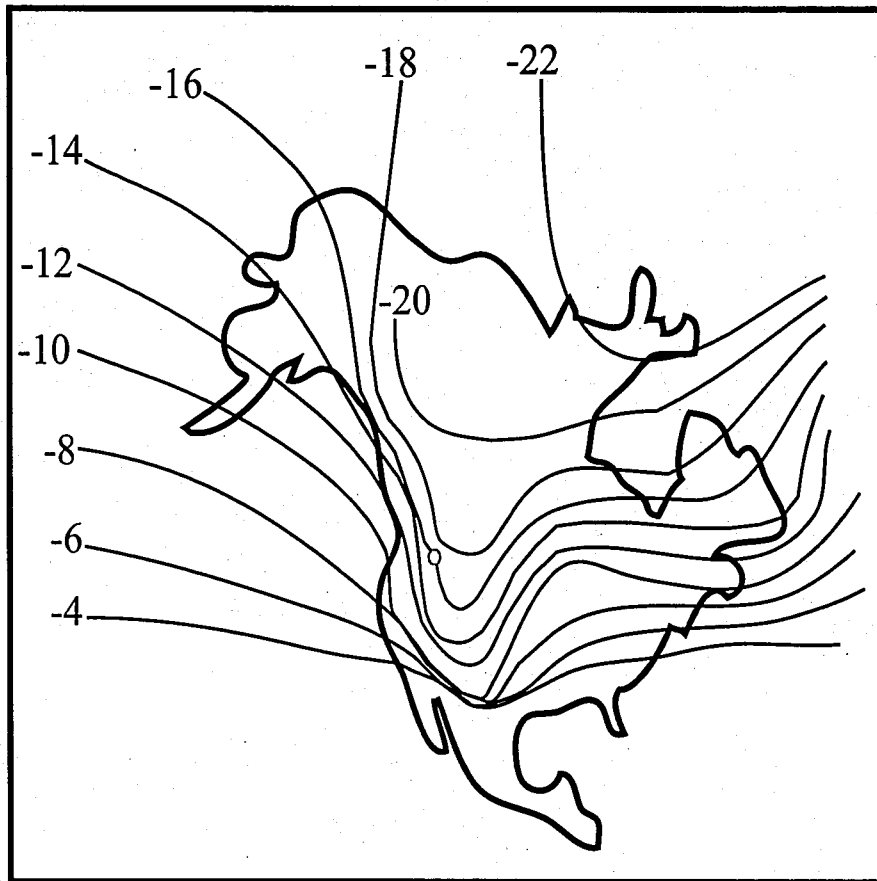


Figure 17. A map of North America showing modern variations in $\delta^{18}\text{O}$ in relation to proximity to the shoreline (modified from Yurtsever and Gat, 1981) with approximate location of the study area in the circle.

Interior Seaway was positioned about 100 km to the east of the study area (Figure 18A). In addition, in the Later Cretaceous the Pacific Ocean was further inland than it is at present. Isotope analyses of $\delta^{18}\text{O}$ for calcareous, phosphatic, and siliceous skeletal material show that isotope compositions of the Western Interior Seaway varied greatly due to eustatic fluctuations and freshwater influxes (from -8 to -1‰) (Cadrin et al., 1995; Cadrin, 1992; Whittaker et al., 1987). During emergence of the thrust sheets the seaway had $\delta^{18}\text{O}$ values of -1‰ (Whittaker et al. 1987), values similar to modern ocean water. Paleoclimate reconstructions show that northern hemisphere circulation and storm tracks were from northwest to southeast across the North American continent (e.g. Kump and Slingerland, 1999; Jewell, 1996; Sageman et al., 1996; Slingerland et al., 1996; Ericksen and Slingerland, 1990) resulting in high volumes of rain on the emerging thrust sheets (e.g. Jewell, 1996). The minimum values found for Cretaceous fluids of -11 to -9‰ (for 80°C and 100°C respectively) are consistent with evolved fluids, the majority of which probably originated from the Pacific Ocean and possibly some less evolved fluids from the Western Interior Seaway (Kendall et al., 1969; Siegenthaler, 1979). The evolution of fluids from -7.5‰ in the Lost River Range to -11 or -9‰ for the Tendoy Mountains is consistent with west-east atmospheric circulation and storm paths coming from the Pacific Ocean.

Movement along detachment faults further hinterland in eastern Idaho have been dated with $^{40}\text{Ar}/^{39}\text{Ar}$ thermochronology of the Pioneer core complex to be Eocene-Oligocene in age, during which time there was hydrothermal activity and fluid flow in that region (Silverburg, 1990). Studies of the Eocene Idaho Batholith and the

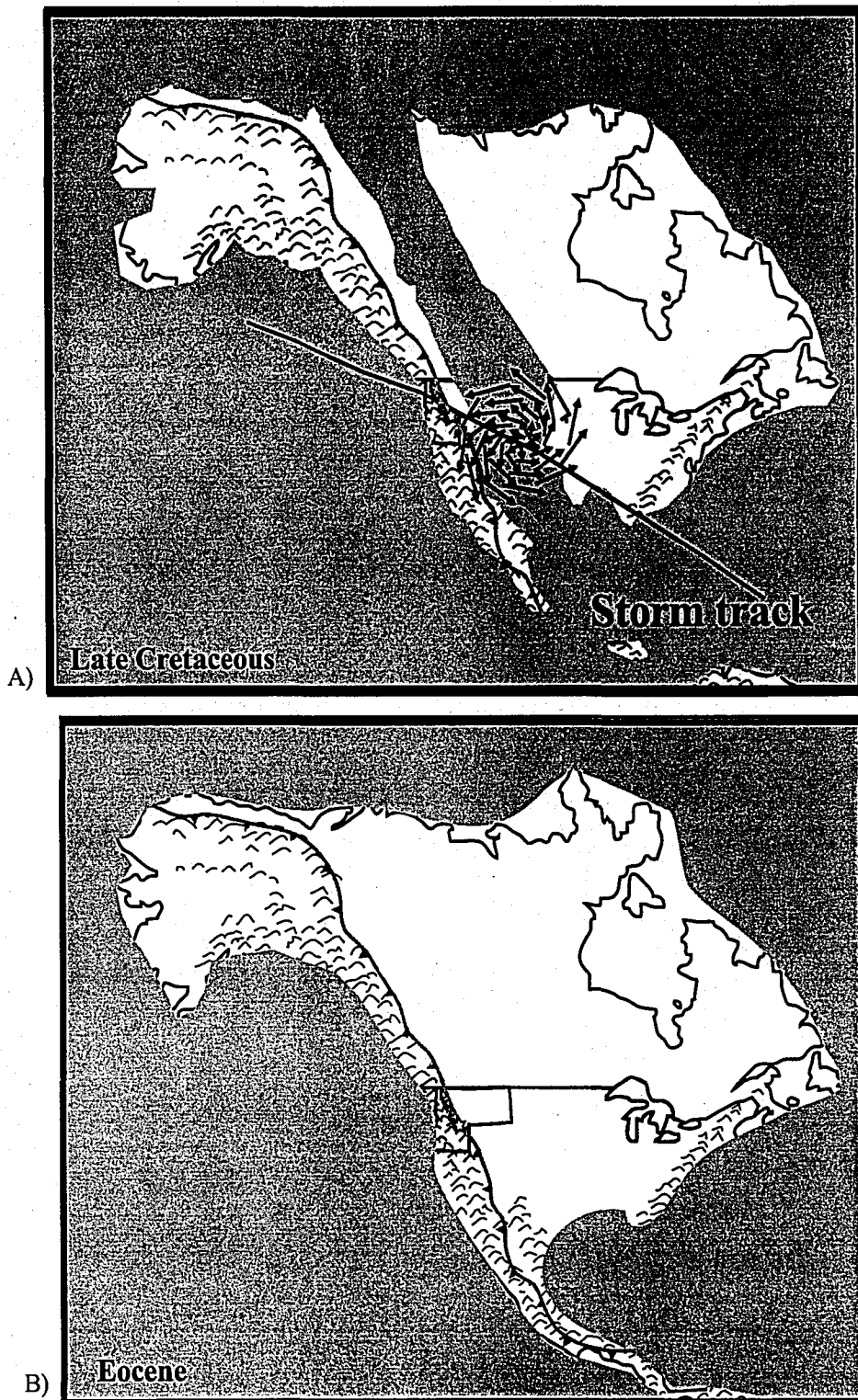


Figure 18. A) Paleogeographic map (Scotese, 2002) and the location of the Western Interior Seaway during the Late Cretaceous (Ericksen and Slingerland, 1990). Climate models have determined that there were large cyclones blowing across the seaway from west to east (e.g. Kump and Slingerland, 1999). The frontal thrust of the Cordilleran Mountain Belt is shown and the study area is marked with a star in SW Montana B) Paleogeographic map of the Eocene (Scotese, 2002).

hydrothermal fluids associated with contact aureoles by Criss and Taylor (1983) interpreted meteoric water values for $\delta^{18}\text{O}$ of about -16‰ for temperatures of 150-400° C at depths of 5-7 km. Fluids in the Eocene Pioneer core complex have meteoric water values of -14.7‰ and -17.7‰ for temperatures of 300° C and 200° C respectively (Bebout et al., 2001). Eocene veins from this study have minimum values of -19‰ or -13‰ (40° C and 80° C respectively). These fluids have compositions consistent with Eocene fluids found in the other studies previously mentioned. During the Eocene the Western Interior Seaway was no longer present and the Pacific Ocean was found slightly further west (Figure 18B). The very ^{18}O -depleted fluids found forming these Eocene veins are consistent with the composition of evolved fluids possibly from the Pacific Ocean (Yurtsever and Gat, 1981). These fluids are more evolved than Cretaceous fluids, possibly due to changes in the location of the Pacific ocean. In addition, during the Eocene since the Western Interior Seaway was no longer present there was no mixing with less evolved fluids with more evolved fluids from the Pacific Ocean that would enrich the overall composition of the fluids, hence these Eocene fluids are more depleted in ^{18}O than the Cretaceous fluids. Also, the poor temperature constraints for the Eocene fluids may be somewhat of a factor in the apparent difference between minimum Cretaceous and Eocene fluids.

During Cretaceous compression and Eocene extension there was fracturing related to the deformation of the Tendoy, Four Eyes Canyon, and Medicine Lodge thrust sheets. These fractures acted as fluid conduits for fresh meteoric fluids, mostly from the Pacific Ocean, and hydrocarbons. These fluids infiltrated into the thrust

sheets to the basal decollement at ~4 km. Studies in the Canadian Cordillera foreland basin show the infiltration of meteoric fluids to depths of 3-4 km (Nesbitt et al., 1991; Hutcheon, 2000). These fluids were driven to these depths by topographic recharge (Ge and Freeze, 1984; Koons and Craw, 1991). The driving mechanism of this flow is the sloping water table, which mimics the topography of the region (Ge and Freeze, 1984; Koons and Craw, 1991). Once at depth, the meteoric water buoyantly flowed updip towards the foreland (Koons and Craw, 1991). During fluid flow there were likely varying degrees of fluid-rock interactions, making for more ^{18}O -enriched fluids. From these fluids calcite precipitated to reseal the fractures to form veins. Hydrocarbons were also migrating through the same fluid conduits in the frontal thrust sheets of the Tendoy Mountains. The evolution of these fluid conduits is recorded in the calcite veins.

Conclusions

In summary, calcite veins from the Sevier frontal thrust sheets in southwestern Montana record syntectonic infiltration of meteoric water. During Cretaceous compression, longitudinal and transverse vein sets formed during Four Eyes Canyon and Medicine Lodge thrust sheet emplacement, but prior to Tendoy thrust sheet emplacement. Bed-parallel veins formed during folding of the Tendoy, Four Eyes Canyon, and Medicine Lodge thrust sheets and brittle deformation zones developed during faulting in the Tendoy thrust sheet in the immediate hanging-wall. During the Eocene, high angle and irregular veins formed coincident with regional extension;

these veins cut Cretaceous compressional structures and reactivated many Cretaceous veins. The Cretaceous and Eocene veins were filled with calcite precipitated from meteoric water derived from the Pacific Ocean with perhaps some mixing of less evolved fluids from the Western Interior Seaway during the Cretaceous. Surficial fluids infiltrated into foreland thrust sheets by topographic recharge and buoyantly flowed through fractures up-dip towards the foreland. In a low temperature environment where the carbonate protolith was very enriched in $\delta^{18}\text{O}$, the presence of more $\delta^{18}\text{O}$ -enriched fluids may be a result of varying degrees of fluid-rock interactions. Not only were fractures conduits for meteoric water, but also hydrocarbons, which migrated with the freshwater. Multi-layered veins that sealed and re-opened numerous times record each flow period. The veins of the Tendoy Mountains were conduits for meteoric surface water generating significant fluid-rock interactions leading to calcite veins of significant isotopic variation.

References

Amoco Production Company, 1986. McKnight Canyon No.1, SE SW Section 21-T12S-R10W, Beaverhead County, Montana. Denver: Amoco Production Company.

Anastasio, David J., Nathan W. Harkins, Diana K. Latta, 2002. Coeval, in-and-out-of-sequence deformation within the frontal thrust sheets of the Tendoy Mountains, SW Montana. *Geological Society of America Rocky Mountain Sectional Meeting Abstracts with Programs*, **34**, A7.

Barker, Charles E. and Mark J. Pawlewicz, 1994. Calculation of Vitrinite Reflectance from Thermal Histories and Peak Temperatures, A comparison of methods. In: *Vitrinite Reflectance as a Maturity Parameter, Applications and Limitations* (Prasanta K. Mukhopadhyay and Wallace G. Dow, eds.), American Chemical Society, Washington, D.C., 1994.

Bebout, Gray B., David J. Anastasio, and James E. Holl, 2001. Synorogenic Crustal Fluid Infiltration in the Idaho-Montana Thrust Belt. *Geophysical Research Letters*, **28**, 429-4298.

Burruss, R. C., 1981. Hydrocarbon fluid inclusions in studies of sedimentary diagenesis. In: *Short Course in Fluid Inclusions: Applications to Petrology* (Hollister, L.S., and Crawford, M.L., eds.), 138-156.

Cadrin, A.A.J., T.K. Kyser, W.G.E. Caldwell, F.J. Longstaffe, 1995. Isotopic and chemical compositions of bentonites as paleoenvironmental indicators of the Cretaceous Western Interior Seaway. *Palaeogeography, Palaeoclimatology, and Palaeoecology*, **119**, 301-320.

Cadrin, A.A.J., 1992. Geochemistry and paleoenvironmental reconstruction of the Greenhorn marine cyclothem in the Western Interior Basin of Canada. Unpublished thesis, University of Saskatchewan.

Cosgrove, John W., 2001. Hydraulic fracturing during the formation and deformation of a basin: A factor in the dewatering of low-permeability sediments. *American Association of Petroleum Geologists Bulletin*, **85**, 737-748.

Criss, R.E. and H.P. Taylor, Jr., 1983. An $^{18}\text{O}/^{16}\text{O}$ and D/H study of Tertiary hydrothermal systems in the southern half of the Idaho batholith. *Geological Society of America Bulletin*, **94**, 640-663.

Davis, D., Suppe J., and J.A. Dahlen, 1983. Mechanics of Fold and Thrust Belts and Accretionary Wedges. *Journal of Geophysical Research*, **88**, 1153-1172.

Durney, D.W., 1972. Solution-transfer, an Important Geological Deformation Mechanism. *Nature*, **235**, 315-317.

Epstein, A.G., J.B. Epstein, and L.D. Harris, 1977. Conodont color alteration – an index to organic metamorphism. *U.S. Geological Survey, Professional Paper 995*, 27.

Ericksen, Marc C. and Rudy L. Slingerland, 1990. Numerical simulations of tidal and wind-driven circulation in the Cretaceous interior seaway of North America. *Geological Society of America Bulletin*, **102**, 1499-1516.

Evans, Mark A. and Denise A. Battles, 1999. Fluid inclusion and stable isotope analyses of veins from the central Appalachian Valley and Ridge province: Implications for regional synorogenic hydrologic structure and fluid migration. *Geological Society of America Bulletin*, **111**, 1841-1860.

Ferrill, David A., 1991. Calcite twin widths and intensities as metamorphic indicators in natural low-temperature deformation of limestone. *Journal of Structural Geology*, **13**, 667-675.

Fisher, Donald M. and Susan L. Brantley, 1992. Models of Quartz Overgrowth and Vein Formation: Deformation and Episodic Fluid Flow in an Ancient Subduction Zone. *Journal of Geophysical Research*, **97**, 20,043-20, 061.

Forester, C. and L. Smith, 1990. Chapter 1: Fluid flow in tectonic regimes. In: Short Course on Fluids in Tectonically Active Regimes of the Continental Crust (Nesbitt, B.E., ed.), *Mineralogical Society of Canada Short Course Handbook Series*, **18**, 1-47.

Garvin, Grant and R. Allen Freeze, 1984. Theoretical Analysis of the Role of Groundwater Flow in the Genesis of Stratabound Ore Deposits. *American Journal of Science*, **284**, 1085-1124.

Ge, Shemin and Grant Garvin, 1994. A theoretical model for thrust-induced deep groundwater expulsion with application of the Canadian Rocky Mountains. *Journal of Geophysical Research*, **99**,13851-13860.

Hubbert, M.K. and Rubey, W.W., 1959. Role of fluid pressure in mechanics of overthrust faulting. I. Mechanics of fluid-filled porous solids and its application to overthrust faulting. *Geological Society of America Bulletin*, **70**, 115-166.

Hutcheon, Ian, John Cody, and Chao Yang. Fluid Flow in the Western Canada Sedimentary Basin – A biased perspective based on geochemistry. In: *Fluids and*

Basin Evolution (Kurt Keyser, ed.), Short Course Series, **28**. Ottawa, Ontario: Mineralogical Association of Canada, 2000.

Janecke, Susanne U., W. McIntosh, and S. Good, 1999. Testing models of rift basins: structure and stratigraphy of an Eocene-Oligocene supradetachment basin, Muddy Creek half graben, south-west Montana. *Basin Research*, **111**, 143-165.

Jewell, Paul W., 1996. Circulation, salinity, and dissolved oxygen in the Cretaceous North American Seaway. *American Journal of Science*, **296**, 1093-1125.

Kalakay, Thomas J., Barbara E. John, David R. Lageson, 2001. Fault-controlled pluton emplacement in the Sevier fold-and-thrust belt of the southwest Montana, USA. *Journal of Structural Geology*, **23**, 1151-1165.

Kalakay, Thomas J., 2001. The role of magmatism during crustal shortening in the Sevier retroarc fold-and-thrust belt of southwest Montana, a Ph.D., from the University of Wyoming, Laramie, WY, May 2001.

Kendall, C., M.M.G. Skalsch, and T.D. Bullen, 1995. Isotope tracers of water and solute sources in catchments. In: *Solute Modelling in Catchment Systems* (Trudgill, S.T., ed.), John Wiley & Sons, Ltd., 261-303.

Koons, P.O. and D. Craw, 1991. Evolution of fluid driving forces and compression within collisional orogens. *Geophysical Research Letters*, **18**, 935-938.

Kump, Lee R. and Rudy L. Slingerland, 1999. Circulation and stratification of the early Turonian Western Interior Seaway: Sensitivity to a variety of forcings.

Geological Society of America, Special Paper 332, 181-190.

Lindholm, R.C., 1974. Fabric and Chemistry of Pore Filling Calcite in Septarian Veins: Models for Limestone Cementation. *Journal of Sedimentary Petrology*, **44**, 428-440.

Lonn, Jeffery D., Betty Skipp, Edward T. Ruppel, Susanne U. Janecke, William J. Perry, Jr., James W. Sears, Mervin J. Bartholomew, Michael C. Stickney, William J. Fritz, Hugh A. Hurlow, and Robert C. Thomas, 2000. Geological Map of the Lima 30' x 60' Quadrangle, Southwest Montana. Montana Bureau of Mines and Geology, Open File Report: MBMG 408.

McCrea, J.M., 1950. The isotopic chemistry of carbonated and paleotemperatures scale. *Journal of Chemical Physics*, **18**, 849-857.

McDowell, Robin John, 1997. Evidence for synchronous thin-skinned and basement deformation in the Cordilleran fold-thrust belt: the Tendoy Mountains, southwestern Montana. *Journal of Structural Geology*, **19**, 77-87.

McDowell, Robin John, 1992. Effects of synsedimentary basement tectonics on fold-thrust belt geometry, southwestern Montana. Unpublished PhD Thesis, University of Kentucky.

Nesbitt, Bruce E. and Karlis Meuhlenbachs, 1989. Orogens and Movement of fluids during deformation and metamorphism in the Canadian Cordillera. *Science*, **245**, 733-736.

Nesbitt, Bruce E. and Karlis Muehlenbachs, 1991. Stable Isotope Constraints on the Nature of the Syntectonic Fluid Regime of the Canadian Cordillera. *Geophysical Research Letters*, **18**, 963-966.

Oliver, Jack, 1986. Fluids expelled tectonically from orogenic belts: their role in hydrocarbon migration and other geologic phenomena. *Geology*, **14**, 99-102.

O'Neil, J.R., R.N. Clayton, and T.K. Mayeda, 1969. Oxygen isotope fractionation in divalent metal carbonates. *Journal of Chemical Physics*, **51**, 5547-5558.

Perry, W.J., Jr. and W. J. Sando, 1983. Sequence of deformation of Cordilleran thrust belt in Lima, Montana, region. In: *Geologic studies of the Cordilleran thrust belt* (Powers, R.B., ed.), 1982: Denver, Colorado, Rocky Mountain Association of Geologists, **1**, 137-144.

Perry, W., J., Jr., B.R. Wardlaw, N.H. Bostick, and E.K. Maughan, 1983. Structure, Burial History, and Petroleum Potential of the Frontal Thrust Belt and Adjacent Foreland, Southwest Montana. *The American Association of Petroleum Geologists Bulletin*, **67**, 725-743.

Perry, W.J., Jr., C. Haley, J. Nichols, M Hammons, O. Ponton, 1988. Interactions of Rocky Mountain foreland and Cordilleran thrust belt in Lima region, southwest Montana. In: *the Interaction of Rocky Mountain Foreland and the Cordilleran Thrust Belt* (Christopher J. Schmidt and William J. Perry, Jr., eds.) Geological Society of America, Memoir 171, 1988.

Perry, W.J., R.T. Ryder, and E.K. Maughan, 1981. Southern Part of the Southwestern Montana Thrust Belt: A Preliminary Re-evaluation of Structure, Thermal Maturation and Petroleum Potential. In: *the Montana Geological Society Field Conference and Symposium Guidebook to Southwest Montana* (Thomas E. Tucker, Richard B. Aram, William F. Brinker, and Robert F. Grabb, Jr., eds.) Montana Geological Society, 1981.

Roedder, Edwin, 1984. Fluid Inclusions; Reviews in Mineralogy. Virginia: Mineralogical Society of America, 12, 1984.

Rye, Danny M. and Harry J. Bradbury, 1988. Fluid Flow in the Crust: An Example from a Pyrenean Thrust Ramp. *American Journal of Science*, 288, 197-235.

Sageman, Bradley B., 1996. Lowstand tempestites: Depositional model for Cretaceous skeletal limestones, Western Interior basin. *Geology*, 24, 888-892.

Schmitt, James G., J. Christopher Haley, David R. Lageson, Brian K. Horton, and Paul A. Azevedo, 1995. Sedimentology and Tectonics of the Bannack-McKnight Canyon-Red Butte Area, Southwest Montana: New Perspectives on the Beaverhead Group and Sevier Orogenic Belt. *Northwest Geology*, 24, 245-313.

Scotese, Christopher, 2002. Paleogeographic maps: <http://www.scotese.com>

Sheppard, Simon M.F., Richard L. Nielsen, and Hugh P. Taylor, Jr., 1969. Oxygen and hydrogen isotope ratios of clay minerals from porphyry copper deposits.

Economic Geology and the Bulletin of the Society of Economic Geologists, 64, 755-777.

Siegenthaler, 1979. Stable hydrogen and oxygen isotopes in the water cycle. In: *Lectures in isotope geology* (Jaeger, E. and J.C. Hunziker, Springer-Verlag,, eds.) Berlin, Germany, 1979.

Silverberg, D.S., 1990. The Tectonic Evolution of the Pioneer Metamorphic Core Complex, South-Central Idaho, a Ph.D., from the Massachusetts Institute of Technology, Massachusetts, 1990.

Skipf, Betty, 1988. Cordilleran thrust belt and faulted foreland in the Beaverhead Mountains, Idaho and Montana. In: *the Interaction of Rocky Mountain Foreland and the Cordilleran Thrust Belt* (Christopher J. Schmidt and William J. Perry, Jr., eds.) Geological Society of America, Memoir 171, 1988.

Slingerland, Rudy, Lee R. Kump, Michael A. Arthur, Peter J. Fawcett, Bradley B.

Sageman, Eric J. Barron, 1996. Estuarine circulation in the Turonian Western Interior Seaway of North America. *Geological Society of America Bulletin*, **108**, 941-952.

Swetland, P. J., J.L. Clayton, and E.G. Sable, 1978. Petroleum source-bed potential of Mississippian-Pennsylvanian rocks in parts of Montana, Idaho, Utah, and Colorado: *The Mountain Geologist*, **14**, 79-87.

Whittaker, S.G., T.K. Keyser, and W.G.E. Caldwell, 1987. Paleoenvironmental geochemistry of the Claggett marine cyclothem in south-central Saskatchewan.

Canadian Journal of Earth Sciences, 24, 967-984.

Williams, Nancy S. and John M. Bartley, 1988. Geometry and sequence of thrusting, McKnight and Kelmbeck Canyons, Tendoy Range, southwestern Montana. In: *the Interaction of Rocky Mountain Foreland and the Cordilleran Thrust Belt* (Christopher J. Schmidt and William J. Perry, Jr., eds.) *Geological Society of America*, Memoir 171, 1988, 307-318.

Wojtal, S., 1986. Deformation within foreland thrust sheets by populations of minor faults. *Journal of Structural Geology*, 11, 669-678.

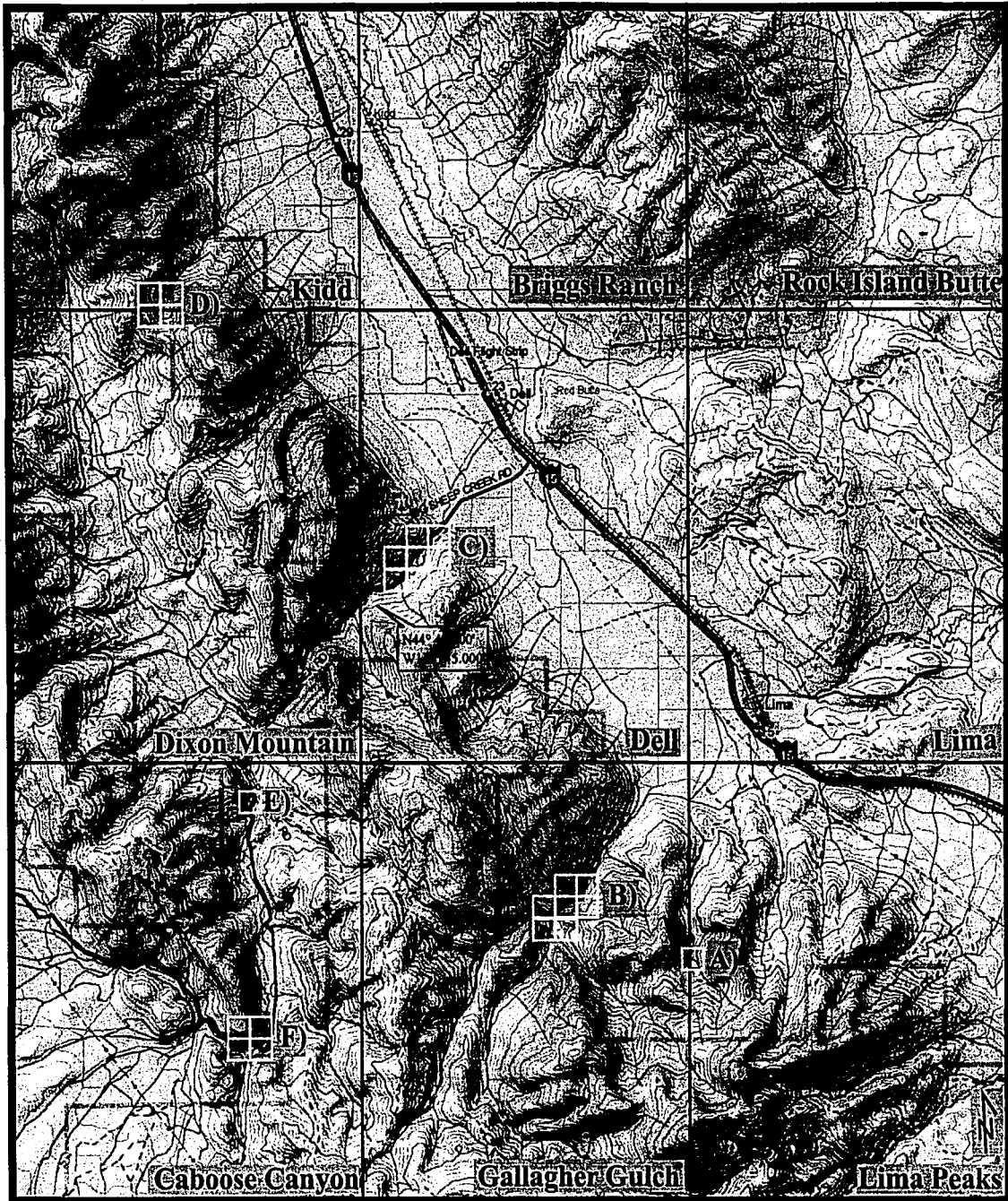
Yurtsever, Y. and J.R. Gat, 1981. Atmospheric water. In: *Stable Isotope Hydrology, Deuterium and Oxygen-18 in the Water Cycle*, Vienna: International Atomic Energy Agency, 103-142.

Whittaker, S.G., T.K. Keyser, and W.G.E. Caldwell, 1987. Paleoenvironmental geochemistry of the Claggett marine cyclothem in south-central Saskatchewan. *Canadian Journal of Earth Sciences*, **24**, 967-984.

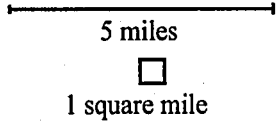
Williams, Nancy S. and John M. Bartley, 1988. Geometry and sequence of thrusting, McKnight and Kelmbeck Canyons, Tendoy Range, southwestern Montana. In: *the Interaction of Rocky Mountain Foreland and the Cordilleran Thrust Belt* (Christopher J. Schmidt and William J. Perry, Jr., eds.) *Geological Society of America*, Memoir 171, 1988, 307-318.

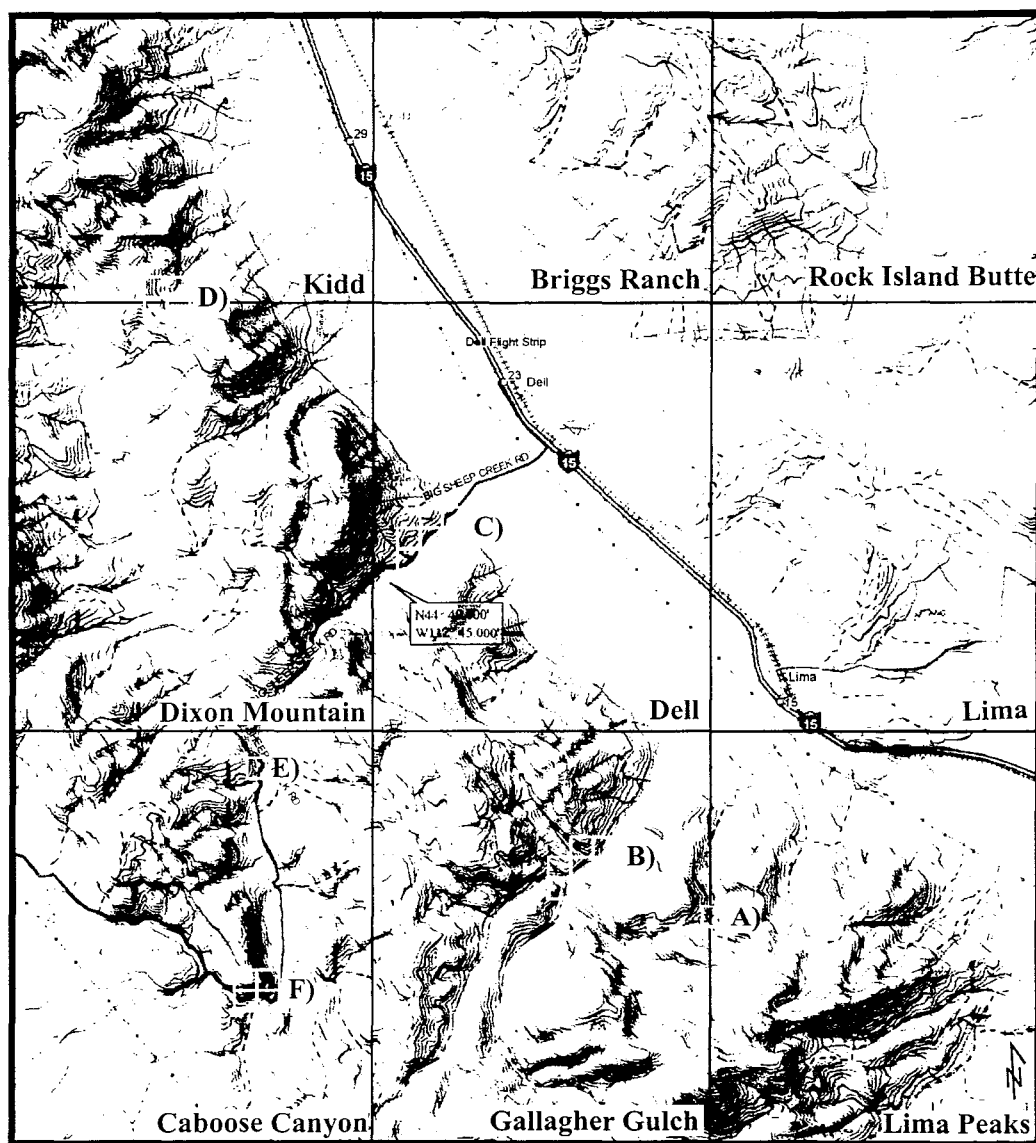
Wojtal, S., 1986. Deformation within foreland thrust sheets by populations of minor faults. *Journal of Structural Geology*, **11**, 669-678.

Yurtsever, Y. and J.R. Gat, 1981. Atmospheric water. In: *Stable Isotope Hydrology, Deuterium and Oxygen-18 in the Water Cycle*, Vienna: International Atomic Energy Agency, 103-142.



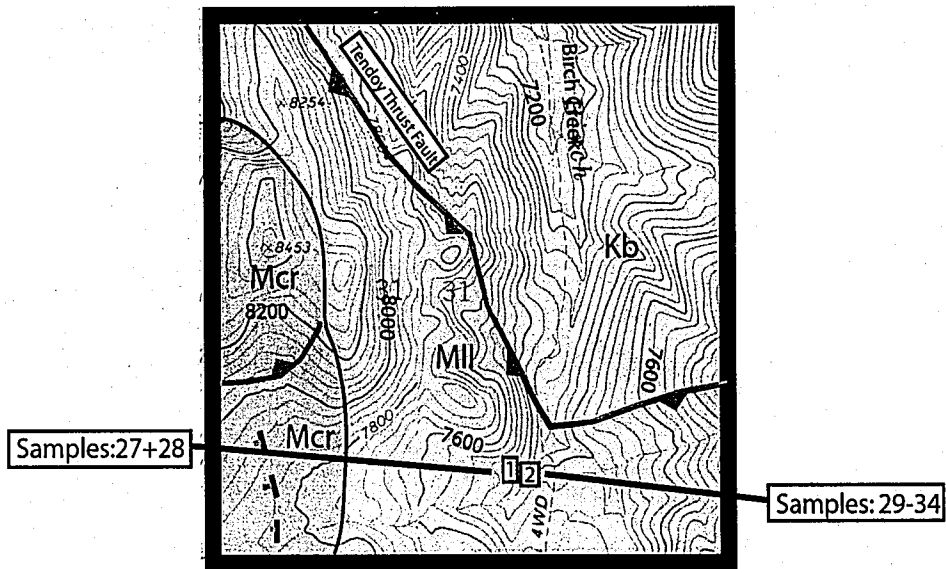
Appendix 1. Topographic Index of quadrangles locating sample traverses in the appropriate township and range (DeLorme. Topo USA 3.0, 2001).
 A) Birch Creek, B) Little Sheep Creek, C) Big Sheep Creek, D) McKnight Canyon, E) UPS, F) Four Eyes Canyon.



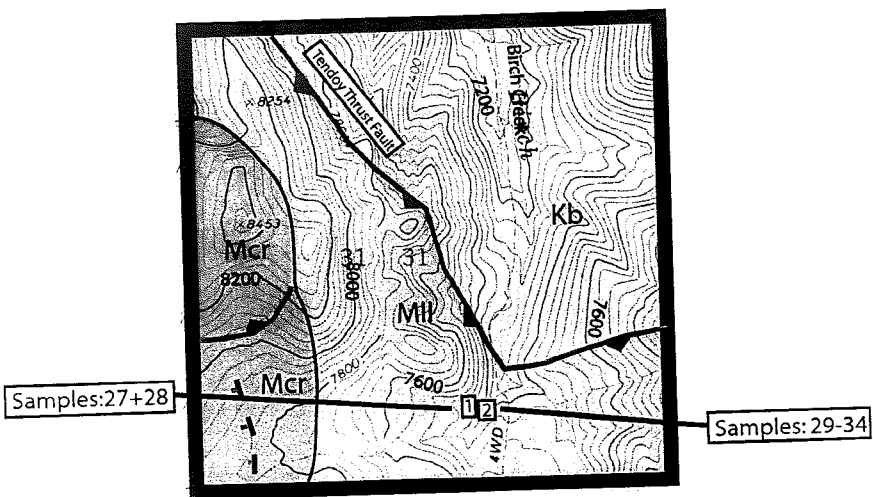


Appendix 1. Topographic Index of quadrangles locating sample traverses in the appropriate township and range (DeLorme. Topo USA 3.0, 2001). A) Birch Creek, B) Little Sheep Creek, C) Big Sheep Creek, D) McKnight Canyon, E) UPS, F) Four Eyes Canyon.

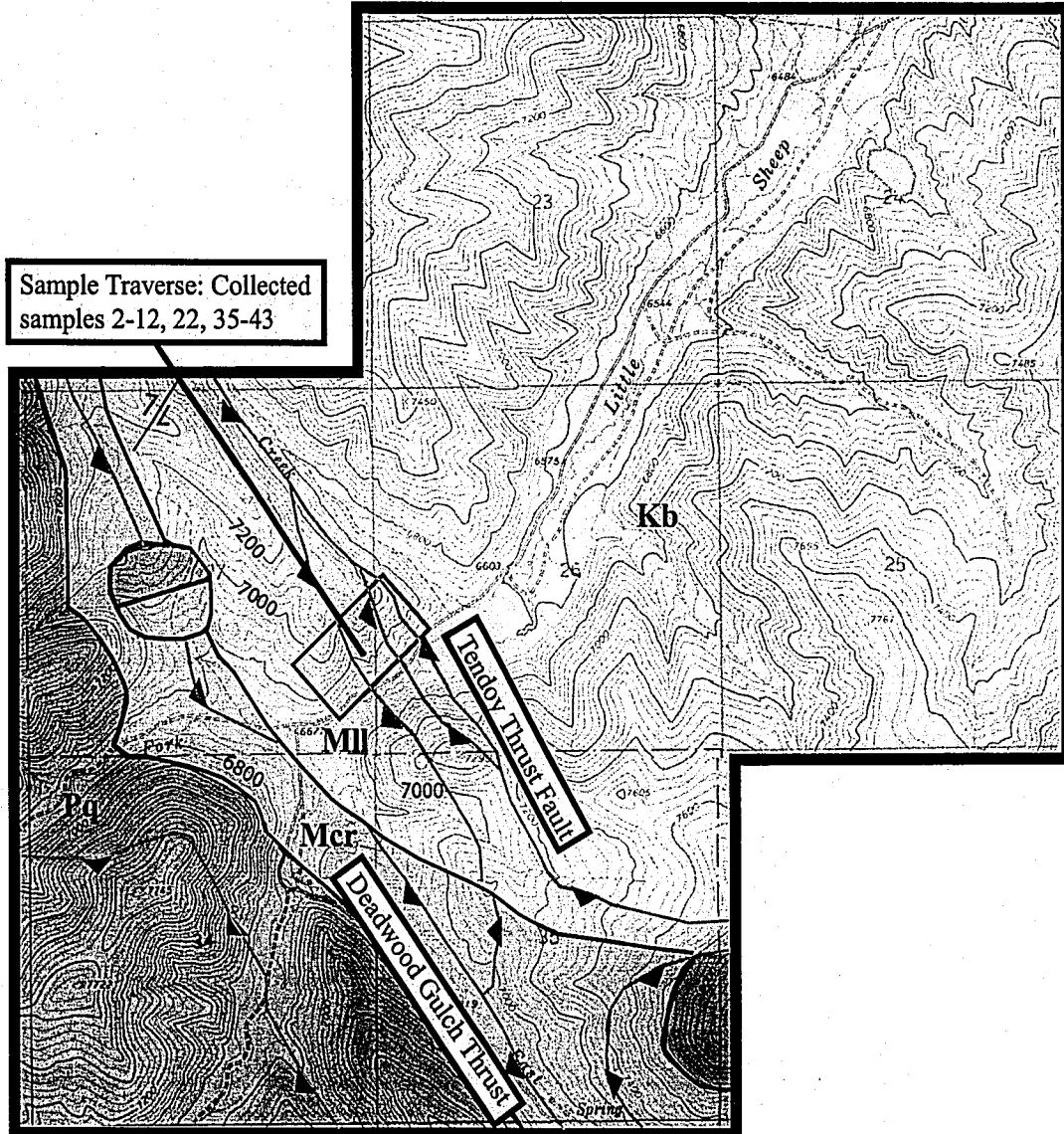
5 miles
 1 square mile



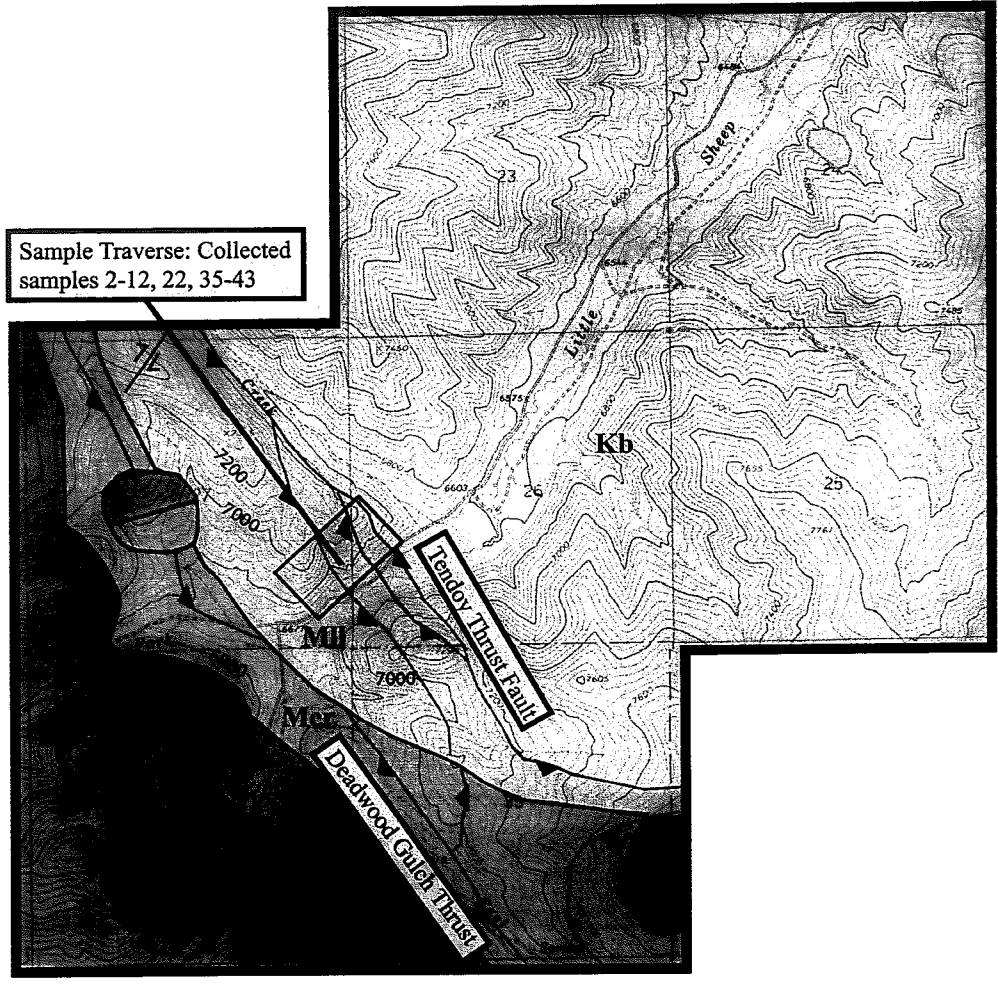
Appendix 1. A) Birch Creek traverse in the Gallagher and Lima Peaks Quadrangles.



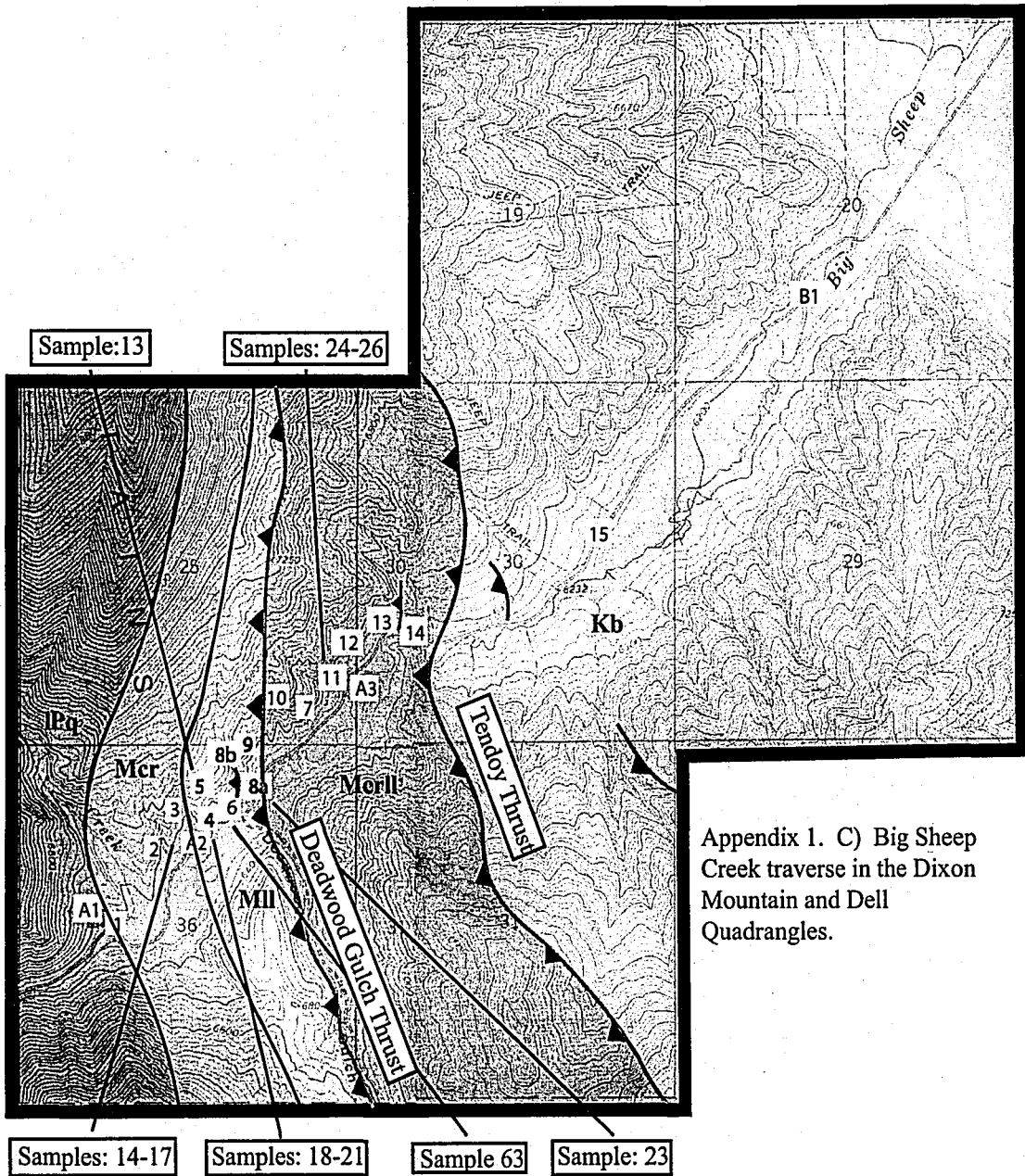
Appendix 1. A) Birch Creek traverse in the Gallagher and Lima Peaks Quadrangles.



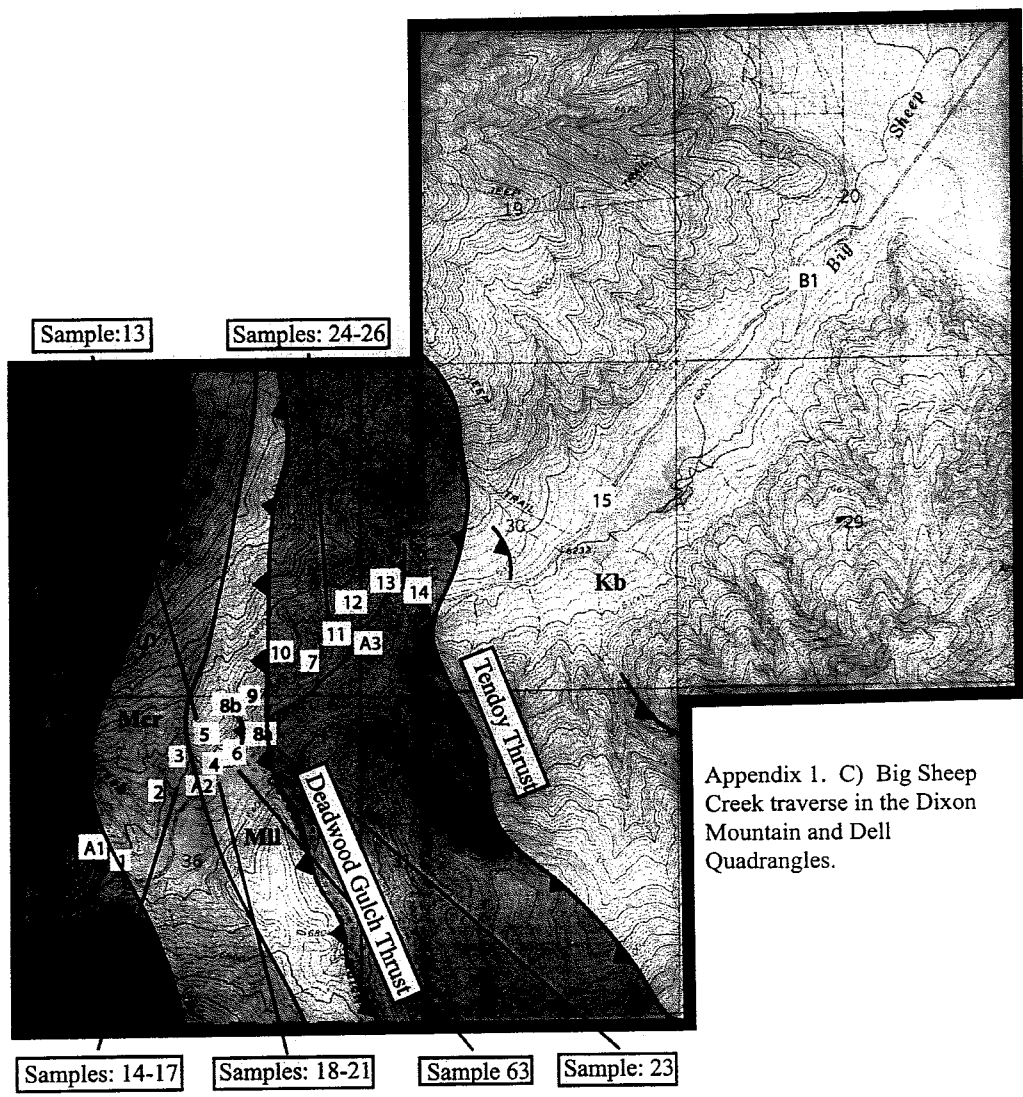
Appendix 1: B) Little Sheep Creek traverse in the Gallagher Gulch quadrangle. Sample sites can be seen in Appendix 2 in the photomosaic of Little Sheep Creek.



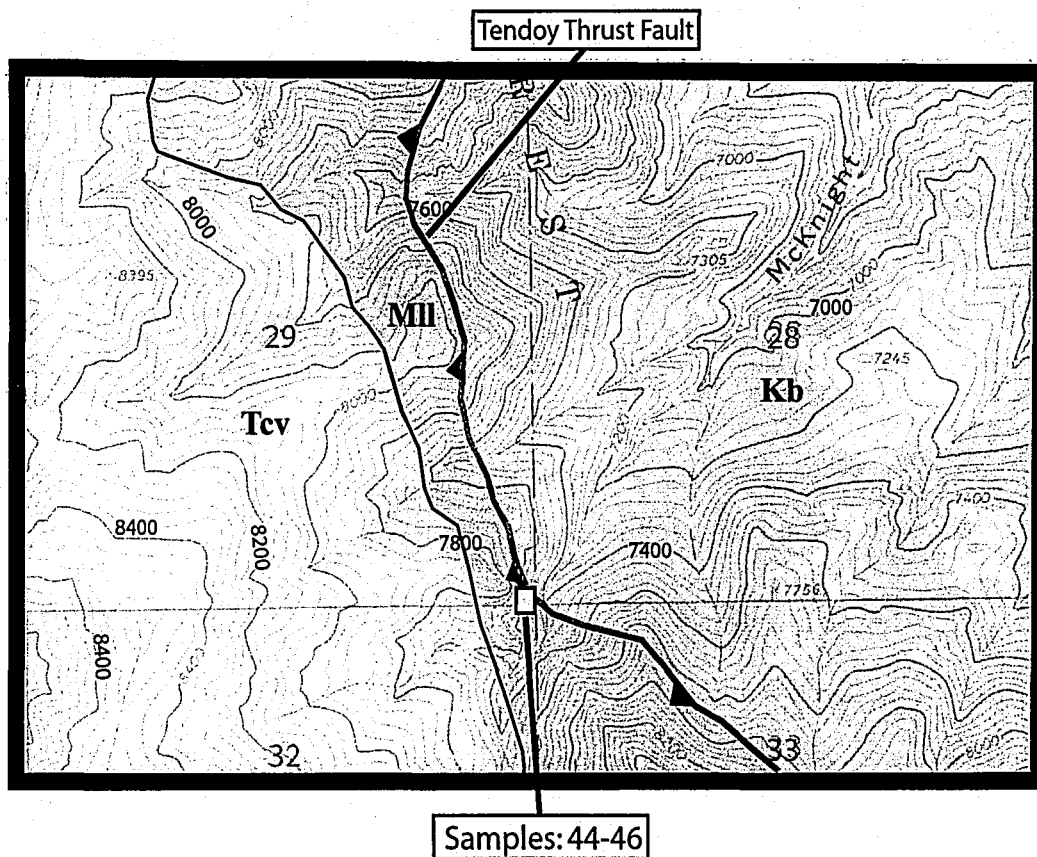
Appendix 1: B) Little Sheep Creek traverse in the Gallagher Gulch quadrangle. Sample sites can be seen in Appendix 2 in the photomosaic of Little Sheep Creek.



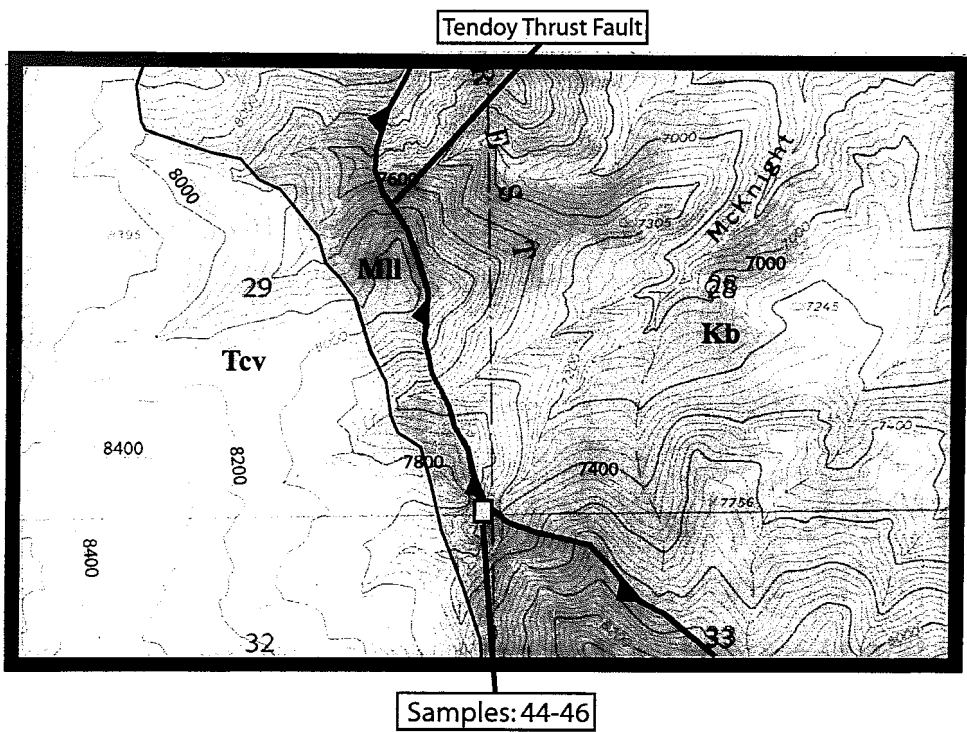
Appendix 1. C) Big Sheep Creek traverse in the Dixon Mountain and Dell Quadrangles.



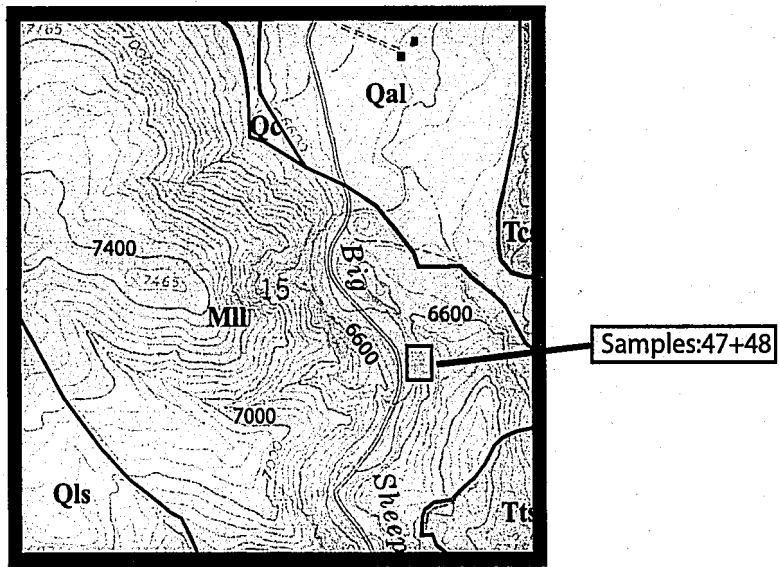
Appendix 1. C) Big Sheep Creek traverse in the Dixon Mountain and Dell Quadrangles.



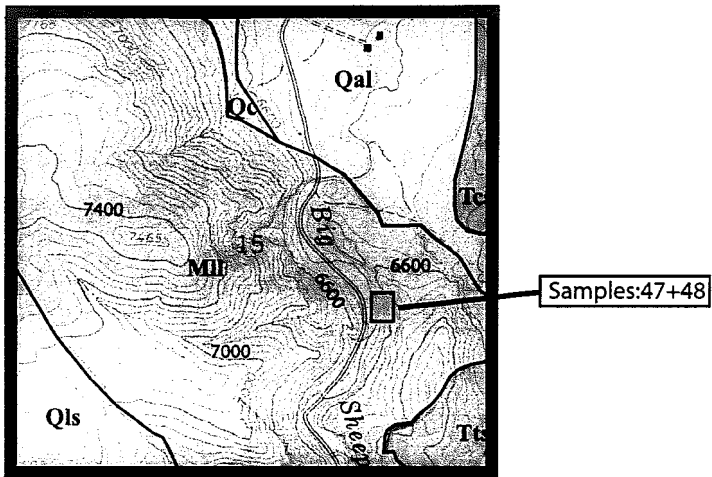
Appendix 1. D) McKnight Canyon traverse in the Kidd Quadrangle.



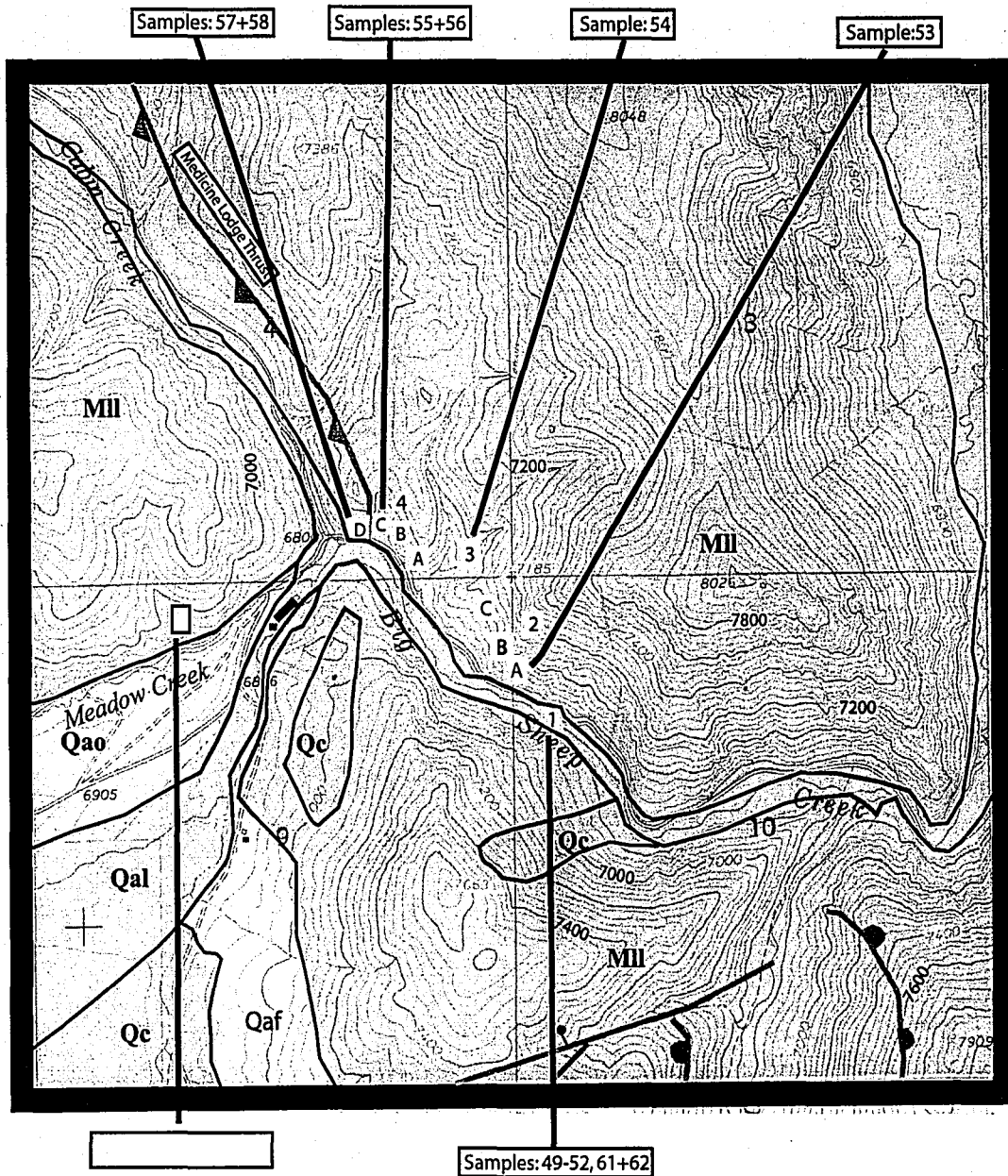
Appendix 1. D) McKnight Canyon traverse in the Kidd Quadrangle.



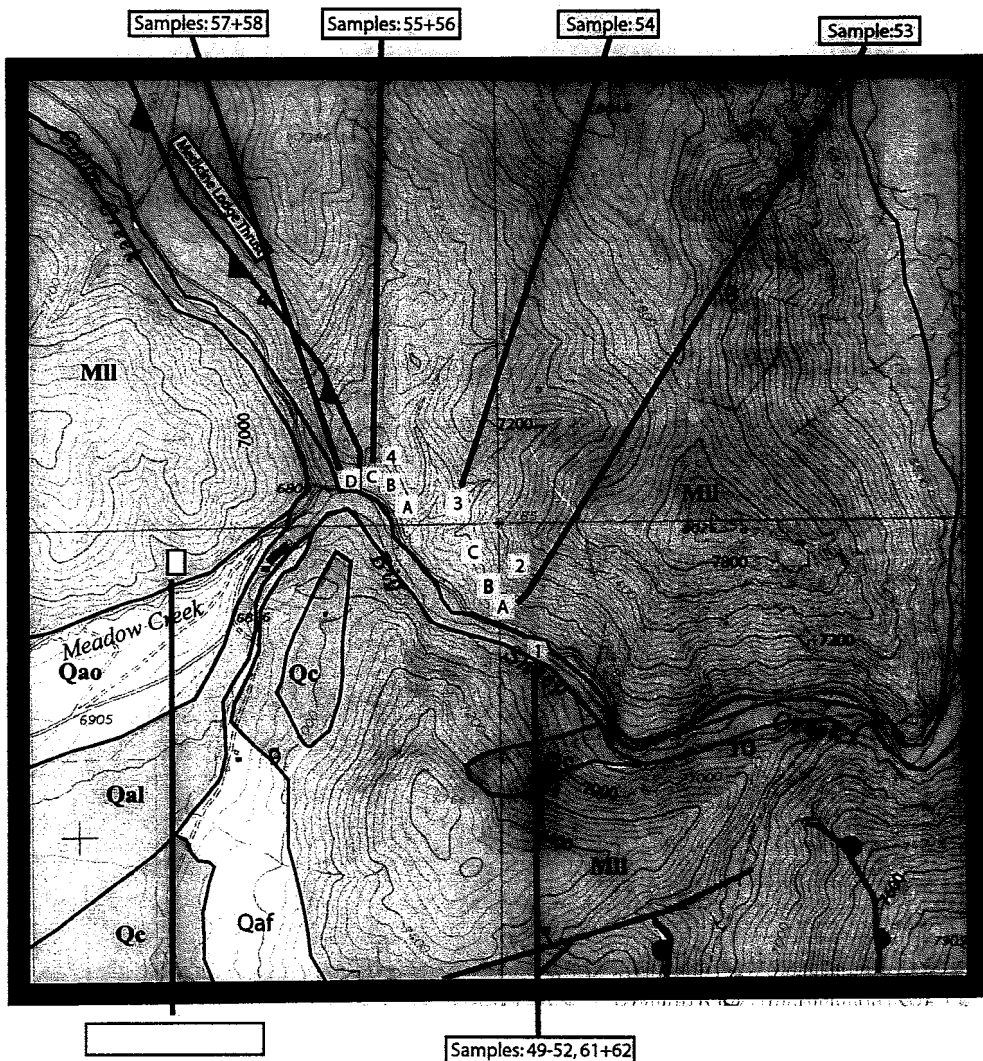
Appendix 1. E) Four Eyes Canyon - United Postal Service (UPS) traverse in the Caboose Canyon Quadrangle.



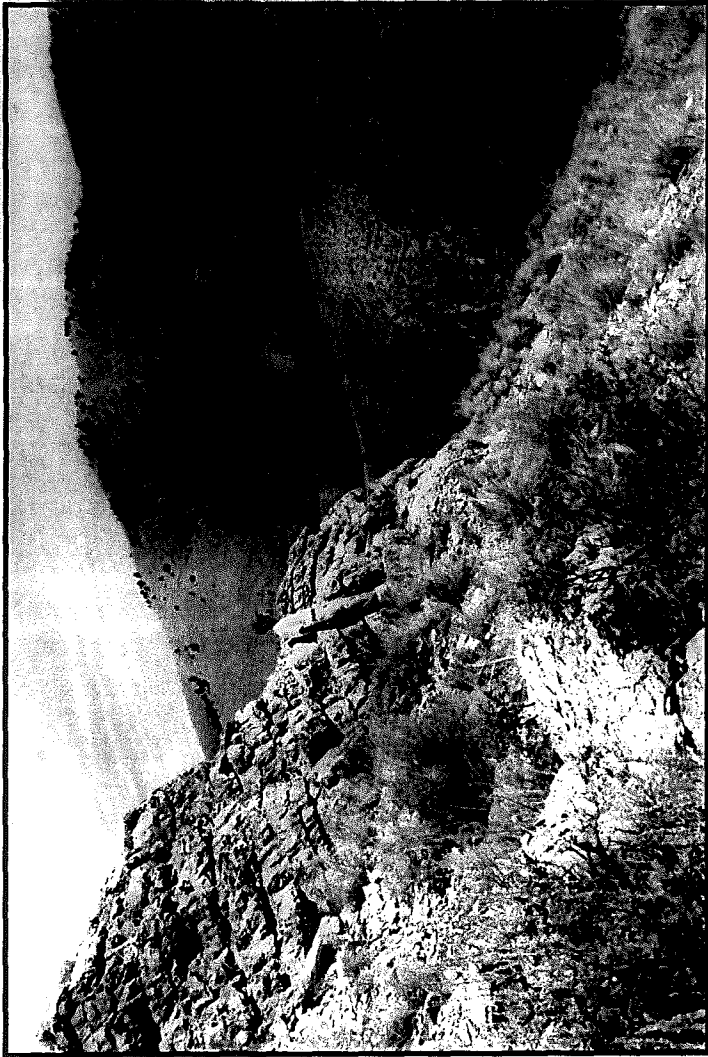
Appendix 1. E) Four Eyes Canyon - United Postal Service (UPS) traverse in the Caboose Canyon Quadrangle.



Appendix 1. F) Four Eyes Canyon and Medicine Lodge traverse in the Caboose Canyon Quadrangle.

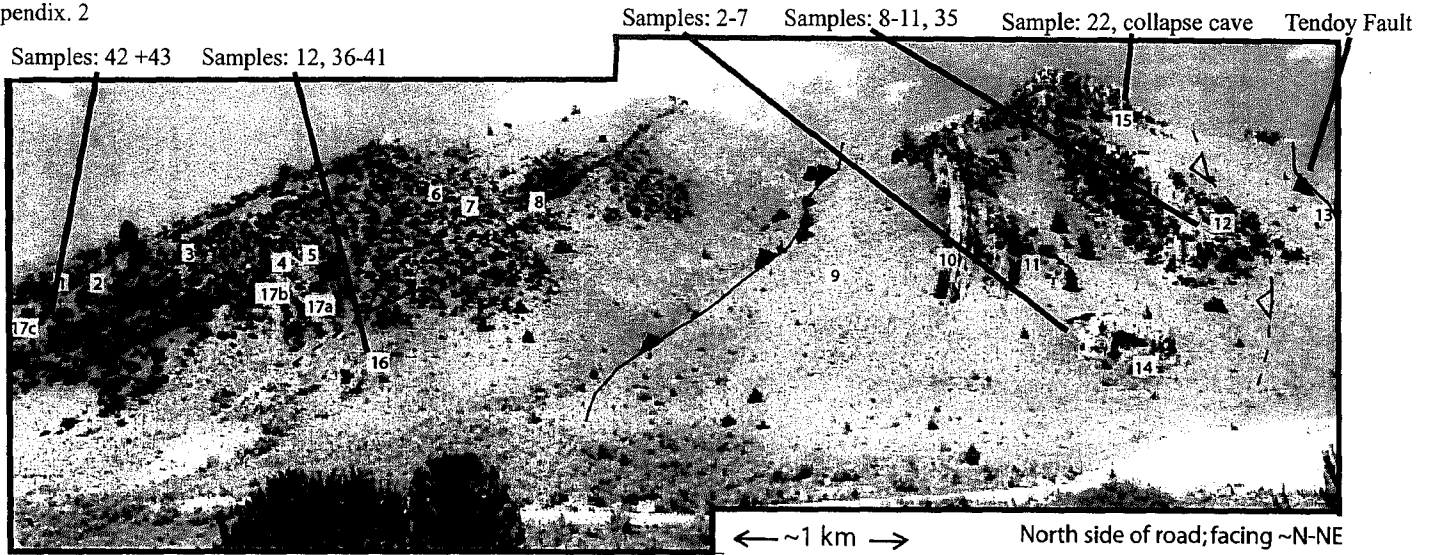


Appendix 1. F) Four Eyes Canyon and Medicine Lodge traverse in the Caboose Canyon Quadrangle.



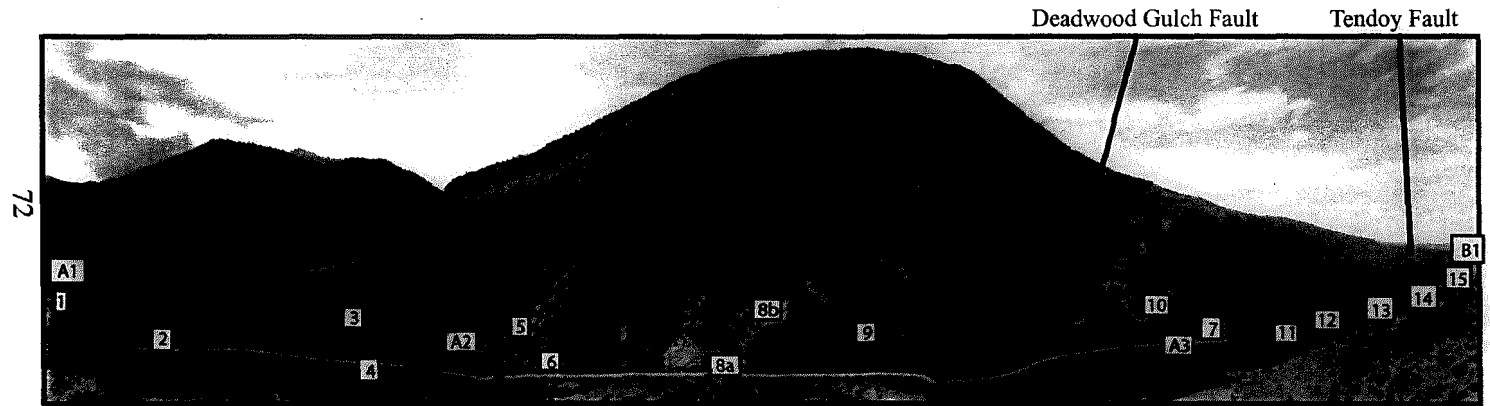
Appendix 2. Birch Creek traverse, facing south.

Appendix. 2



Little Sheep Creek traverse with data and sample collecting stations.

Appendix 2.



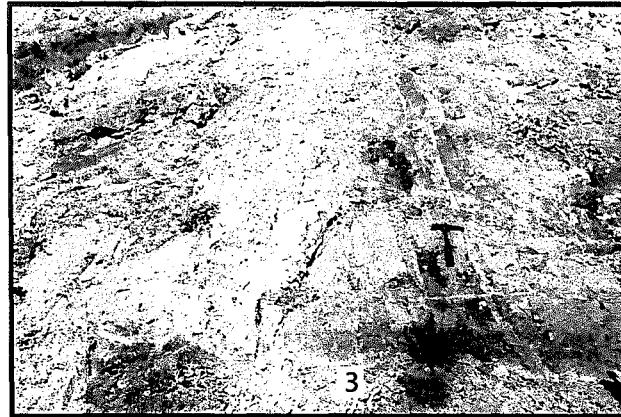
North Side of Road; facing ~N
Scale: ~2km

Big Sheep Creek traverse with data and sample collecting stations.

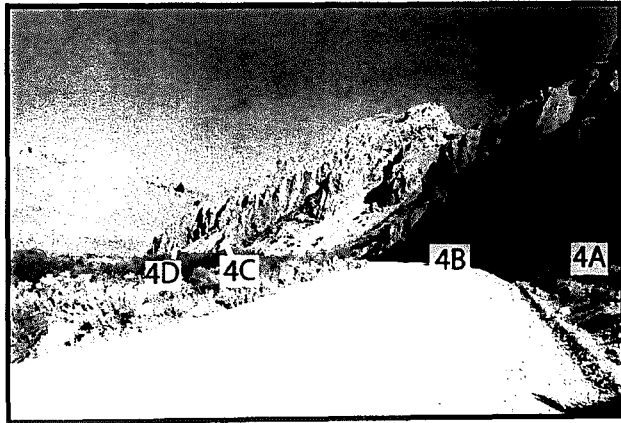


Appendix 2. Eastern Four Eyes Canyon - United Parcel Service (UPS) traverse, just upstream.

Hinge

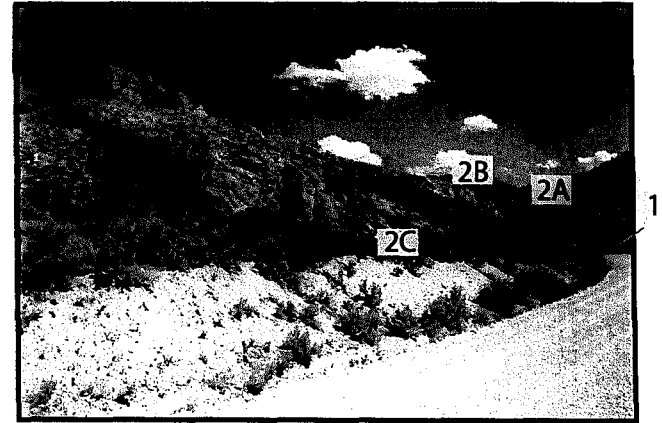


West Limb of Anticline (4C+D)



Hinge cont'd (4A+B)

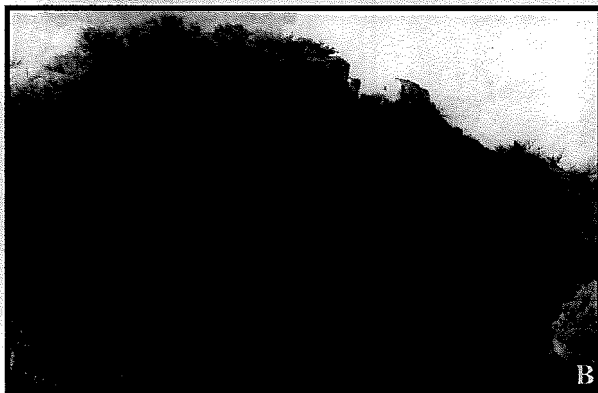
East Limb of Anticline



Appendix 3. Collapse cave at Little Sheep Creek



A) Collapse cave in the Lombard Limestone at Little Sheep Creek traverse. B) The cave is surrounded by undisturbed, near vertical beds contained within the imbricate faults that formed out of sequence behind the Tendoy fault, just approximately 100m to the East. Cave believed to have formed prior to deformation.



Sediment layer in collapse cave at Little Sheep Creek. Picture taken facing ~North. The stratigraphic top of the sediment layer runs vertical on the western side. Calcite deposits behaved as a cement holding sediment layer and collapse blocks in place during folding and faulting.

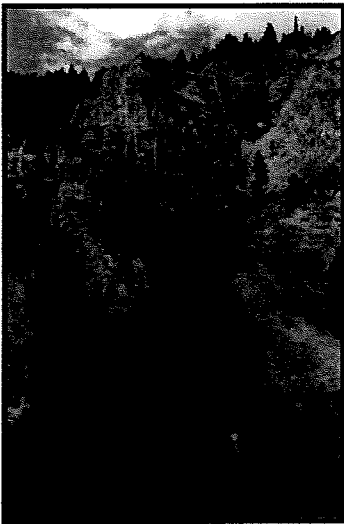
Appendix 4. Styles of Veining



Single layered veins at Little Sheep Creek.



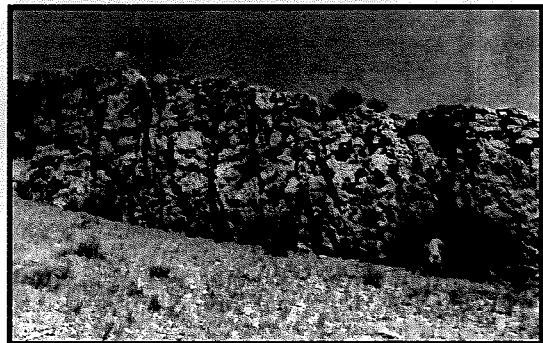
Post-compression multi-layered vein in the Four Eyes Canyon thrust sheet.



High angle post-compression veins in the Four Eyes Canyon thrust sheet, cutting all Sevier structures. Across the stream from UPS stop.



Monster post-compression vein, ~3m, in the Four Eyes Canyon thrust sheet.



Compressional veins at Little Sheep Creek. Longitudinal veins run left to right and transverse veins run up and down.

Appendix 5. Orientation Results

- Key for Abbreviations and Sample Traverses
- Sample Log
- Orientations for Veins
- Orientations for Joints
- Orientations for Joints or Veins (undistinguishable)
- Orientations for Beds
- Orientations for Faults

Key for Abbreviations and Sample Traverses

Little Sheep Creek (LSC)

South Side of Road: was not sampled or measure, but was photographed

North Side of Road: all sampling, ect. occurred here

Station1 western limb of large anticline

Station2 western limb of large anticline

Station3 western limb of large anticline

Station4 western limb of large anticline

Station5 eastern limb of large anticline

Station6 west limb of snycline

Station7 hinge of syncline

Station8 eastern limb of syncline

Station9 small upright ribbon of rock within imbricates to east of mini drainage

Station10 western large fin of rock, extensive, within imbricates to east of mini drainage

Station11 western large fin of rock, extensive, within imbricates to east of mini drainage

Station12 eastern large fin of rock, extensive, within imbricates to east of mini drainage, subdivided into A-E

Station13 unexposed Tendoy fault in small drainage, Kb float on east, Mll float on west

Station14 large isolated block between two major fins, near base of hill, east of mini drainage, subdivided into A,B,C

Station15 collapse cave in eastern large rock fin, within imbricates

Station16 small isolated block, eastern most mini fin, near Tendoy fault

Station 16* below large anticline to west of mini drainage, small tight anticline

Key for Abbreviations and Sample Traverses Continued

Big Sheep Creek (BSC)

- Station 1
- Station2
- Station3
- Station4
- Station5
- Station6
- Station7
- Station8
- Station9
- Station10
- Station11
- Station12
- Station13
- Station14

79

Birch Creek (BC)

- Station1
- Station2

McKnight Canyon (McK)

Key for Abbreviations and Sample Traverses Continued

Four Eyes Thrust Sheet

Station1

Station2

Station3

Station4

Station5

Station6

Station7

Station8

Station9

Station10

Station11

Key for Abbreviations and Sample Traverses Continued

TdF = Tendoy thrust fault

UPS = frontal portion of Four Eyes thrust sheet, near Muddy Creek Basin

V = Vein

J = Joint

B = Bedding

F = Fault

Orientations measured with a quadrant Brunton

Mll = Lombard limestone

Con.R. = Conover Ranch formation

Pq = Quadrant sandstone

Kb = Beaverhead conglomerate

HW = hanging wall

FW = footwall

Long (L) = longitudinal veins

Trans (T) = transverse veins

Bed // = bed parallel

Sample Log

Sample ID #	Page	Station	Description	Vein(s)/other	Orientations
Td01-ACJ-	1 p.42	LSC, B2		Conv. R. lm	B: N55W, 47SW
Td01-ACJ-	2 p.52-52	LSC, stat.14		V: a-d	B: N33W, 18S
Td01-ACJ-	3 p.51-52	LSC, stat.14		V: z, ff, gg	B: N35W, 89N
Td01-ACJ-	4 p.51-52	LSC, stat.14		V: hh, ii, jj, kk, v	B: N32W, 77S
Td01-ACJ-	5	LSC, stat.14		V: P(?) and below	B: N35W, 87S
Td01-ACJ-	6 p.53	LSC, stat.14		V: i, j, k, n (2 pieces)	B: N32W, 77S
Td01-ACJ-	7 p.56+57	LSC, stat.14		V: n, o, p	B: N32W, 70S
Td01-ACJ-	8 p.60+61	LSC, stat.12		V: h, i, j, k	B: N10E, 81S
Td01-ACJ-	9 p.60+61	LSC, stat.12		V: c ?	B: N15W, 75S
Td01-ACJ-	10 p.60+61	LSC, stat.12		V: d	B: N5W, 80W
Td01-ACJ-	11 p.63	LSC, sect.12		V: 4	B: N40W, 70W
Td01-ACJ-	12 p.70	LSC, stat.16		Vein and fault	B: N75W, 68W; V: N10E, 65S;
					F: N25E, 25S
Td01-ACJ-	13 p.77	BSC, stat.5		Vein	V: N52E, 32S
Td01-ACJ-	14 p.83	BSC, stat.4A		V: I	V: N45W, 39E
Td01-ACJ-	15 p.83	BSC, stat.4A		V: g	V: N46W, 35N
Td01-ACJ-	16 p.83	BSC, stat.4A		V:a	V: N47W, 31N
Td01-ACJ-	17 p.83	BSC, stat.4A		V: c	V: N56E, 88N
Td01-ACJ-	18 p.86	BSC, stat.4B		Vein	V: N65E, 89N; B: N12W, 47W
Td01-ACJ-	19 p.87	BSC, stat.4B		Vein	V: N81E, 87S; B: N14E, 31N
Td01-ACJ-	20 p.87	BSC, stat.4B		Vein	V: N82E, 86S
Td01-ACJ-	21 p.87	BSC, stat.4B		Vein	V: N25E, 62S
Td01-ACJ-	22	LSC stat.15		coll. Cave, calc.+clasts	
Td01-ACJ-	23 p.90	BSC, stat.9		Vein	V: N75W, 60S
Td01-ACJ-	24 p.93	BSC, stat.11		V: b	V: N5E, 81W
Td01-ACJ-	25 p.93	BSC, stat.11		V:c	V: N4E, 78W; B: N26W, 14W
Td01-ACJ-	26	BSC, stat.11		V:e	V: N33?, 59NW; B: N40W, 28NE
Td01-ACJ-	27 p.98	BC, stat.1		Vein	V: N55E, 88NW; B: N44W, 22NW
Td01-ACJ-	28 p.98	BC		V: b	V: N71E, 52S; B: N70E, 21N
Td01-ACJ-	29 p.98	BC		V: 9	V: N48E, 52N; B: N89W, 12S

Sample Log Continued

Sample ID #	Page	Station	Vein(s)/other	Orientations
Td01-ACJ-	30 p.99	BC	V: 10	V: N78E, 47N
Td01-ACJ-	31	BC	V: 7, 8	V7: N88E, 45N; V8: N10E, 70E; B: N75W, 32S
Td01-ACJ-	32 p.99	BC	V: 11	V: N73E, 58N; B: N79W, 32S
Td01-ACJ-	33 p.99	BC	V: 12, 13, 14	V: N78E, 52N; N82E, 58N; N81E, 52N; B: N83W, 30S
Td01-ACJ-	34	BC	V: 15	V: N84E, 54W; B: N75E, 40S
Td01-ACJ-	35 p.123	LSC, stat.12	V: b	N60E, 73S
Td01-ACJ-	36 p.126	LSC, stat.16	shear fibers	N10E, 67S
Td01-ACJ-	37 p.126	LSC, stat.16	protolith	N10E, 67S
Td01-ACJ-	38 p.127	LSC, stat.16	Vein material in wedge	
Td01-ACJ-	39 p.128	LSC, stat.16	protolith	B: N70W, 65NE; N65W, 65NE
Td01-ACJ-	40 p.129	LSC, stat.16	longitudinal vein	N65E, 75S
Td01-ACJ-	41 p.129	LSC, stat.16	perpendicular vein	N35W, 80W; N19W, 62W
Td01-ACJ-	42 p.130	LSC	V: b	V: N18W, 50E; N20W, 57E; N15W, 60E
Td01-ACJ-	43 p.130	LSC	V/F: d	V: N70E, 30N
Td01-ACJ-	44 p.132	McK	Kb	
Td01-ACJ-	45 p.132	McK	breccia	
Td01-ACJ-	46 p.132	McK	float with veins	
Td01-ACJ-	47 p.133	BSC, UPS	Vein	V: N68E, 75N
Td01-ACJ-	48 p.133	BSC, UPS	Veins within beds	
Td01-ACJ-	49 p.135	4Eyes, stat.1	V: a	N65W, 44S (bed-//)
Td01-ACJ-	50 p.135	4Eyes, stat.1	V: c	N40E, 75W
Td01-ACJ-	51 p.135	4Eyes, stat.1	V: d	N57W, 40S
Td01-ACJ-	52 p.137	4Eyes, stat.1	V: k+j	N4E, 85W; N25W, 79S
Td01-ACJ-	53 p.139	4Eyes, stat.2A	V: A, B, C, L, M, O	N56E, 67W; N14Q, 84S; N80E, 68NW; N68E, 89N N28W, 88S; N78W, 32S
Td01-ACJ-	54 Book2 p.1-3	4Eyes, stat.3	V: b, E, L	N70E, 83S; N9W, 77N; N84E, 74S
Td01-ACJ-	55 p.8	4Eyes, stat.4C	V: a	N12W, 32W (bed-//)
Td01-ACJ-	56 p.8	4Eyes, stat.4C	thin B paral., Td fluid?	

Sample Log Continued

Sample ID #	Page	Station	Vein(s)/other	Orientations
Td01-ACJ-	57 p.12	4Eyes, stat.4D	Monster Vein	N60E, 20W
Td01-ACJ-	58 p.13	4Eyes, stat.4D	V: c	N23E, 84N
Td01-ACJ-	59 p.14	Medicine L.	Vein	V: N10E, 83W; B: N20W, 16SW
Td01-ACJ-	60 p.14	Medicine L.	Fault	F: N12E, 15W
Td01-ACJ-	61 p.15	4Eyes, stat.1	Vein	V: N26W, 86W; 11P7, 3S24
Td01-ACJ-	62 p.15	4Eyes, stat.1	Vein	V: N26W, 86W; 11P8, 3S25
Td01-ACI-	63	BSC, stat.6	Black shale	

Orientations of Veins

sample site	orientation	notes about that vein	notes about site
LSC - stat.14a3	N45W, 10SW	a: 8cm long, 1mm wide	vein spacing (m)
	N70E, 16NW	b: 9cm long, 5mm wide, xlin	0.02, 0.02, 0.01, 0.03
	N78E, 5SE	c: 5cm long, 2mm wide, cut by a	0.05, 0.04
	"	d: 5cm long, 2mm wide, same as c	irregulare, no apparent pattern
	N88W, 16NE	e: 11cm long, 5mm wide	
	?	f: 4cm long, 1-2mm wide	
		g: ? About orien, 12cm long, 5-2 mm wide	vein thickness (mm)
	?	h: 6cm long, 1mm wide	varies from 0.25-5mm
	N2W, 35SW	i: 5cm long, 2mm wide	most are 1-2mm
	N15W, 37SW	j: 13.5cm long, 1-4mm wide, fibrous?	
	N9W, 41SW	k: 9cm long, 1-5mm wide	pictures
	N1E, 20W	l: 18cm long, 5mm wide	2P18+19
	?	m: 9cm long, 0.5mm wide	1S11+12
	N38W, 30NE	n: 9cm long, 1mm wide	
	?	o: 6cm long 1mm wide	p.51-52
	N38W, 25SW	p: 15cm long, 3mm wide	
	N1E, 36W	q: 16cm long, 3mm wide	sketch
	N54W, 34SW	r: 25cm long, 5mm wide	
	N15W, 25SW	3cm long, 5mm wide	
	N54E, 40NW	s: 5.5cm long, 1mm wide	
	N77W, 15NE	t: 11cm long, 3mm wide	
	?	u: 6cm long, 2mm wide	
	N75E, 25NE	v: 50cm long, 5mm wide, cut by bb, x, y, z	
	N60E, 84SE	w: 15cm long, 1mm wide	
	N50E, 82SE	x: 4cm long, 0.5mm wide	
	N45E, 82SE	y: 4cm long, 0.5mm wide	
	N46E, 70SE	z: 7cm long, 1mm wide	
	N62W, 37SW	ff: ??? ff-kk very hard to measure orien	
	N19W, 22SW	gg:???	
	N34W, 50SW	hh:???	

Orientations of Veins Continued

sample site	orientation	notes about that vein	notes about site
	N35W, 64NE	ii:???	
	N45E, 70SE	jj:???	
	N36E, 84SE	kk:???	
	N70E, 89N	ll: longit vein	p.122
	N30W, 72W	mm: bed //, shear vein	
	N25W, 87W	nn: bed //	
LSC, stat.14a2	N48W, 28NE	cc: 5mm wide	p.52
	N75E, 14W	dd: 5-10mm wide	pictures
	N75E, 52NW	ee: 4mm wide	2P25, 1S18
LSC, stat.14a4	N60E, 88S	a: 5mm wide, xlin	
	N5E, 17W	b: 2mm wide	veins a,c,e,h,I,k,L are
	N72W, 24NE	c: same as aa ~1cm wide	drawn to scale as far
	N32W, 26SW	d: 3mm wide	as placement
	N63W, 16NE	e: 3mm wide	
	N43E, 35S	f: ? 2-5mm wide	sketch
	N77W, 35NE	g: 3mm wide, xlin	
	N84E, 15NE	h: 3mm wide, split in middle	p.53
	N76E, 14N	I: 2mm wide	
	N88E, 18S	j: ? 2-6mm side	
	see h+I	k: same as h+I, 3mm wide	
	N10E, 24W	L: ?, 3m wide?	
	N70E, 87S	m: vein material on surface, can't get width	
	N14E, 84W	n:	
LSC, stat. 14B	N21W, 44SW	j: 2-5mm wide	p.54-55
	N18E, 35NW	k: 2-5mm wide	
	N47E, 35SE	l: 2mm wide	sketch (all to scale)
	N41E, 41NW	o: 2mm wide	
	N57E, 72SE	p: ~1mm wide	
	N17W, 34SW	q: ~3mm wide	
	N30W, 32SW	r: ~3cm wide, sim orien to q	
LSC - stat.14C	N80W, 29NE	h: ?	p. 56-57

Orientations of Veins Continued

sample site	orientation	notes about that vein	notes about site
	N31W, 68NE	I: 1mm wide	sketch (outline and faults a+b are to scale)
	N42W, 52NE	j: 1mm wide	
	N28E, 29NW	n: 1mm wide	
	N14W, 55SE	o: 1mm wide	
	?	p: 1mm wide	
	N15W, 16NE	q: 2 diff veins, 2-3mm wide	
	N75W, 45NE		
	N70E, 79S	1: -	p.122
	N60E, 84SE	2: -	sketch
	N62E, 82S	3: -	spacing: 6 veins per 2m
	N69E, 79S	4: -	spacing bet Vs:
	?	5: set with 6	.6m, .5m, .4m, .35m, .25m
	N45W, 35N	6: set with 5	
LSC - stat.12A	N81W, 40S	a:	p.60-61
	N42E, 26S	b: 4cm long, 2mm wide	sketches (all to scale)
	N78E, 48S	c: 28cm long, 2-4mm wide	
	N89W, 46S	d: 28cm long, 3mm-1.2cm wide	
	N78E, 19S	e: 9cm long, 1mm wide	
	N65W, 29S	f: 18cm long, 2mm wide	
	N45W, 14S	g: 3mm wide, xlin	
	N81E, 82N	h: 1mm wide	
	N86W, 80N	I: 0.5mm wide	
	N80E, 50S	j: 8cm long, 3-4mm wide	
	N75W, 44S	k: 8cm long, 2-6mm wide	
	N38E, 25S	L: 10 cm long, 5mm wide	
	N75W, 28S	m: 1m wide	
	N42E, 35S	n: 1mm wide	
	N20W, 14W	o: 2mm wide	
	N62E, 86N		
LSC - stat.12B	N28W, 36S		p.62
	N29W, 22S		

Orientations of Veins Continued

sample site	orientation	notes about that vein	notes about site
	N2W, 35E		
	N30W, 30SW		
LSC-stat.12C	N68W, 50NE		p.62
	N71W, 55NE		
	N15E, 9NW	a: shear vein on fault	p.123
	N60E, 73S	b: long vein, 2 per ext - 1st thin xlin 2nd open fract xls	
	N4E, 19W	c: shear vein perp to bed, cut by b	timing - c+d to b shear
	N71W, 22S	d: gash vein formed w/ c, spaced 0.05m	to b ext to a
LSC - - stat.12D	N85W, 41N	poss 3mm wide	p.62
LSC - stat.12E	N68E, 58S		p.63
	N60E, 64S	sim to above	
	N70E, 60S	sim to above	
	N88W, 22N		
	N35W, 24E		
	N63E, 82S		
	N61E, 60S		
	N20W, 10W		
	N5W, 32E		
	N45W, 30N	1: see p.59	
	N45W, 30N	2: see p.59	
	N62W, 18N	3: see p.59	
	N20E, 31S	4: no in pic/sampled	
LSC - stat.11	N25E, 35S	1: 4mm wide	p.65
	N69E, 34N	2: 2mm wide	sketch
	N58W, 30N	3: 1mm wide	
	N25E, 88S		
	N77W, 76S		
LSC - stat.16.	N10E, 65S		
	N88E, 70W	shear fibers, also fault, bed //	
	N80W, 88E		
	N58W, 68E		

Orientations of Veins Continued

sample site	orientation	notes about that vein	notes about site
	N78W, 72S	a: shear fibers, bed //, cuts c	p.126
	N32E, 62NW	b: long, ext vein, cuts c?	bed // cuts ext veins
	N63E, 56E	c: ext vein	
	N10E, 67S	d: trend and plunge, fiber on a	
	N70W, 88SW	bed // shear fibers, fiber lin N5W, 72S	
BSC - stat.5	N52E, 32S	sampled, thick, course text, layers	p.77
BSC - stat.4A	N21E, 35S	~2m long, near Martin nest	p.81
	N47W, 31N	a: ranges from 5mm-1.5cm wide, xlin	p.82
	N59E, 75N	b: about 1cm wide, very xlin	sets
		c: see blowup sketch too	d+e = transverse
	N11E, 42S	d:	h+I = longitudinal
	N41W, 72N	e: 3-4mm wide, xlin	g+k = conj set, disp
	N11W, 48S	f: major surface, many like it	beds
	N46W, 35N	g: ~5mm wide	? = bed //, cant see
	N56E, 88N	h:	any, may be to dirty
	N52E, 74S	I:	or not there
	N45W, 39E	j: sampled	
	N76E, 89N	j:	
	N10E, 74S	k:	
	N55E, 56S	~7.5m to west along road, further down	p.84
BSC - stat.4B	N82W, 74S	a:	p.85
	N85W, 79S	b: 5mm	sets
	N87E, 75S	c: 1m wide	a-e = longit set
	N89E, 84S	d: 7mm wide	f = transv set
	N87W, 80S	e:	poss longit cuts trans
	N26E, 65S	f: set	see no bed // poss
	N84E, 82S	g: 5mm wide	since no folding
	N81E, 88S	h:	
	N70E, 89N	I:	
	N89W, 79S	k:	
	N86E, 84S	same as k	

Orientations of Veins Continued

sample site	orientation	notes about that vein	notes about site
	N26E, 67S	sim to f	
	N23E, 60S	sim to f	
	N50E, 84S		p.86
	N62E, 84N		
	N49E, 77S	very xlin, 3mm wide	
	N30E, 71S		
	N76E, 86N		
	N65E, 89N	~1cm wide	
	N81E, 87S	4mm wide	p.87
	N82E, 86S	mult periods of flow, complex text	
	N12E, 61E	1.5-2.5cm wide, very xlin	
BSC - stat.8b	N69W, 67NE		p.89
	N85W, 70NE		
	N65E, 61S		p.90
	N7E, 50E		
BSC - stat.9	N74W, 72S		p.90
	N75W, 60S	in biopackestone	
BSC - stat.7A	N14W, 86S		p.91
	N38W, 63S		
	N74W, 71S		
	N41W, 88NE		
	N25W, 74W		
	N30W, 84S		
BSC - stat.7B	N31W, 70N		p.91
	N38W, 82NE		
	N19W, 62E	East of fault	p.92
	N1W, 76E		
	N16E, 88E		
	N52W, 71SW		
BSC - stat.11	N72E, 71N	a:	p.94
	N5E, 81W	b:	

Orientations of Veins Continued

sample site	orientation	notes about that vein	notes about site
	N4E, 78W	c:	
	N1E, 79W	d:	
	N33E, 59NW	e:	
BC - stat.1	N50E, 64SE	1: plane exposed	p.98
	N55E, 89NW	2: sample 27	
BC - stat.2	N81E, 62S	3: a	9.98-99
	N71E, 52S	4: b, sample 28	
	N65E, 51S	5: c	
	N58E, 57S	6: -	
	N88E, 45N	7: -	
	N10E, 70E	8: -	
	N48E, 52N	9: -	
	N78E, 47N	10: from very dark thin bedded mudst, no fossils	
	N73E, 58N	11: from very dark thin bedded mudst, no fossils	
	N78E, 52N	12: same as above + same bed but higher up	
	N82E, 58N	13: " "	
	N81E, 52N	14: " "	
	N84E, 54N	15: sample 34	
LSC - stat.10	N55E, 33N	3cm wide, doesn't cross bed	p.124
	N10W, 15E	a:	bed has shear v which
	N1W, 24E	b:	cuts perp V
	N65E, 86S	c:	bed // cuts perp
	N60E, 89S	d:	a+b poss cut others
	N61E, 84S	e:	spacing: c-e over 0.8m
	N55E, 85S	f:	a+b is 3V per 1.4m
	N70W, 11N	a: cuts b+d ?	p.125
	N62E, 75N	b: poss cuts e ?	
	N74E, 74N	c:	
	N52E, 52S	d:	
		e: long vein, spacing (cm) 6,4,7,6,22,13,9,5,12,3,5	
LSC - stat.17	N28E, 55N	sample #39, east limb	p.128

Orientations of Veins Continued

sample site	orientation	notes about that vein	notes about site
	N45E, 86N	set, 1 every ~15cm, east limb	
	N41E, 80N	east limb	
	N55E, 84S	east limb	
	N57E, 76S	east limb	
	N60E, 72S	set, east limb	
	N60E, 62S	east limb	
	N85E, 25N	a: bed with shear, hinge	p.129
	N65E, 75S	b: trans, hinge	a cuts d (// cuts tran)
	N35W, 80W	c: long, hinge	poss b cut by c
	N19W, 62W	d: long, hinge	d offset by bed
	N60E, 61S	poss cong pair, hinge	c+d same set
	N55E, 88N	poss cong pair, hinge	
	N20W, 57E	b: sample #42	p.130
	N18W, 50E	b:	b cut by c
	N15W, 60E	b:	no bed // shear
	N75E, 82S	c:	c spaced every 6-10cm
	N66E, 84S	c:	d cut by c
	N70E, 30N	d: sample #43, shear fault with gashes	e poss cuts c
	N40W, 64N	e:	
LSC - bet 12+13	N86E, 75N	set, spaced ~ 1'	p.131
	N55E, 89S	set spaced ~ 0.5'	on road, thin lime
	N51W, 67N	set spaced ~ 6cm	mudstone with veins
	N82W, 62N		

Orientations of Joints

sample site	orientation	notes about that joint	notes about that site
B1-	N66E, 86NW	p.41	
	N55E, 80NW	p.41	
B1a-	N40W, 87NE	p.42	
	N45W, 81NE	p.42, same joint as above	2 joint sets
	N38W, 79NE	p.42	
	N49W, 78NE	p.42	
LSC - stat.12E	N58E, 81S		p.63
	N60E, 85S		
	N70E, 86S		
LSC - stat.11	N61E, 78N	1: p.65	
	N60E, 81N	2: p.65	
BSC - stat.4A	N55W, 32E	p.81	
	N81W, 88N	p.82	
BSC - stat.4B	N28W, 46E	p.85	
	N57E, 79S	p.86	
	N45W, 63N		
	N31E, 53S	p.87	

Orientations of Joints or Veins (undistinguishable)

sample site	orientation	notes about that fracture	notes about site
LSC - stat.14a	N87W, 35NE	vein?, #6, p.50	
	N87E, 39NE	vein?, #7, p.50	
	N10W, 25SW	j/v?, #8	
LSC - stat.14a3	N89E, 31N	aa: >3m long, ~1cm wide, poss truncated by fault around corner	
	N55E, 86SE	bb: >2m long, reopened	
LSC - stat.14B	N82E, 64N	b: poss aa from A, truncated by a	p.54-55
	N75W, 58SW	c: too weathered to tell	sketch
	N28W, 78SW	d: bedding/joint?	
	N19W, 70SW	e: bedding/joint?, sim to d	
	N60E, 64S	g: j/v? too weathered, in massive bed	
	N12W, 82W	h: j/v?	
	N31W, 71W	I: j/v?	
	N80E, 81N	m: planes sim to b, j/v?	
	N88E, 74N	n: planes sim to b, j/v?	
	LSC - stat.14B	N58W, 25NE	b: v/j?
N20W, 72SW		c: bedding?	sketch
N36E, 50NW		d: j/v?	
N37W, 75SW		e: fracture/bedding?	
N41W, 65SW		g: fracture/bedding?	
N49E, 67NW		L: some conjugate plane with m	
	N44E, 25NW	M: some conjugate plane with L	
LSC - stat.12E	N87E, 61N	j/v?	p.63
LSC - stat.11	N23W, 35E	j/v?	p.65
	N18W, 36E	j/v?	
BSC - stat.4B	N75W, 27N		

Orientations of Beds

sample site	orientation	notes about that bed	notes about site
B1	N20E, 23NW	p.41	
	N15E, 30NW	p.41	
B2	N25W, 45SW	p.42	Conv.R.
	N30W, 50SW	p.42	
	N55W, 47SW	sampled, p.42	
LSC - stat.1	N27W, 51SW	p.44	
	N44W, 45SW	p.44	
	N46W, 32SW	p.44	
	N35W, 37SW	p.44	
LSC - stat.2	N45W, 46SW	p.44	
LSC - stat.3	N38W, 33SW	p.44	
	N35W, 40SW	p.44	
LSC - stat.4	N22W, 35SW	p.44	
	N30W, 32SW	p.44	
LSC - stat.5	N40W, 48NE	p.44	
	N50W, 50NE	p.44	
LSC - stat.6	N58W, 50NE	p.44	
LSC - stat.7	N35E, 10SE	?, p.44	
LSC - stat.8	N32W, 39SW	also fault plane, p.44	
	N38W, 49SW	also fault plane, p.44	
LSC - stat.9	N35W, 65SW	p.44	
LSC - stat.10	N32W, 73SW	p.44	
	N33W, 70SW	p.44	
	N25W, 74SW	uneven, p.124	
LSC - stat.11	N38W, 75SW	p.46	
LSC - stat.12	N31W, 76SW	p.46	
LSC, stat.14	N34W, 85NE	p.46	
LSC, stat.14a	N30W, 79SW	#2, p.50	
	N34W, 80SW	#9, p.50	
LSC, stat.14B	N30W, 81SW	f: argill layer, p.54-55	

Orientations of Beds Continued

sample site	orientation	notes about that bed	notes about site
LSC, stat.14C	N31W, 74SW	k: p.56-57	
	N26W, 75SW	r: p.56-57	
LSC, stat.12A	N5W, 89W		1 p.60-61
	N10E, 81W		2 sketch
	N15W, 71W		3
	N5W, 80W		4
	N15W, 75E		5
LSC - stat.12E	N40W, 70W	approx, uneven surface	
LSC - stat.11	N25W, 71W		p.65
	N32W, 73W		
	N28W, 76W		
LSC - stat.15	N25W, 78W		
	N26W, 80W		
	N20W, 81W		
	N2W, 78W	cave sed. Layer	
LSC - stat.16	N75W, 68W		p.70-71
	N35W, 68W	west limb	these four are tight
	N20E, 25N	hinge	fold, ~3m bet limbs
	N75E, 56E	east limb	fold axis ~N55W
	N72W, 72E	east limb	
	N78W, 72S	shear vein, fault	p.127
	N70W, 88SW	shear vein, fault	
BSC - stat.5	N38E, 65N		p.77
	N28E, 42NW		
	N25E, 31NW		
BSC - stat.4A	N21W, 70W	top limb	p.81
	N89W, 85E	hinge	sketch
	N20W, 62W	bottom limb	
	N22W, 61W	big sketch	p.82
	N25W, 62W	mini sketch	
BSC - stat.4B	N12W, 25N		

Orientations of Beds Continued

sample site	orientation	notes about that bed	notes about site
	N12W, 47W	p.86	
	N14E, 31NW	p.87	
BSC - stat.8b	N1E, 87W	upturned bed, top	p.89
	N45W, 27NW	upturned bed	
	N1E, 40NW	upturned bed	
	N15E, 52NW	upturned bed	
	N67E, 44N	higher on hill	
	N41E, 57N	lower on hill	
	N25E, 16N	lower on hill	
	N40E, 39N	lower on hill	
BSC - stat.7A	N15E, 34N		p.91
BSC - stat.7B	N26E, 28N		p.91
	N35E, 39N	west of fault	
	N44E, 50N	west of fault	
	N81E, 65N	east of fault	
	N45E, 64NW	east of fault	
	N42E, 22NW	east of fault	
	N30E, 54NW	east of fault	
	N19W, 60NW	east of fault	
	N10W, 70NW	east of fault	
BSC - stat.11	N28W, 38W	west limb of fold	p.93
	N40W, 12W	west limb of fold	trend of fold is ~N25W
	N1E, 11W	west limb of fold	
	N19W, 12E	hinge	
	N45W, 89W	east limb of fold	
	N20W, 74SW	east limb of fold	
	N25W, 75NE	east limb of fold	
	N40W, 28NE		
	N26W, 14W		
BC - stat.1	N45E, 22NW	west limb of fold	p.98
BC - stat.2	N20E, 21N	with vein 5	p.98-99

Oriations of Beds Continued

sample site	orientation	notes about that bed	notes about site
	N75W, 32S	with vein 8	
	N89W, 42S	with vein 9	
	N79W, 32S	with vein 11	
	N83W, 30 S	with vein 14	
	N52W, 28N	east limb of fold	
	N80W, 41N		
	N75E, 40S	with vein 15	
LSC - stat.17	N70W, 65NE	east limb	p.128-129
	N64W, 65NE	east limb	
	N85E, 75S	shear vein, hinge	
	N27W, 39W	west limb	p.130
LSC - bet 12+13	N38W, 67W		p.131, on road

Orientations of Faults

sample site	orientation	notes about that fault	notes about site
LSC - stat/8			
	N32W, 39SW	bedding plane, HW up to E, p.44	
	N38W, 49SW	bedding plane, HW up to E, p.44	
LSC - stat.14a	N38W, 27SW	HW up to E, #1, p.50	
	"	similar to above, no evid, #10, p.50	
LSC, stat.14B	N39W, 35SW; rake 88S	a: offset beds, slicks, HW up, p.55	
LSC, stat.14C		a: sim to fault a at B (above), too high	
LSC - stat.12B	N49W, 20W	? Slicks rake ~perp to strike HW up to E, p.62	
LSC - stat.12C	N15E, 9NW	3: go with this, HW up to E	
	N15E, 9NW	same as above, rake is N55W, 8W (trend + plunge)	p.123
	N4E, 19W	has gash veins, see sketch	
LSC - stat.12D	N15E, 17W	3: HW up to E	p.62
	N35W, 9W	rake ~perp to strike, if anything to S, Normal fault, HW down to SW	
	N30W, 20W	HW up to E	
LSC - stat.12E	N7W, 22W	2: see sketch	p.63
	N56W, 21SW	1: see sketch	
	N58W, 27SW	2: bed drag, HW up to E	
LSC - stat.16	N88E, 70W, rake 70N	bedding plane, HW down to W	p.70-71
	N80W, 88E	same as above	
	N58W, 68E, rake 55N	same as above	
	N25E, 25S	HW up to NE	
	N49W, 64NE	HW up to W, back thrust	
BSC - stat.4B	N80W, 85N	slicks, HW out to road SE, p.85	
	N77E, 72SW, rake 28W	HW to west, p.87, slicks	
BSC - stat.8a	N77E, 71N	like fault on p.87, no rake, slicks //to strike, p.88	
BSC - stat.7B	N27W, 51NW	p.92	

Sample	Inclusions Present	Th (°C)	Tm ice (°C)	Flouress	Conclusions
6 (BSC)	potential fluid and hydrocarbon	-----	-----	-----	decrepitated
11 chip 1 (LSC)	-----	-----	-----	-----	decrepitated
16 chip 1 (LSC)	potential fluid and hydrocarbon	heated to 100°	-----	-----	either fresh/empty/degraded hydrocarbon; not methane or hydrocarbon
16 chip 2 (LSC)	potential fluid and hydrocarbon	+48° to +66°	-----	-----	low temperature fluid
20a (BSC)	potential fluid and hydrocarbon	heated to 320°	-----	-----	decrepitated
21 chip 1 (BSC)	potential fluid, hydrocarbon, calcite	-----	+1.8°	-----	freshwater, metastable superheated ice
21 chip 2 (BSC)	potential fluid and hydrocarbon	+159.4°	+3.6°	-----	freshwater, metastable superheated ice
21 chip 3 (BSC)	potential fluid and hydrocarbon	expanded-no return -----	-0.6°	-----	freshwater, metastable superheated ice - decrepitated
25 (BSC)	potential fluid and hydrocarbon	-----	-----	-----	decrepitated
33 (BC)	potential fluid	-----	-----	-----	decrepitated
45 chip 1 (McK)	potential fluid and hydrocarbon	+216°	-----	-----	don't trust, bubble formed when frozen- didn't return after heating
61a chip 1 (4Eyes)	potential fluid, hydrocarbon, calcite	heated to 200°	-----	-----	solid calcite and degraded hydrocarbon
61a chip 2 (4Eyes)	potential fluid and hydrocarbon	-----	-----	-----	decrepitated

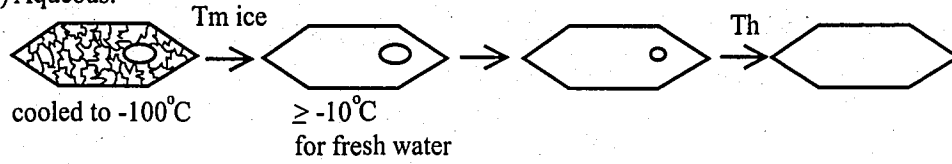
Appendix 6. Results from fluid inclusion analyses

Appendix 6.

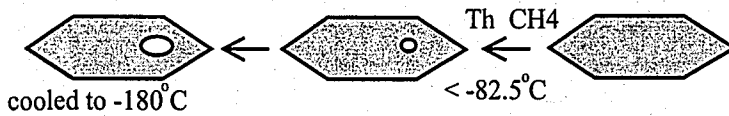
Fluid Inclusion Results

Expected:

1) Aqueous:

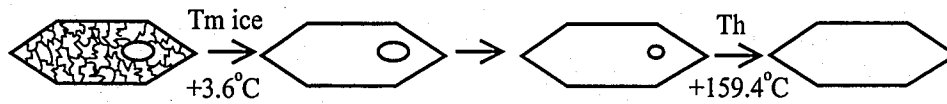


2) Hydrocarbon (CH_4) (can fluoresce blue if light or yellow if heavy)

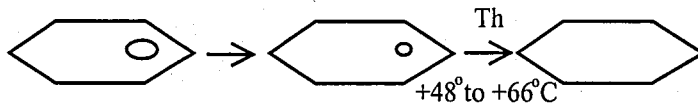


Results:

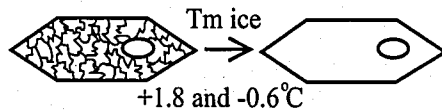
1) Aqueous Freshwater



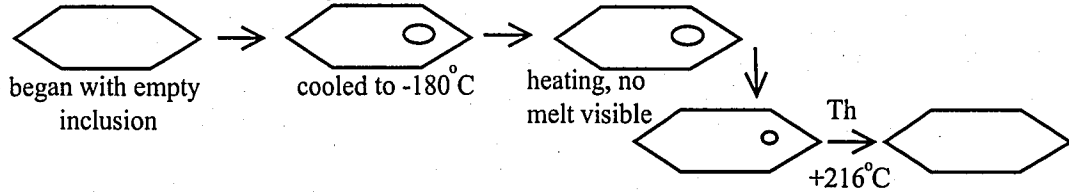
2) Aqueous



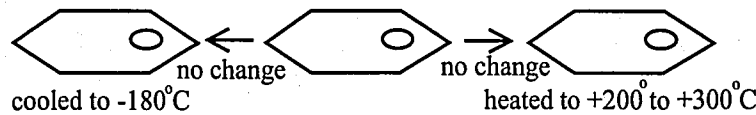
3) Aqueous Metastable Superheated Ice



4) Aqueous? Ended up decrepid

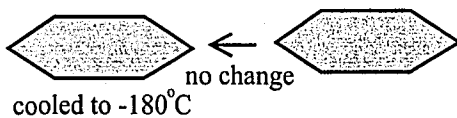


5) Aqueous? Ended up decrepid

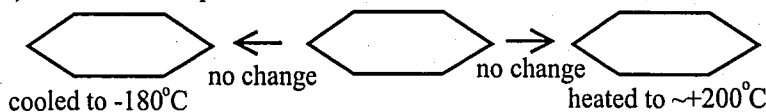


don't trust due to possible expansion from freezing

6) Degraded Hydrocarbon (CH_4) (did not fluoresce)



7) Calcite or decrepid



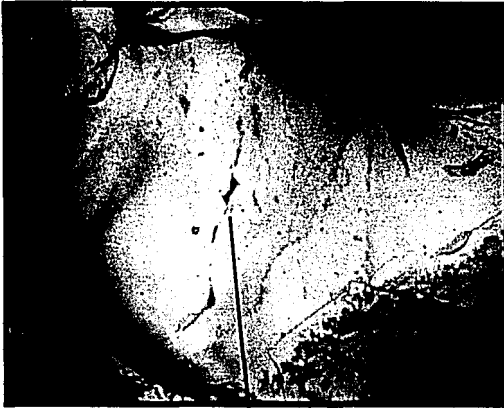
Appendix 6. Fluid Inclusion Analyses



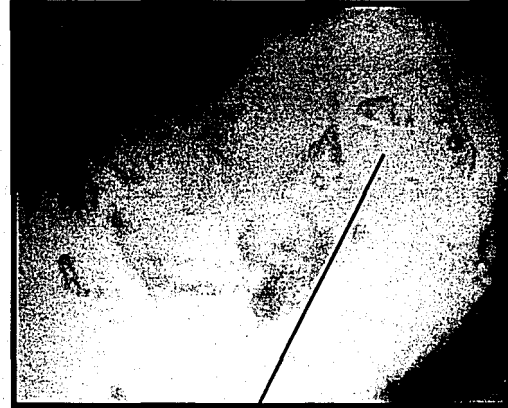
Trains of inclusions healing microfractures and running in parallel lines from left to right at an acute angle to twim lamellae. Inclusions are 2 to 5 μ .



Planar cluster of inclusions, 2 to 5 μ .



Train of degraded hydrocarbon inclusions healing a microfracture. Inclusions are ~2 to 5 μ .



Cluster of three aqueous fluid inclusions with vapor bubbles. Inclusion are 2 to 5 μ .



Degraded hydrocarbon inclusion, ~5 μ

Appendix 7. Stable Isotope Data

- Run 1: April, 2001
- Run 2: October, 2001
- Run 3: December, 2001
- Previous Studies Data
- Veins by Timing and Thrust Sheet
- Veins by Set
- Protolith, Microlithons, and Selvages
- Fluid Compositions of Veins
- Individual Samples

Run 1: April, 2001
 used standard 8-3-7vCO3

Sample #	Location	True Vein Set	delta 13 [^] C	delta 18 [^] O	corrected delta 18 [^] O
A1	4Eyes	bed-parallel	1.80	22.96	12.59
A2	4Eyes	bed-parallel	1.73	22.69	12.32
A4	4Eyes	bed-parallel	1.77	23.62	13.23
A5	4Eyes	bed-parallel	1.80	22.87	12.49
A6	4Eyes	bed-parallel	1.83	23.47	13.08
A7	4Eyes	bed-parallel	3.00	33.82	23.33
B1	4Eyes	?	1.45	23.20	12.82
B2	4Eyes	?	2.17	22.89	12.51
B3	4Eyes	?	1.86	17.98	7.65
B5	4Eyes	?	1.76	16.18	5.87
B6	4Eyes	?	1.74	22.74	12.36
B7	4Eyes	?	1.76	16.52	6.20
A3	4Eyes	protolith	2.84	31.86	21.39
B4	4Eyes	protolith	2.88	31.61	21.15
B8	4Eyes	protolith	2.82	32.01	21.54
STD - A			-4.18	25.52	15.11
STD - B			-4.67	24.11	13.71

Run 2 : October 8+9, 2001

used standard 8-3-7v CO2 (both were lost, but should be ok)

Sample #	Location	True Vein Set	delta 13C	delta 18O	corrected delta 18O
20a	BSC-DWG-4B	Transverse	2.046	20.936	10.55
20b	BSC-DWG-4B	Transverse	1.805	20.34	9.98
22	LSC - col cave	-----	2.619	20.997	10.64
25	BSC-11	Longitudinal	-0.391	19.317	8.89
33	BC	Transverse	0.168	31.308	20.84
36	LSC-16	Bed-parallel	-0.639	36.162	25.65
40	LSC-16	Longitudinal	-0.854	31.664	21.2
42	LSC-17c	Longitudinal	1.206	37.345	26.82
45	McK	-----	2.131	24.89	14.49
47	UPS	post def.	1.689	20.178	9.83
48	UPS	-----	2.772	31.652	20.89
56	4Eyes-4C	Transverse	1.905	16.724	6.41
61	4Eyes-1	Longitudinal	1.529	23.812	13.42
STD A		-----	lost	lost	lost
STD B		-----	lost	lost	lost

Run 3: December 10-14, 2001

used standard 8-3-7v CO3

Sample #	Location	True Vein Set	delta 13C	delta 18O	corrected delta 18O
13-1	BSC DWG 5	Longitudinal	4.82	35.42	24.91
13-2	BSC DWG 5	Longitudinal	2.54	39.39	28.84
13-3	BSC DWG 5	Longitudinal	0.95	20.09	9.74
13-4	BSC DWG 5	Longitudinal	4.96	35.30	24.79
13-5	BSC DWG 5	Longitudinal	2.40	36.62	26.10
13-6	BSC DWG 5	Longitudinal	0.22	20.86	10.50
59(p)	Med Lodge	protolith	1.83	32.79	22.31
59(v)	Med Lodge	Transverse	1.37	32.04	21.57
14(p)	BSC DWG 4A	protolith	1.01	31.84	21.37
14(v)	BSC DWG 4A	Longitudinal	2.67	34.00	23.51
33(p)	BC	protolith	1.24	35.40	24.89
25(p)	BSC 11	protolith	1.42	31.48	21.01
6(p)	LSC 14	protolith	0.71	35.98	25.47
6(v1k)	LSC 14	Longitudinal	0.15	30.30	19.85
6(v2n)	LSC 14	Transverse	0.00	33.48	22.99
45(p)	Mck	protolith	4.14	33.56	23.07
48(p)	UPS	protolith	3.00	25.77	15.36
53(v)	4Eyes 2A	Longitudinal	1.78	22.99	12.61
56(p)	4Eyes 4C	protolith	2.73	29.14	18.70
42(p)	LSC 17c	protolith	0.62	37.22	26.70
Std-A	-----	-----	-4.24	25.21	14.80
Std-B	-----	-----	-4.25	25.15	14.75

4. Previous Studies Data (Chizmadia and Bebout)

Sample	Delta18O	vein	microlithon	selvage
		Delta13C Bhvein	Delta13CBH μ l	Delta13C Bhselv
BH96-SP-3hr	26.06		5.31	
BH96-15hr	26.51		1.23	
BH96-21 wr/cg per	22.23		2.88	
BH96-SP-(18)	21.71		4.97	
IrvCrkBF brec fill	24.67		2.57	
UPS- μ s-7 (2)	23.78		5.36	
UPS- μ s-8 (7)	22.63		5.03	
UPS- μ s-10 (6)	23.12		4.75	
UPS- μ s-414 (1)	23.32		5.02	
BH96-17(fibcgrv)	12.38	1.62		
BH96-SP-3 (vn)	16.67	1.95		
BH96-191vn	5.18	1.42		
BH96-14vein	9.65	2.90		
BH96-21 v/cg perp	12.68	1.82		
BH96-IC-101	13.83	0.94		
BH96-5 vn	12.80	1.60		
BH96-15 vnnrwsa	15.88	-0.30		
BH96-16	9.93	1.57		
BH96-TF-103vn	16.84	1.43		
UPS- μ s-14 (3)	10.64	3.30		
UPS- μ s-20 (10)	16.99	3.15		
UPS- μ s-4 (8)	21.92			4.12
UPS- μ s-11 (4)	21.16			4.02
UPS- μ s-21 (9)	20.82			3.80
UPS- μ s-22 (5)	22.36			4.42
BH96-14wr	13.78			3.92

Veins By Timing and Thrust Sheet

Sample #	Location	Timing	delta 13 [^] C	corrected delta 18 [^] O
A1	4Eyes	Eocene	1.80	12.59
A2	4Eyes	Eocene	1.73	12.32
A4	4Eyes	Eocene	1.77	13.23
A5	4Eyes	Eocene	1.80	12.49
A6	4Eyes	Eocene	1.83	13.08
61	4Eyes-1	Eocene	1.53	13.42
47	UPS	Eocene	1.69	9.83
B1	Med Lodge	Eocene	1.45	12.82
B2	Med Lodge	Eocene	2.17	12.51
B3	Med Lodge	Eocene	1.86	7.65
B5	Med Lodge	Eocene	1.76	5.87
B6	Med Lodge	Eocene	1.74	12.36
B7	Med Lodge	Eocene	1.76	6.20
59(v)	Med Lodge	Eocene	1.37	21.57
56	4Eyes-4C	Cretaceous	1.91	6.41
53(v)	4Eyes 2A	Cretaceous	1.78	12.61
48	UPS	Cretaceous	2.77	20.89
BH96-SP-3 (vn)	4Eyes	Cretaceous	1.95	16.67
BH96-5 vn	4Eyes	Cretaceous	1.60	12.80
UPS-μs-14 (3)	4Eyes UPS	Cretaceous	3.30	10.64
UPS-μs-20 (10)	4Eyes UPS	Cretaceous	3.15	16.99
BH96-17(fibcgrv)	Med Lodge	Cretaceous	1.62	12.38
BH96-191 vn	Med Lodge	Cretaceous	1.42	5.18
BH96-16	Med Lodge	Cretaceous	1.57	9.93
20a	BSC-DWG-4B	Cretaceous	2.05	10.55
20b	BSC-DWG-4B	Cretaceous	1.81	9.98
13-1	BSC DWG 5	Cretaceous	4.82	24.91
13-2	BSC DWG 5	Cretaceous	2.54	28.84
13-3	BSC DWG 5	Cretaceous	0.95	9.74
13-4	BSC DWG 5	Cretaceous	4.96	24.79

Veins By Timing and Thrust Sheet Continued

Sample #	Location	Timing	delta 13 [^] C	corrected delta 18 [^] O
13-5	BSC DWG 5	Cretaceous	2.40	26.10
13-6	BSC DWG 5	Cretaceous	0.22	10.50
14(v)	BSC DWG 4A	Cretaceous	2.67	23.51
25	BSC-11	Cretaceous	-0.39	8.89
BH96-TF-103vn	BSC	Cretaceous	1.43	16.84
36	LSC-16	Cretaceous	-0.64	25.65
40	LSC-16	Cretaceous	-0.85	21.20
42	LSC-17c	Cretaceous	1.21	26.82
6(v1k)	LSC 14	Cretaceous	0.15	19.85
6(v2n)	LSC 14	Cretaceous	0.00	22.99
22	LSC - col cave	Cretaceous	2.62	10.64
33	BC	Cretaceous	0.17	20.84
45	McK	Cretaceous	2.13	14.49
BH96-14vein	?	Cretaceous	2.90	9.65
BH96-21 v/cg per	?	Cretaceous	1.82	12.68
BH96-IC-101	?	Cretaceous	0.94	13.83
BH96-15 vnmrwsa	?	Cretaceous	-0.30	15.88

Veins By Set

Veins by set in Tendoy Thrust Sheet (Cretaceous)

Sample	Location	13^C	18^O	vein set
	22 LSC - col cave	2.62	10.64	Mississippian cave dep.
14(v)	BSC DWG 4A	2.67	23.51	Longitudinal
	42 LSC-17c	1.21	26.82	Longitudinal
6(v1k)	LSC 14	0.15	19.85	Longitudinal
	25 BSC-11	-0.39	8.89	Longitudinal
13-1	BSC DWG 5	4.82	24.91	Longitudinal
13-2	BSC DWG 5	2.54	28.84	Longitudinal
13-3	BSC DWG 5	0.95	9.74	Longitudinal
13-4	BSC DWG 5	4.96	24.79	Longitudinal
13-5	BSC DWG 5	2.40	26.10	Longitudinal
13-6	BSC DWG 5	0.22	10.50	Longitudinal
	40 LSC-16	-0.85	21.20	Longitudinal
20a	BSC-DWG-4B	2.05	10.55	Transverse
20b	BSC-DWG-4B	1.81	9.98	Transverse
6(v2n)	LSC 14	0.00	22.99	Transverse
	33 BC	0.17	20.84	Transverse
	36 LSC-16	-0.64	25.65	Bed-parallel
	45 McK	2.13	14.49	fault breccia
BH96-TF-103vn	BSC	1.43	16.84	?

Veins in Four Eyes Canyon and Medicine Lodge Thrust Sheets (Cretaceous)

Sample	Location	13^C	18^O	vein set
53(v)	4Eyes 2A	1.78	12.61	Longitudinal
56	4Eyes-4C	1.91	6.41	Transverse
48	UPS	2.77	20.89	?
BH96-17(fibcgrv)	Med Lodge	1.62	12.38	?
BH96-SP-3 (vn)	4Eyes	1.95	16.67	?
BH96-191vn	Med Lodge	1.42	5.18	?
BH96-5 vn	4Eyes	1.60	12.80	?
BH96-16	Med Lodge	1.57	9.93	?
UPS- μ s-14 (3)	UPS	3.30	10.64	?
UPS- μ s-20 (10)	UPS	3.15	16.99	?

Veins in Four Eyes Canyon and Medicine Lodge Thrust Sheets (Eocene)

Sample	Location	13^C	18^O	vein set
61	4Eyes-1	1.53	13.42	Longitudinal
59(v)	Med Lodge	1.37	21.57	Transverse
A1	4Eyes	1.80	12.59	Bed-parallel
A2	4Eyes	1.73	12.32	Bed-parallel
A4	4Eyes	1.77	13.23	Bed-parallel
A5	4Eyes	1.80	12.49	Bed-parallel
A6	4Eyes	1.83	13.08	Bed-parallel
B1	Med Lodge	1.45	12.82	Longitudinal or Transverse
B2	Med Lodge	2.17	12.51	Longitudinal or Transverse
B3	Med Lodge	1.86	7.65	Longitudinal or Transverse
B5	Med Lodge	1.76	5.87	Longitudinal or Transverse
B6	Med Lodge	1.74	12.36	Longitudinal or Transverse
B7	Med Lodge	1.76	6.20	Longitudinal or Transverse
47	UPS	1.69	9.83	high angle vertical set

Protolith			
Sample #	Location	delta 13 [^] C	corrected delta 18 [^] O
B8	4Eyes	2.82	21.54
56(p)	4Eyes 4C	2.73	18.70
59(p)	Med Lodge	1.83	22.31
14(p)	BSC DWG 4A	1.01	21.37
33(p)	BC	1.24	24.89
25(p)	BSC 11	1.42	21.01
6(p)	LSC 14	0.71	25.47
42(p)	LSC 17c	0.62	26.70
45(p)	McK	4.14	23.07
48(p)	UPS	3.00	15.36
A7	4Eyes	3.00	23.33

Microlithon

Sample	Delta13CBH μ l	Delta18O
A3 - 4Eyes	2.84	21.39
B-4 4Eyes	2.88	21.15
BH96-SP-3hr	5.31	26.06
BH96-15hr	1.23	26.51
BH96-21 wr/cg perprd.	2.88	22.23
BH96-SP-(18)	4.97	21.71
IrvCrkBF brec fill	2.57	24.67
UPS- μ s-7 (2)	5.36	23.78
UPS- μ s-8 (7)	5.03	22.63
UPS- μ s-10 (6)	4.75	23.12
UPS- μ s-414 (1)	5.02	23.32

Selvage

Sample	Delta13C Bhselv	Delta18O
UPS- μ s-4 (8)	4.12	21.92
UPS- μ s-11 (4)	4.02	21.16
UPS- μ s-21 (9)	3.80	20.82
UPS- μ s-22 (5)	4.42	22.36
BH96-14wr	3.92	13.78

Fluid compositions of veins under different temperature conditions continued

Sample #	Location	Timing	corrected delta 18°C	20 deg C	40 deg C	at 80 deg C	at 100 deg C
13-4	Tendoy	Cretaceous	24.79	-4.00	-1.01	5.00	7.02
13-5	Tendoy	Cretaceous	26.10	-2.73	0.27	6.29	8.30
13-6	Tendoy	Cretaceous	10.50	-17.89	-14.94	-9.01	-7.03
14(v)	Tendoy	Cretaceous	23.51	-5.25	-2.26	3.75	5.76
25	Tendoy	Cretaceous	8.89	-19.46	-16.51	-10.59	-8.61
36	Tendoy	Cretaceous	25.65	-3.17	-0.17	5.84	7.86
40	Tendoy	Cretaceous	21.20	-7.49	-4.51	1.48	3.48
42	Tendoy	Cretaceous	26.82	-2.03	0.97	6.99	9.01
6(v1k)	Tendoy	Cretaceous	19.85	-8.80	-5.83	0.16	2.16
6(v2n)	Tendoy	Cretaceous	22.99	-5.75	-2.77	3.24	5.24
22	Tendoy	Cretaceous	10.64	-17.76	-14.81	-8.88	-6.89
33	Tendoy	Cretaceous	20.84	-7.84	-4.86	1.13	3.13
45	Tendoy	Cretaceous	14.49	-14.01	-11.05	-5.10	-3.11
BH96-TF-103vn	Tendoy	Cretaceous	16.84	-11.73	-8.76	-2.80	-0.80
BH96-14vein	Unknown	Unknown	9.65	-18.72	-15.77	-9.85	-7.87
BH96-21 v/cg perp	Unknown	Unknown	12.68	-15.77	-12.82	-6.88	-4.89
BH96-IC-101	Unknown	Unknown	13.83	-14.65	-11.69	-5.75	-3.75
BH96-15 vnrwrsar	Unknown	Unknown	15.88	-12.66	-9.70	-3.74	-1.74

Individual samples

Sample	Location	13C	18O	width across (mm)
A1	4Eyes	1.80	12.59	11
A2	4Eyes	1.73	12.32	16
A3 microlith	4 eyes	2.84	21.39	21
A4	4Eyes	1.77	13.23	25
A5	4Eyes	1.80	12.49	28
A6	4Eyes	1.83	13.08	35
A7 Rock	4Eyes	3.00	23.33	39

Sample	Location	13C	18O	width across (mm)
B1	Med Lodge	1.45	12.82	3
B2	Med Lodge	2.17	12.51	7
B3	Med Lodge	1.86	7.65	14
B4 microlith	Med Lodge	2.88	21.15	20
B5	Med Lodge	1.76	5.87	27
B6	Med Lodge	1.74	12.36	35
B7	Med Lodge	1.76	6.20	42
B8 Rock	Med Lodge	2.82	21.54	47

Sample	Location	13C	18O
13-1	BSC DWG 5	4.82	24.91
13-2	BSC DWG 5	2.54	28.84
13-3	BSC DWG 5	0.95	9.74
13-4	BSC DWG 5	4.96	24.79
13-5	BSC DWG 5	2.40	26.10
13-6	BSC DWG 5	0.22	10.50

Individual samples continued

L. Chizmadia and G. Bebout sample; Four Eyes Canyon thrust sheet, downstream from this study's UPS

microlithons	Delta13CBH μ l	Delta18O
UPS- μ s-7 (2)	5.36	23.78
UPS- μ s-8 (7)	5.03	22.63
UPS- μ s-10 (6)	4.75	23.12
UPS- μ s-414 (1)	5.02	23.32

vein		
UPS- μ s-14 (3)	3.30	10.64
UPS- μ s-20 (10)	3.15	16.99

selvages		
UPS- μ s-4 (8)	4.12	21.92
UPS- μ s-11 (4)	4.02	21.16
UPS- μ s-21 (9)	3.80	20.82
UPS- μ s-22 (5)	4.42	22.36

Vita

Adrienne Claire Johnson

Born in Washington, D.C. on February 9, 1978 to Robert L. Johnson and Susan W. Johnson.

Education

- **Lehigh University – Bethlehem, Pennsylvania**

Masters Candidate, Department of Earth and Environmental Sciences

GPA: 3.18/4.0, expected graduation June 2002

- **Bucknell University – Lewisburg, Pennsylvania**

B.S. in Geology, Department of Geology; Minor in Music

Overall GPA: 3.2/4.0, Geology GPA: 3.16/4.0, Graduated May 2000

- **Indiana University – Bloomington, Indiana**

Field Geology in the Rocky Mountains (G429), June-July 1999

Overall GPA: 3.33/4.0

Professional Experience

- **Teaching Assistant, Lehigh University**

Introduction to Planet Earth, Fall 2000, Spring 2001, Fall 2001; Introduction to Rocks and Minerals, Fall 2001; Geology 7 Week Field Course in the Rocky Mountains, Summer 2000

- **Teaching Assistant, Bucknell University**

Physical Geology, Fall 1999; Historical Geology, Spring 2000

Abstracts and Publications

- Johnson, Adrienne, 2001. Syntectonic Fluid Flow, Paleohydrology, and Vein Development within the Tendoy and Four Eyes Thrust Sheets of the Sevier Foreland, Tendoy Mountains, SW Montana, USA. *American Association of Petroleum Geologists Bulletin*, 85, no. 11, 2053.
- Ault, A.L., Burnett, B.N., Johnson, A.C., Knipscher, W.P., and Pazzaglia, F.J., 2001. Active Tectonism in the Northern Apennines and the southeastern Po Plain, Italy. *Uplift and Erosion: Driving Processes and Resulting Landforms*, INQUA Workshop, 11-12.
- Johnson, Adrienne, 2002. Syntectonic Fluid-Rock Interactions Involving Surficial Waters in the Sevier Thrust Belt, Tendoy Mountains, Southwest Montana. American Geophysical Union Abstracts, in press.

Research Grants

- **Marchand Fund, Bucknell Department of Geology, 1999**
“A Structural Study of Silurian-Devonian carbonates in the National Limestone Quarry, Middleburg, Pennsylvania.”
- **Geological Society of America, 2001**
“Syntectonic Fluid-Rock Interactions Involving Surficial Waters in the Sevier Thrust Belt, Tendoy Mountains, Southwestern Montana”
- **American Association of Petroleum Geologists, 2001**
“Syntectonic Fluid-Rock Interactions Involving Surficial Waters in the Sevier Thrust Belt, Tendoy Mountains, Southwestern Montana”
- **Palmer Fund, Lehigh Department of Earth and Environmental Sciences, 2001**

“Syntectonic Fluid-Rock Interactions Involving Surficial Waters in the Sevier Thrust Belt,
Tendoy Mountains, Southwestern Montana”

Scholarships, Academic Awards, and Honors

- **Phi Sigma Pi National Honor Fraternity**, Beta Chi Chapter, Bucknell University, Secretary, 1999-2000
- **Dean’s List**, Bucknell University, Fall 1998

Related Geological and University Organization Memberships

- **Geological Society of America**, 1999 thru present
- **American Geophysical Union**, 2002
- **American Association of Petroleum Geologists**, 2002
- **Graduate Student Council Representative**, Lehigh University Representative for the Department of Earth and Environmental Sciences; Fall 2000 thru Spring 2002
- **Bucknell University Geological Society**, President 1999-2000, member 1996-2000
- **Alpha Chi Omega**, Eta Chapter, Bucknell University, 1997 thru 2000, alumni status 2000 thru present

**END OF
TITLE**